universität wien

DISSERTATION

Titel der Dissertation

„FUNCTIONAL CHARACTERIZATION OF THE *ARABIDOPSIS* SMG7 PROTEIN“

Verfasserin

Mag. rer.nat. Nina Riehs

angestrebter akademischer Grad

Doktorin der Naturwissenschaften (Dr. rer.nat.)

Wien, 2009

Studienkennzahl lt. Studienblatt:	A 091 490
Dissertationsgebiet lt. Studienblatt:	Molekulare Biologie
Betreuer:	Dr. Karel Riha

“To appreciate nonsense requires
a serious interest in life.”
Frank Gelett Burgess (1866–1951)

ABSTRACT

During gene expression, mutations and errors in the processing of mRNA can lead to premature termination codons (PTC) or so called nonsense mutations. PTCs can lead to the production of truncated proteins which are potentially harmful to the cell. Nonsense mediated RNA decay (NMD) is a mechanism that has evolved to specifically target PTC containing mRNAs for degradation. The evolutionary conserved Est1/SMG5-7 proteins have been shown to play a role in NMD as well as telomere biology. However, due to their essential nature the characterization of these proteins in higher eukaryotes has been limited. The *Arabidopsis thaliana* genome encodes two EST1/SMG7 proteins, which are named SMG7 and SMG7-like. The major goal of my PhD thesis was to investigate the role of the SMG7 protein at an organismal level utilizing *Arabidopsis thaliana* as model system. I aimed to understand the function of SMG7 by studying T-DNA insertion lines. I found that naturally occurring NMD targets were stabilized in *smg7* mutants in a translation dependent manner, indicating that their degradation via the NMD machinery was impaired. These results demonstrated that the *Arabidopsis* SMG7 protein has a conserved function in NMD. Additionally, *smg7* mutant plants displayed two striking phenotypes. First, mutants were completely sterile. Cytological examination of the meiotic cell cycle revealed a strict arrest at the anaphase stage of the second meiotic division, indicating that SMG7 is essential for the exit from meiosis. Second, *smg7* mutants display severe growth and developmental defects as well as necrotic lesions on the leaves. The latter is a typical feature of lesion mimic mutants, in which the pathogen stress response is miss-regulated. Analysis of marker molecules revealed an up-regulation of the pathogen stress response in *smg7* even though the plants are not challenged with pathogens. Attenuation of the pathogen response signaling cascade in *smg7* mutants by a mutation in *pad4-1*, rescued all the vegetative growth and developmental defects in *smg7*. These data showed that SMG7 is involved in the regulation of pathogen response. Finally, I compared the defects observed in *smg7* with mutants of the NMD factors UPF1 and UPF3. I could not find any indication that either UPF1 or UPF3 showed an up-regulation of the pathogen response or defects in meiosis. This leads us to the conclusion that the function of SMG7 is more complex and not limited to NMD.

ZUSAMMENFASSUNG

Während der Genexpression können Mutation oder eine fehlerhafte Prozessierung der Boten RNA zu vorzeitigen Stopcodons (PTCs) führen, die ein vorzeitiges Translationsende und folglich die Produktion verkürzter und potentiell schädlicher Proteine verursachen. Der "Nonsense mediated RNA decay" (NMD) ist ein Mechanismus, der dieser Gefahr vorbeugt und die Degradierung dieser Boten RNAs veranlasst. Die evolutionär konservierten Est1/SMG5-7 Proteine spielen sowohl in NMD als auch in der Telomerbiologie eine entscheidende Rolle. Leider sind sie essenziell, und ihre Charakterisierung daher begrenzt. Das *Arabidopsis thaliana* Genom kodiert zwei EST1/SMG7 Proteine, welche SMG7 und SMG7-like genannt werden. Das Ziel meiner Doktorarbeit bestand darin, die Rolle des SMG7 Proteins auf Ebene des Pflanzenorganismus zu untersuchen. Daher verwendete ich mutante Pflanzenlinien, um die Funktion von SMG7 zu studieren. Ich stellte fest, dass in *smg7* Mutanten natürlich vorkommende und von NMD regulierte Transkripte in einem translationsabhängigen Prozess stabilisiert wurden, was darauf hindeutet, dass ihr Abbau, welcher normalerweise durch NMD veranlasst wird, verhindert wurde. Diese Ergebnisse zeigen, dass das *Arabidopsis* SMG7 Protein eine konservierte Rolle im NMD spielt. Zusätzlich zeigten *smg7* Mutanten eine Reihe an sichtbaren Defekten. *Smg7* Mutanten waren steril, wobei eine zytologische Untersuchung der Meiose zeigte, dass ein Arrest in der Anaphase der zweiten meiotischen Teilung diese Sterilität verursachte. Daher ist SMG7 essenziell für den Abschluss der meiotischen M phase. Weiters waren *smg7* Mutanten stark in Wachstum und Entwicklung beeinträchtigt und zeigten abgestorbene Zellen an den Blättern, welche ein typisches Zeichen von "lesion mimic" Mutanten sind. In diesen Mutanten ist die Stressantwort auf pathogene Organismen, selbst in deren Abwesenheit aktiviert. *Smg7* Mutanten zeigten auch ohne Pathogenstress einen Anstieg von Marker Molekülen, was auf eine ständige Aktivierung der Pathogenantwort deutet. Eine Abschwächung der Pathogenantwort mittels der *pad4-1* Mutation führte zu einer kompletten Aufhebung aller vegetativen Defekte in *smg7*, was darauf hindeutet, dass SMG7 an der Regulierung der Pathogenantwort beteiligt ist. Weiters verglich ich die Defekte in *smg7* Mutanten mit den Phänotypen von anderen NMD Mutanten, wie *upf1* und *upf3*. Allerdings zeigten *upf* Mutanten weder einen Defekt in der Pathogenantwort noch eine reduzierte Fertilität. Daher kam ich zum Schluss, dass SMG7 eine komplexere Funktion zu haben scheint und nicht auf NMD limitiert ist.

TABLE OF CONTENTS

1 INTRODUCTION

1.1 Nonsense Mediated RNA decay (NMD)

1.1.1 NMD function

Gene expression is a complex task comprised of many processes, and thus not immune to mistakes. In addition to mutations in genomic DNA, errors in transcription or mRNA processing can lead to aberrations including premature termination codons (PTCs). Translation of mRNAs that bear a PTC can lead to truncated proteins with harmful gain-of-function or dominant negative effects. Thus, quality control mechanisms are highly important for cell survival. One of these mechanisms is the nonsense mediated RNA decay (NMD) pathway which specifically eliminates PTC-carrying mRNAs (reviewed in Conti and Izaurralde 2005, Chang, Imam et al. 2007, Isken and Maquat 2008).

It is speculated that one third of human genetic diseases are caused by nonsense transcripts, as, for instance, is the case for beta-thalassaemia (Holbrook, Neu-Yilik et al. 2004). Therefore NMD is an interesting target for drug development (reviewed in Linde and Kerem 2008). However, it was also shown that NMD degrades naturally occurring nonsense transcripts that often arise due to alternative splicing of cryptic splice sites (Morrison, Harris et al. 1997; Mitrovich and Anderson 2000; Lewis, Green et al. 2003) and that NMD can compensate for inefficient splicing (Jaillon, Bouhouche et al. 2008).

An increasing body of evidence suggests that a variety of physiological NMD targets exist and that NMD is an important regulatory mechanism of gene expression. For instance, the existence of upstream open reading frames (uORFs) in the 5´UTR of a gene can regulate its expression level in an NMD dependent manner as was shown with the CYC1 gene in yeast (Pinto, Na et al. 1992) (reviewed in Frischmeyer and Dietz 1999). In a recent publication it was shown that even mRNA-like nonprotein-coding RNAs (mlncRNAs) and natural antisense transcript RNAs (nat-RNAs) were upregulated in NMD mutants in *Arabidopsis thaliana* (Kurihara, Matsui et al. 2009).

Nonsense mediated RNA decay is an evolutionarily conserved mRNA pathway that can not only modulate the pathology of a disease but has important physiological functions on the regulation of gene expression. Although many studies have contributed to a better understanding of the basic principle of NMD, many questions remain. For instance, how are the physiological targets defined and targeted for decay and what is the biological relevance of their regulation? In this respect our knowledge only scratches the surface and further investigation will prove beneficial not only for therapeutic aspects but for the understanding of the complex nature of gene expression.

1.1.2 Mammalian NMD

How PTC containing transcripts are defined and recognized by the NMD machinery differs between invertebrates and mammals. Whereas invertebrate NMD employs the faux 3´UTR model, mammalian NMD relies on the exon-junction complex (EJC). A current scheme of the mammalian NMD pathway is shown in figure 1.

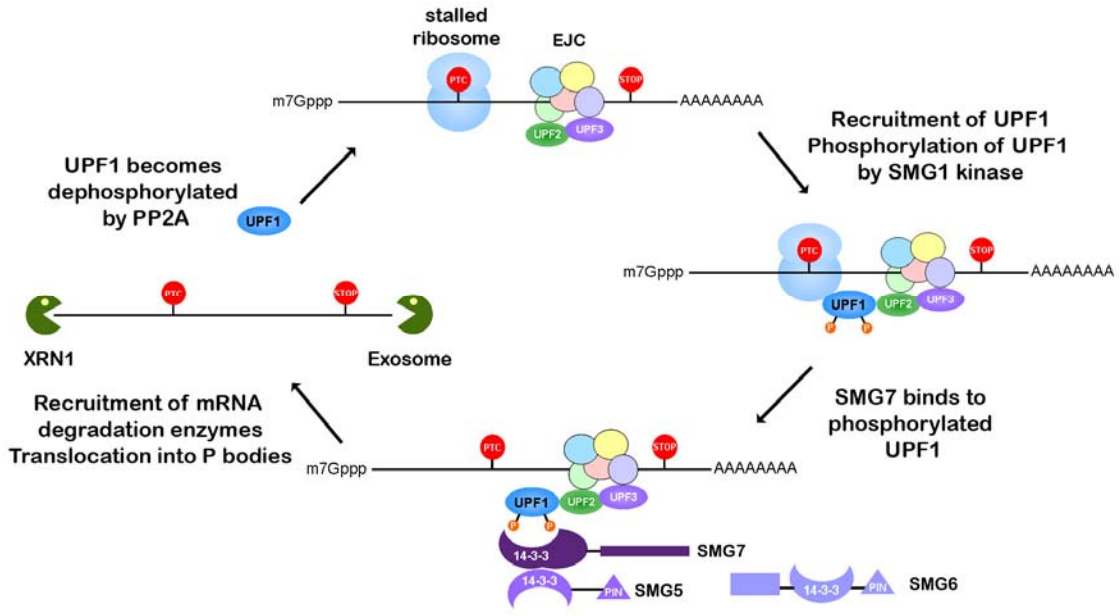

Figure 1. Overview of the mammalian nonsense mediated RNA decay pathway. EJC = exon-junction complex. Picture adapted from (Conti and Izaurralde 2005).

NMD can distinguish between a normal and a premature stop codon according to its location. Proteins of the exon-junction complex (EJC) remain attached to the spliced mRNA until the mRNA becomes translated. A normal stop codon, that is typically located in the last exon, will not trigger NMD, since all EJC proteins will be removed

by the translating ribosome. However, if a PTC is located upstream of the last exon-exon junction, the downstream EJC proteins can not be removed by the ribosome that is stalled at the PTC. Then the EJC proteins together with UPF2 and UPF3 activate NMD. This scanning mechanism occurs during a pioneer round of translation to ensure that no potentially harmful proteins can be produced.

Once NMD is elicited, UPF1, an RNA helicase, becomes phosphorylated by SMG1, a phosphoinositide-3-kinase related protein kinase. The 14-3-3-like domain of SMG7 can recognize and bind to phosphorylated UPF1 leading to translocation of the mRNA-protein complex to processing bodies or P-bodies, the cytoplasmic sites of mRNA degradation (reviewed in Eulalio, Behm-Ansmant et al. 2007). PP2A phosphatase dephosphorylates UPF1 and the mRNA is degraded via the exosome and XRN1 exoribonuclease. Finally, UPF1 is released and recycled for the next round of NMD (reviewed in Conti and Izaurralde 2005).

1.1.3 NMD in other model organisms

In higher eukaryotes some NMD factors are essential for cell survival. For instance, UPF1 is important for larval development and cell proliferation in *Drosophila melanogaster* (Rehwinkel, Letunic et al. 2005; Metzstein and Krasnow 2006) and *Arabidopsis* plants homozygous for the *upf1-3* allele are seedling lethal (Arciga-Reyes, Wootton et al. 2006). However, NMD mutants in budding yeast and nematodes are viable (Behm-Ansmant, Kashima et al. 2007). Another major difference is the recognition of PTC containing mRNAs. In yeast and invertebrates the distance of the PTC to the 3´UTR of the mRNA is crucial. Usually the longer the distance the more efficient is NMD processing (Amrani, Ganesan et al. 2004). This model of PTC recognition is called the faux 3´UTR model.

NMD was first described in yeast (Losson and Lacroute 1979). So far only the three core transacting factors UPF1, UPF2/NMD2 and UPF3 have been shown to be crucial for NMD in budding yeast (Culbertson, Underbrink et al. 1980; Leeds, Peltz et al. 1991; He and Jacobson 1995). Although a yeast SMG1 homolog has not been found, phosphorylation of UPF1 hints to another unidentified kinase (Wang, Cajigas et al. 2006). In multicellular organisms the SMG5-7 proteins are required for the

dephosphorlyation of UPF1. Although ScEbs1p behaves in a similar manner to the SMG5-7 proteins, it is not essential for NMD. Interestingly, the N-terminal conserved region (NCR) of UPF1, which is involved in the binding of UPF1 to SMG5, is conserved only in metazoa but not in yeast (Ohnishi, Yamashita et al. 2003). This might indicate that dephosphorylation of UPF1 underlies a different mechanism in yeast compared to higher eukaryotes.

1.1.4 Plant NMD

NMD in plants displays an interesting feature. It has been reported that both the faux 3´UTR and intron based NMD co-exist in plants (Kertesz, Kerenyi et al. 2006; Hori and Watanabe 2007; Kerenyi, Merai et al. 2008), which indicates that the plants adapted both types of NMD from invertebrates and mammals.

Functionally homologous proteins have been identified and characterized in plants based on homology to known NMD factors (listed in table 1).

Sc	*Ce*	*Dm*	*At*	*Mm, Hs*	**Protein domains**
-	SMG-1	SMG1	-	SMG1	PI3K-related kinase
Upf1p	SMG-2	UPF1	UPF1	UPF1	RNA helicase
Upf2p	SMG-3	UPF2	UPF2	UPF2	nucleic acid binding
Upf3p	SMG-4	UPF3	UPF3	UPF3 / UPF3X	nucleic acid binding
-	SMG-5	SMG5	-	SMG5	EST1 (14-3-3-like), PIN
-	SMG-6	SMG6	-	SMG6	EST1 (14-3-3-like), PIN
Ebs1p	SMG-7	-	SMG7, SMG7L	SMG7	EST1 (14-3-3-like)

Table 1. Evolutionary conserved NMD factors (Sc = *Saccaromyces cerevisiae*, Ce = *Caenorhabditis elegans*, Dm = *Drosophila melanogaster*, Mm = *Mus musculus*, Hs = *Homo sapiens*, PI3K = phosphoinositide-3-OH-kinase).

The core trans acting factors UPF1, UPF2, UPF3 (Hori and Watanabe 2005; Arciga-Reyes, Wootton et al. 2006; Yoine, Nishii et al. 2006; Yoine, Ohto et al. 2006) are conserved in plants like in every eukaryote. Surprisingly, homology searches for the

SMG5-7 proteins in *Arabidopsis thaliana* identified only two proteins, both of which showed closer homology and similar domain architecture to hSMG7 and thus were named SMG7 and SMG7-like (Riehs, Akimcheva et al. 2008). Their characterization was the major aim of this thesis. Data supporting the role of *Arabidopsis* SMG7 in NMD was also provided by another laboratory (Kerenyi, Merai et al. 2008).

Analysis of the nucleolar proteome revealed that, except for SMG7, many plant NMD and exon junction proteins localize to the nucleolus, which could indicate that a first round of translation may occur inside the nucleus (Pendle, Clark et al. 2005).

The fact that both the invertebrate and mammalian types of NMD recognition are present in plants and that the NMD machinery is conserved and essential makes *Arabidopsis* an interesting model system for the investigation of NMD.

1.2 The EST1/SMG5-7 protein family

Protein homology searches based on the budding yeast Est1p as well as SMG5-7 proteins of *Caenorhabditis elegans* defined a new protein family that is characterized by the EST1 domain (Reichenbach, Hoss et al. 2003; Snow, Erdmann et al. 2003). The EST1 domain is also known as the EST1-TPR domain since it contains two tetratricopeptide repeats. Analysis of the crystal structure of the EST1 domain showed that it has a 14-3-3-like fold, indicating that the EST1 domain functions as a protein-protein interaction domain that binds phosphorylated serine containing peptides (Fukuhara, Ebert et al. 2005). The EST1/SMG5-7 protein family is evolutionarily conserved and essential in higher eukaryotes. Their functions have mainly been implicated in RNA surveillance and telomere maintenance. The features of this interesting group of proteins will be described in more detail below.

1.2.1 Budding yeast Est1p and Ebs1p

The *Saccharomyces cerevisiae EST1* (ever shorter telomere 1) gene was first identified in a screen for mutants defective in telomere elongation (Lundblad and Szostak 1989). In order to fully replicate telomeres, many eukaryotes rely on a reverse transcriptase

called telomerase. Lack of telomerase (Est2p), its RNA subunit (*TLC1*), Est1p, or Est3p leads to gradual loss of telomeric DNA and eventually to senescence of the yeast cell. The work of several studies demonstrated that the Est1 protein is needed to mediate the access of telomerase to the telomeres. On the one hand Est1p interacts with Cdc13p, a single-stranded DNA binding protein that specifically binds to the telomeric single-stranded 3´overhang (Qi and Zakian 2000; Pennock, Buckley et al. 2001). On the other hand Est1p binds to *TLC1* via a C-terminal RNA recognition motif (Zhou, Hidaka et al. 2000; Seto, Livengood et al. 2002). Final evidence that Est1p bridges telomerase to telomeres came from a study were a fusion of Cdc13p with Est2p fully rescued the ever shorter telomere phenotype of Est1p (Evans and Lundblad 1999).
The second EST1 domain containing protein in *Saccharomyces cerevisae* is Ebs1p. The Ebs1 protein has been implicated in regulating translation via binding to elF-4E. *Ebs1* mutants show only a very modest defect in NMD, but interestingly NMD regulates the expression of *EBS1* (Ford, Guan et al. 2006). In a more recent publication it was found that Ebs1p binds Upf1p and localizes to P-bodies; it also leads to Upf1p concentration in P-bodies when overexpressed (Luke, Azzalin et al. 2007). Even though Ebs1p is not required for NMD, it acts in a manner similar to its orthologs in higher eukaryotes, indicating that Ebs1p is at least partially a functional homolog of the SMG5-7 proteins.

1.2.2 Fission yeast Est1p and Est1-like protein

In the fission yeast *Schizosaccaromyces pombe* two EST1 domain containing proteins named Est1p and another Est1-like protein (SPBC2F12) were identified (Beernink, Miller et al. 2003). SpEst1p is, like its homolog in budding yeast, necessary for telomere elongation and its binding to telomerase is dependent on telomerase RNA TER1 (Leonardi, Box et al. 2008). However neither the Est1 nor Est1-like protein have been characterized with respect to NMD.

1.2.3 *Caenorhabditis elegans* SMG-5, SMG--6 and SMG-7

Almost all known NMD factors (*smg-1* to *smg-6*) of *C .elegans* were found in a screen for informational suppression of mutations in three different genes (Hodgkin, Papp et al. 1989). One of the genes was *unc-54*, a myosin heavy chain of the body wall muscle. Heterozygous worms for a mutation allele that lacks the polyadenylation signal are

phenotypically normal since the transcripts derived from the mutant allele contributed only ~5% to the total amount of UNC-54 mRNA. Due to the impaired NMD machinery in the *smg* mutant background the amount of *unc-54* transcripts increased to the level of the normal unc-54 allele, leading to paralysis of the worms because of its dominant negative effect. In addition, the *smg* mutant worms displayed defects in the morphogenesis of male and female genitalia, thus they were named *smg-1* to *smg-6* (suppressor with morphogenetic effect on genitalia). Due to a temperature sensitive effect on NMD the *smg-7* null allele was only identified in a modified screen (Cali, Kuchma et al. 1999). Furthermore, the fact that SMG-5 and SMG-7 proteins interact with each other and that both are needed to dephosphorylate SMG-2 (UPF1) was first described in *C. elegans* (Page, Carr et al. 1999; Anders, Grimson et al. 2003).

1.2.4 Mammalian SMG5, SMG6 and SMG7

In human the SMG5, SMG6 and SMG7 proteins (also known as EST1B, EST1A and EST1C, respectively) were independently identified as homologs of ScEst1p (Reichenbach, Hoss et al. 2003; Snow, Erdmann et al. 2003) and of the CeSMG5-7 proteins (Chiu, Serin et al. 2003; Ohnishi, Yamashita et al. 2003). Biochemical analysis of hSMG5-7 (or hEST1A-C) revealed that all three proteins are required for functional NMD (Unterholzner and Izaurralde 2004) and also play a role in telomere maintenance. For instance, it was shown that hEST1A/hSMG6 associates with active telomerase and that hEST1A/hSMG6 overexpression leads to defects in telomere capping. With respect to NMD, it was shown that SMG5 and SMG7 form a complex that binds to phosphorylated UPF1 and, via interaction with protein phosphatase 2A (PP2A), leads to dephosphorylation of UPF1. All three proteins were reported to be mainly cytoplasmic but shuttle between the cytoplasm and nucleus (Ohnishi, Yamashita et al. 2003). Interestingly SMG5 and SMG7 localize to cytoplasmic P-bodies, whereas SMG6 is found in separate cytoplasmic foci (Unterholzner and Izaurralde 2004).

Valuable insights into the function of SMG7 came from a tethering assay experiment (Unterholzner and Izaurralde 2004). In this assay candidate proteins are fused to λN, a peptide that binds a five-BoxB site that is cloned into the 3´UTR of a β-globin reporter mRNA. NMD and EJC components such as UPF3b, Y14 and MAGOH, which are

tethered to this reporter transcript, induce the degradation of the reporter mRNA since the normal stop codon is upstream of the tethering site and is therefore perceived as premature (Fribourg, Gatfield et al. 2003; Gehring, Neu-Yilik et al. 2003). Unterholzner and colleagues (Unterholzner and Izaurralde 2004) found that SMG7 tethered to the reporter mRNA led to degradation of the mRNA, while tethering SMG5 and SMG6 did not decrease the transcript levels. In contrast to other NMD factors, SMG7 was even able to degrade the tethered mRNA when it did not contain a premature stop codon. Further they could show that degradation of the SMG7 tethered mRNA was independent of UPF1. Hence, the authors suggest that SMG7 links the nonsense mediated RNA decay with the mRNA degradation machinery.

An important hint to the molecular function of SMG7 came from crystal structure analysis of the first 500 amino acids. Even with very low sequence conservation (~10%), SMG7 has a very high structural similarity to 14-3-3 proteins. The typical feature of 14-3-3 protein is a pocket-like structure that mediates binding to phosphorylated peptides. Interestingly, the residues important for binding to phopshorylated serines are highly conserved in all organisms and are also required for the binding of hSMG7 to phosphorylated hUPF1 (figure 2, Fukuhara, Ebert et al. 2005).

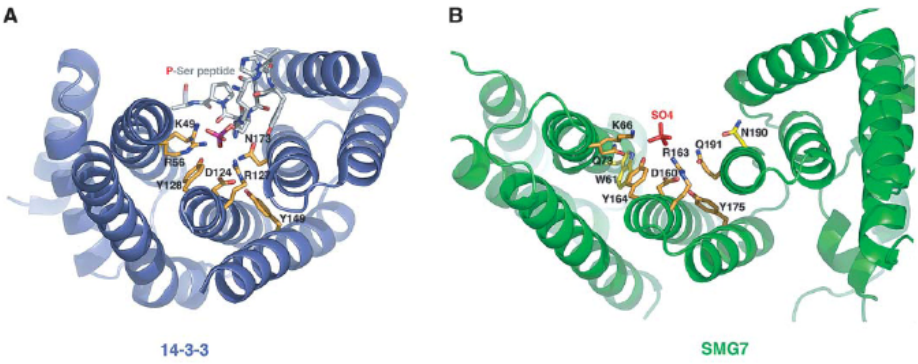

Figure 2. The EST1-TPR domain of human SMG7 (B) has a similar fold to 14-3-3 proteins (A). Picture taken from Fukuhara, Ebert et al. 2005.

An explanation for the diverse roles of the SMG5-7 proteins came from a more recent study, where it was found that NMD proteins are involved in processing of telomeric transcripts called TERRA molecules, and thus link the function of NMD with

telomeres (Azzalin, Reichenbach et al. 2007). The authors speculate that the displacement of TERRA molecules from the telomeres, which is crucial for telomere integrity, is promoted by NMD factors such as UPF1, SMG1 and hEST1A/hSMG6.

However, SMG5-7 proteins were only characterized in cell cultures and no knock out mouse has yet been described.

1.3 Aim of the PhD thesis

SMG5-7 proteins belong to a novel protein family defined by an N-terminal EST1 domain. The founding members Est1p in budding yeast and the SMG5-7 proteins in *C. elegans* were implicated in telomere biology or mRNA surveillance, respectively. Homologous proteins in higher eukaryotes are essential for cell survival which hinders their functional characterization at the organismal level.

Work in both our and Dorothy Shippen's (Texas A&M University, USA) laboratory led to the identification of *Arabidopsis* EST1 domain containing proteins, which were originally named EST1B (now SMG7) and EST1A (now SMG7-like). However in the course of our study we decided to rename them to SMG7 and SMG7-like. Initial characterization of *SMG7* and *SMG7-like* T-DNA insertion mutants did not reveal a function for these proteins in telomere integrity (Rachel Idol, Dorothy Shippen. unpublished data).

The aim of my PhD thesis was to further characterize SMG7 with respect to NMD and to understand the biological relevance of SMG7 by studying its function in the organismal context.

Objective 1: Basic characterization of AtSMG7 and AtSMG7-like
In order to unravel the biological role of the SMG7 orthologs in *Arabidopsis thaliana* I aimed to characterize the *SMG7* genes and transcripts, as well as to obtain and to characterize *smg7* mutant lines. In addition I aimed to perform a phenotypic analysis of all available mutant lines in order to gain insights in the function of SMG7 at the organismal level.

Objective 2: Is SMG7 involved in NMD?

Homologous proteins in higher eukaryotes are involved in the nonsense mediated RNA decay. Therefore I aimed to test if the function of *Arabidopsis* SMG7 in NMD is evolutionarily conserved.

Objective 3: What causes the sterility defect?

NMD factors are not essential in yeast and in *C. elegans* but are usually required for cell survival in higher eukaryotes. Therefore characterization of mammalian NMD mutants was limited. The ability to study the function of SMG7 in the context of the whole organism using a series of *Arabidopsis* hypomorphic mutants provides a clear advantage to uncovering the biological significance of SMG7. *Smg7* mutant plants are almost completely sterile. I aimed to discover the cause of the sterility and to gain valuable insights into the biological role of SMG7.

Objective 4: What underlies the vegetative defects?

Some *smg7* mutations cause a pleiotropic phenotype with respect to vegetative growth and plant development. I aimed to investigate the cause of the vegetative defects in order to gain knowledge about the biological significance of SMG7.

Objective 5: Can the defects observed in mutant plants be linked to NMD?

Analysis of the defects in *smg7* mutants gives a first glimpse to the biological role NMD plays in an organism that undergoes complex development. In order to evaluate what aspects of plant development and growth can be associated with NMD function I wanted to compare the *smg7* mutants with all available mutant lines of the other characterized NMD factors UPF1 and UPF3. If defects in *smg7* mutants are not observed in other NMD mutants, it would indicate that SMG7 plays a role beyond NMD.

2 RESULTS

2.1 Characterization of AtSMG7

2.1.1 Identification of *Arabidopsis* EST1 domain proteins

Previously identified homologues of *S. cerevisiae* Est1p showed sequence homology within a region spanning approximately 250 amino acids at the N-terminus. This region contained two tertratricopeptide repeats (TPR) and was named the EST1 or EST1-TPR domain (Reichenbach, Hoss et al. 2003; Snow, Erdmann et al. 2003). Based on position-specific iterative (PSI)-BLAST searches of the EST1-TPR domain of the Est1p protein of *Kluyveromyces lactis* against the non-redundant NCBI database (National Center for Biotechnology Information) the *Arabidopsis* proteins NP_197441 and AAF98429 were identified (Riehs, Akimcheva et al. 2008). A multiple sequence alignment of the conserved EST1-TPR domain was compiled (figure 3).

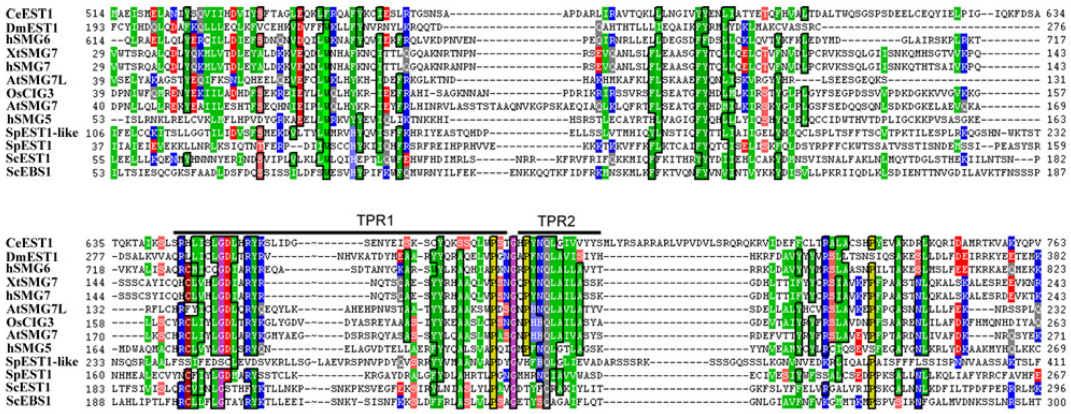

Figure 3. Multiple sequence alignment of the EST1 domain by clustalW. The following protein sequences were used for the alignment: *Caenorhabditis elegans* CeEST1 (AAK27880), *Drosophila melanogaster* DmEST1 (CAD89221), human hSMG6/EST1A (AAN46114), hSMG5/EST1B (NP_056142), hSMG7/EST1C (NP_775179), *Xenopus tropicalis* XtEST1C (AAH63908), *Arabidopsis thaliana* AtSMG7L (AAF98429), AtSMG7 (NP_197441), *Oryza sativa* OsCIG3 (BAD30942), *Schizosaccharomyces pombe* SpEst1-like (CAB10152), SpEst1 (CAA21171) and *Saccharomyces cerevisiae* Est1p (NP_013334) and Ebs1p (NP_010492). Putative tertratricopeptide repeats (TPR) are indicated. The alignment of the EST1 domains was performed with BioEdit Sequence Alignment Editor (Hall 1999). The following amino acid color code is used: green (Y, F, A, I, L, M, V), pale green (W), violet (G), yellow (P), red (S, D, E, T), blue (R, N, K), pale blue (H), gray (Q) and brown (C).

Besides the sequence homology of the EST1-TPR domain, the two identified *Arabidopsis* proteins share ~25% sequence identity to human SMG7 and SMG6 over a region spanning ~300aa-550aa, which we called the EST1- central domain (CD). A PilT N terminus (PIN) domain, which is present in human SMG5 and SMG6, is lacking in both *Arabidopsis* homologs. As the *Arabidopsis* proteins show a similar domain architecture and size to the human SMG7 we named them AtSMG7 (NP_197441) and AtSMG7-like (AAF98429) (figure 4).

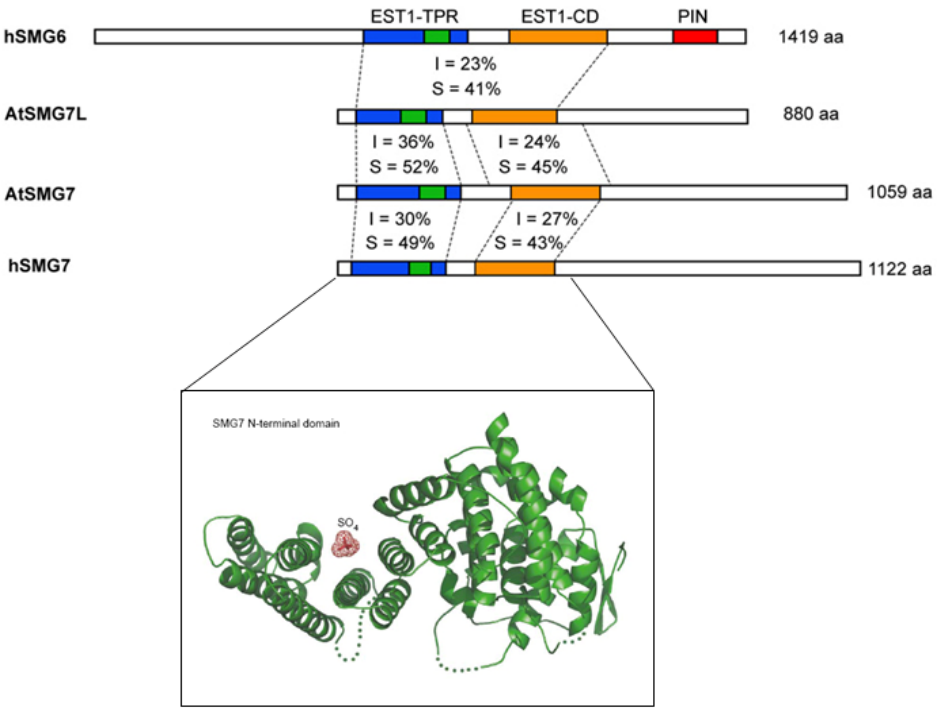

Figure 4 *Arabidopsis* SMG7 and SMG7-like share homology to hSMG7 and hSMG6 over the EST1-TPR and EST1-CD domain. Green box = Tetratricopeptidrepeat (TPR), blue box = EST1-TPR domain, orange box = EST1- conserved domain (CD), red box = PilT N terminus (PIN) domain. Crystal structure analysis revealed that the EST1-TPR domain folds similar to 14-3-3 proteins.

Analysis of the hSMG7 crystal structure revealed that the EST1-TPR domain has a similar fold to 14-3-3 proteins (Fukuhara, Ebert et al. 2005). 14-3-3 proteins are small proteins that can bind phosphorylated peptides. All EST1-TPR residues required for the binding to phosphoserines are conserved in AtSMG7 and AtSMG7L.

Using ClustalW1.81 (http://www.ebi.ac.uk/Tools/clustalw, Larkin, Blackshields et al. 2007), phylogenetic relationships were calculated based on a multiple sequence

alignment of full length EST1/SMG5-7 proteins and visualized in a phylogenetic tree (figure 5, TreeView, http://taxonomy.zoology.gla.ac.uk/rod/treeview.html, Page 1996).

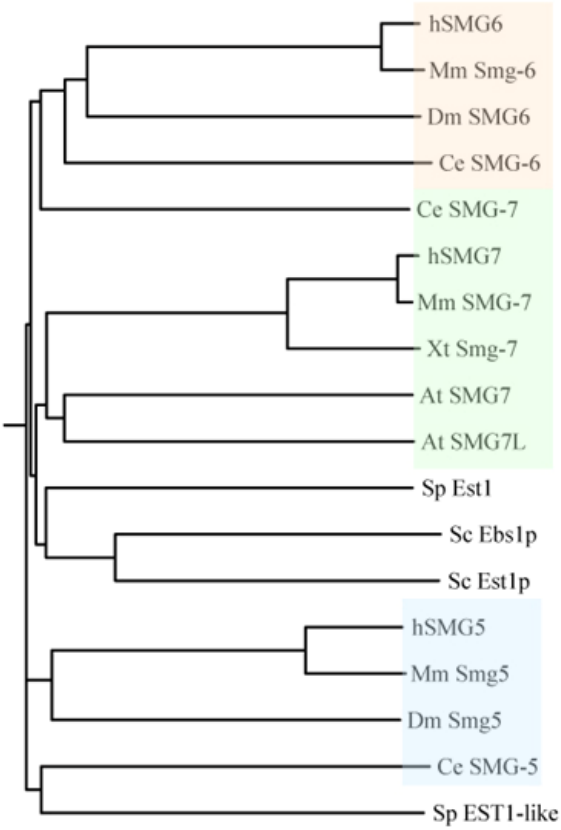

Figure 5. Phylogenetic tree of the EST1/SMG5-7 protein family. The following protein sequences were used: hSMG6 (NP_060045), hSMG5 (NP_056142), hSMG7 (NP_775179), Mm Smg5 (AAH24683), Mm SMG7 (NP_001005507), Mm Smg-6 (NP_001002764), Dm SMG6 (CAD89221), Dm Smg5 (NP_609685), Xt Smg-7 (NP_989258), Ce SMG-7 (NP_501033), Ce SMG-6 (NP_001040885), Ce SMG-5 (NP_491929), Sp Est1 (NP_596232), Sc Ebs1p (NP_010492), Sc Est1p (NP_013334), At SMG7 (NP_197441) and At SMG7L (AAF98429). (Abbreviations: At = *Arabidopsis thaliana*, Ce = *Caenorhabditis elegans*, Dm = *Drosopila melanogaster*, h = human, Mm = *Mus musculus*, Sp = *Schizosaccharomyces pombe*, Sc = *Saccharomyces cerevisiae*, Xt = *Xenopus tropicalis*).

The *Arabidopsis* genome encodes two SMG7 homologs but lacks clear homologs of the SMG5 and SMG6 proteins of higher eukaryotes. Phylogenetic analysis of the plant EST1/SMG5-7 protein family showed that SMG7 homologs were present in all plant species where sequence data was available (figure 6). An interesting observation was that orthologs of the SMG7 protein are present in every analyzed plant species. However the existence of proteins homologous to AtSMG7-like is restricted to dicots. This data indicates that the SMG7 protein is highly evolutionary conserved in plants and that the SMG7-like protein evolved later.

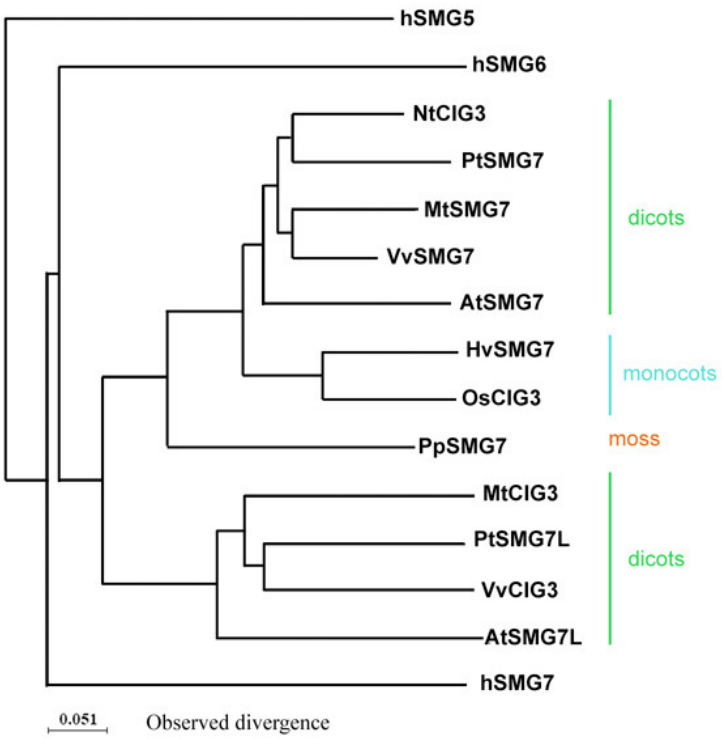

Figure 6. Phylogenetic tree of the plant SMG7 proteins. Selected homologues were aligned using Probcons (Do, Mahabhashyam et al. 2005) and the phylogenetic tree was prepared with PHYLO_WIN (Galtier, Gouy et al. 1996) using the neighbour-joining method with observed divergence distances. The scale bar corresponds to 0.051 estimated amino acid substitutions per site. The following sequences were used for the alignment: hSMG5, hSMG6, hSMG7, AtSMG7, AtSMG7L, OsCIG3, *Nicotina tabacum* NtCIG3 (BAB82502), *Medicago truncatula* MtCIG3 (ABD32367), *Hordeum vulgare* HvSMG7 (AK248878), *Vitis vinifera* VvCIG3 (CAN78121). *V. vinifera* VvSMG7 and *M. truncatula* MtSMG7 were derived from unannotated genome sequences (AM465968 and CT033769, respectively). *Populus trichocarpa* PpSMG7 and PpSMG7L, and *Physcomitrella patens* PpSMG7 sequences were obtained from the land plant genome sequence database "Phytozome" (http://dev.phytozome.net/index.php).

2.1.2 Cloning of *SMG7* cDNA and RACE

I cloned the predicted full-length cDNA of *AtSMG7* via RT-PCR and confirmed the sequence of the cDNA by sequencing. 3´RACE analysis revealed an alternative splice site in the 7th intron of the cloned *SMG7* cDNA compared to the published *SMG7* cDNA (NM_121945) in the GenBank database of NCBI (http://www.ncbi.nlm.nih.gov). The new exon seven is shifted 10bp to the 3´ end of the gene and uses a different stop codon (TGA) instead of the previous TAA stop codon (figure 7). The new cDNA sequence was deposited in GenBank under the accession number EU126544. However, this splice variant does not lead to a change in the 1059aa long protein sequence of SMG7. Alternative splicing as well as a non-coding exon in the 3´UTR are interesting features of the *SMG7* gene structure, which hint that

SMG7 itself might be a natural target of NMD. In fact data in tobacco suggests that *SMG7* is indeed regulated by NMD (Kerenyi, Merai et al. 2008).

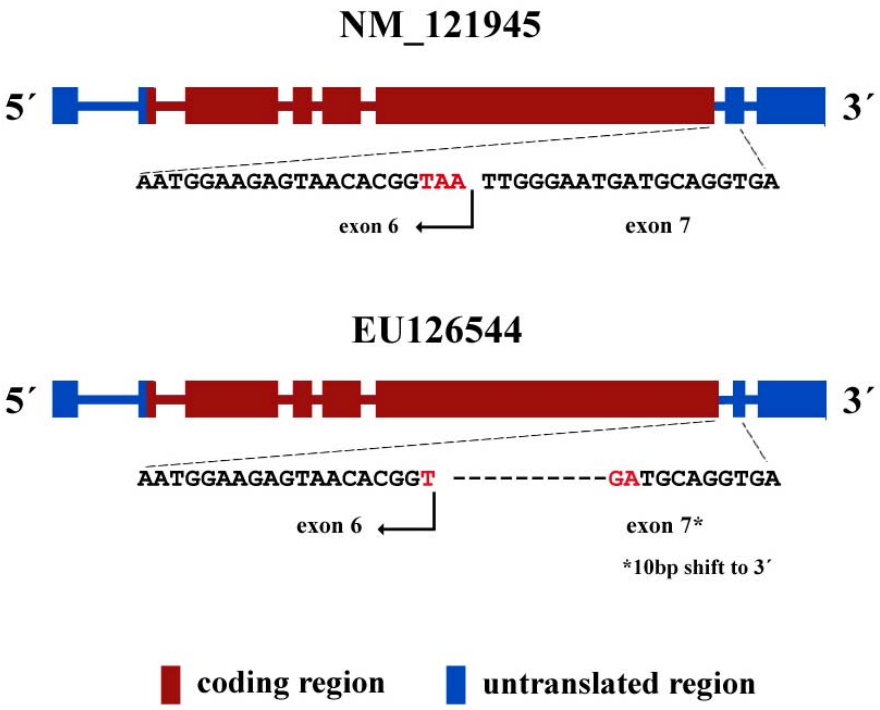

Figure 7. Alternative splicing of *AtSMG7*. The new splice variant (EU126544) contains a 10bp shift of exon 7. Stop codons are depicted in red.

2.1.3 Expression analysis of *SMG7*

Where and to which extent a gene is expressed can give valuable hints to its function. The Genevestigator tool (https://www.genevestigator.com/gv/index.jsp, (Hruz T 2008) provides an estimation of the expression levels based on microarray data deposited in a public database. *SMG7* shows high and ubiquitious expression in almost all tissues. Particularly elevated levels were seen in cell culture, pollen, senescent leaves and xylem (figure 8A). In general the *SMG7-like* gene showed lower expression levels compared to *SMG7*. I extracted total RNA from several tissues and measured the *SMG7* mRNA levels via northern blot. The ubiquitous expression of *SMG7* in a variety of *Arabidopsis* tissues was verified by this method (figure 8B).

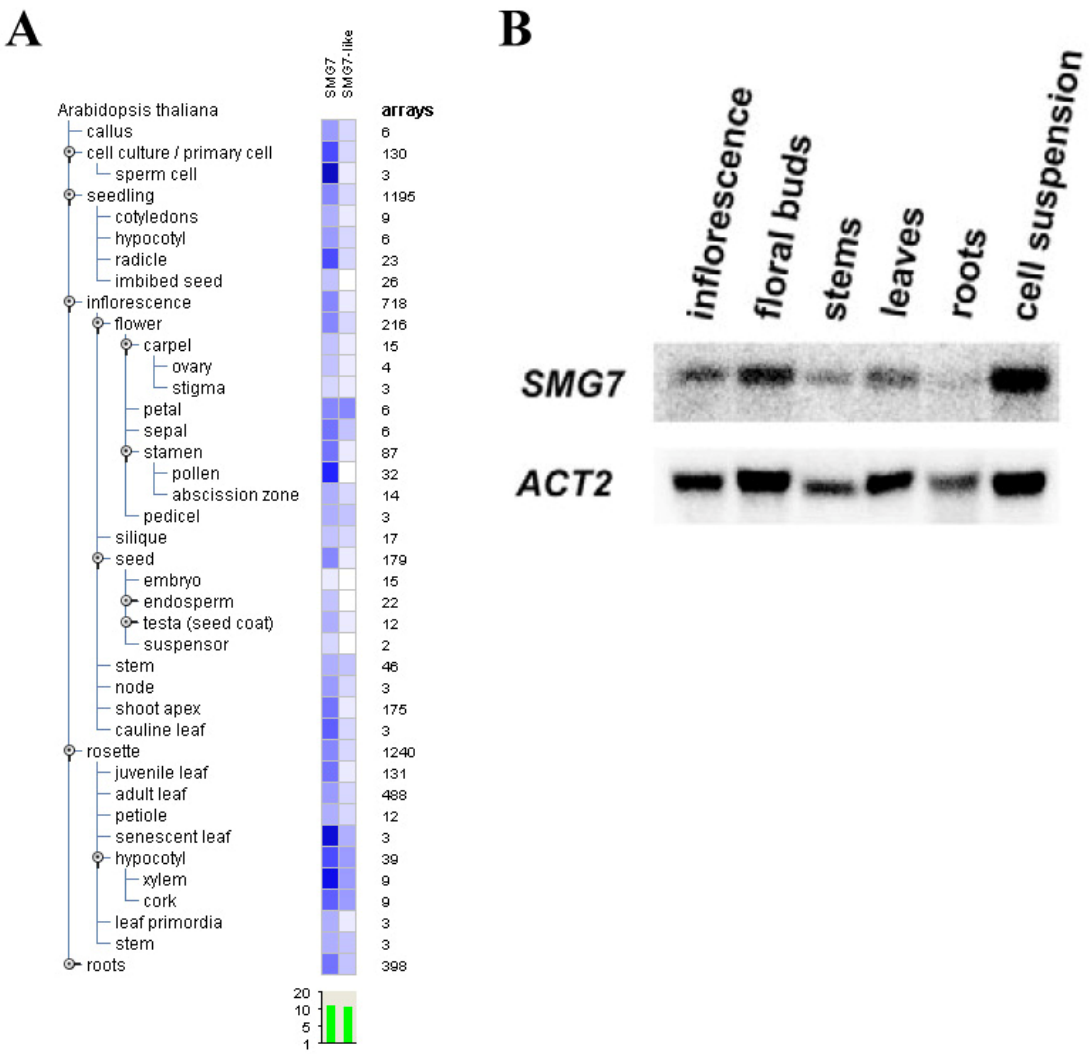

Figure 8. Expression of *AtSMG7*. (A) Transcription profiles of *SMG7* mRNA analyzed by Genevestigator (Hruz T 2008). (B) *SMG7* mRNA levels were analyzed with northern blot hybridization in the indicated tissues. *ACT2* RNA was used as loading control.

2.1.4 Characterization of *AtSMG7* T-DNA insertion lines

In order to understand the function of *Arabidopsis* SMG7 I analyzed mutant plants. A range of *Arabidopsis* lines carrying T-DNA insertions at different positions in the *SMG7* gene were obtained from seed stock centers. The obtained alleles are listed in table 2 and figure 9.

allele	seed stock ID	position of insertion (distance from ATG)	phenotype
smg7-1	SALK_073354	6th exon (1547bp) deletion: 15bp (1547-1562bp) Two T-DNA insertions[a] LB: filler sequence: 9 + 25bp	defects in vegetative growth and development, sterility
smg7-2	SALK_025699	6th exon (2488bp) LB: 2bp microhomology with SMG7 RB: not verified	defects in vegetative growth and development, sterility
smg7-3	SALK_112476	6th exon (2516bp) deletion: 13bp (2516-2529bp) LB: 4bp microhomology with SMG7 RB[b]: 14bp inserted filler sequence	defects in vegetative growth and development, sterility
smg7-4	SAIL_63F08	6th exon (3212bp) deletion 34bp (3212-3246bp) LB: 3bp inserted filler sequence RB[b]: 2bp microhomology with SMG7	no visible defects
smg7-5	SALK_144162	5th exon (1256bp) LB: 3bp microhomology with SMG7 RB: not verified	embryo lethality
smg7-6	SALK_052532	6th exon (2719bp) deletion of 11bp (2719-2730bp) LB: 3bp inserted filler sequence RB: 3bp microhomology with SMG7	sterility

Table 2. List of *SMG7* T-DNA insertions. Inserted filler sequences are of unknown origin. LB= left border, RB = right border. [a]The *smg7-1* allele has at least two T-DNA inserted in a head to head orientation. [b]Rearrangement of the T-DNA insertion: a duplication of the LB sequence follows the right border.

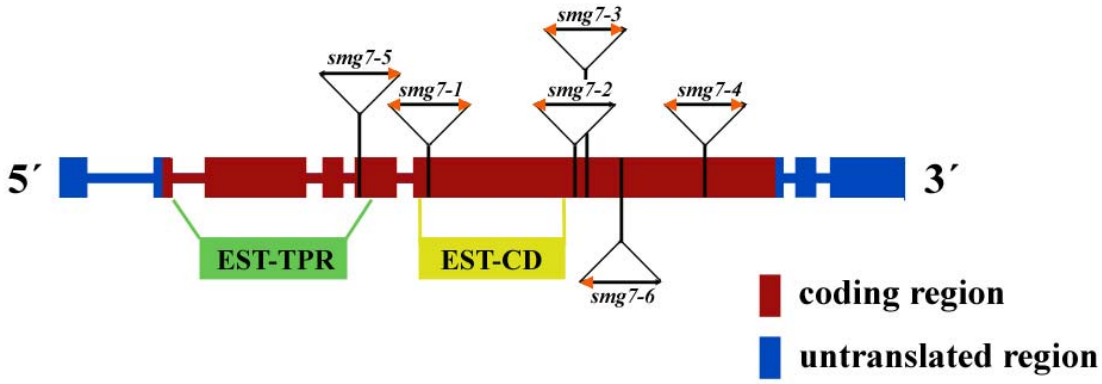

Figure 9. Schematic representation of the *SMG7* gene with the T-DNA insertions *smg7-1*, *smg7-2*, *smg7-3*, *smg7-4*, *smg7-5* and *smg7-6*. Left borders of the insertions are indicated by orange arrowheads.

The *smg7-5* allele carries a T-DNA insertion that lies the furthest upstream within the open reading frame and is the only one that disrupts the EST1-TPR domain. I was unable to obtain homozygous *smg7-5* mutants out of 63 plants segregating from a heterozygous parent with a ratio of wild-type to heterozygous plants of 2:1 ($\chi^2 = 1.78$). In addition the siliques of heterozygous plants showed a portion of aborted seeds (figure 10) which indicates that *smg7-5* homozygous mutation causes embryonic lethality.

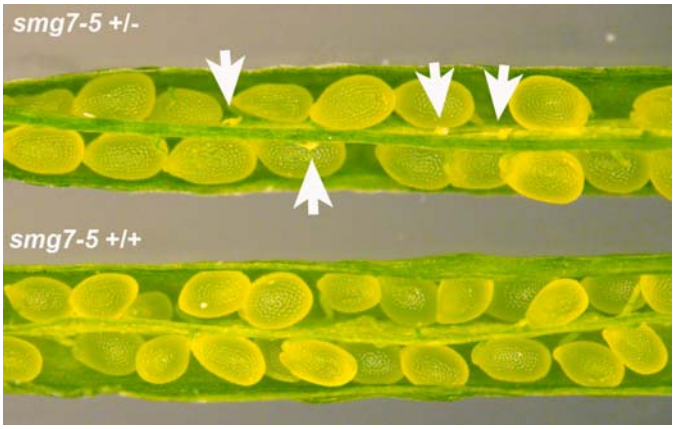

Figure 10. Embryo lethality of *smg7-5*. Siliques of heterozygous plants for the *smg7-5* allele contain a fraction of aborted seeds (indicated with the white arrows).

Homozygous plants for all the other T-DNA insertions (*smg7-1, -2, -3, -4 and -6*) gave rise to viable homozygous mutant plants (figure 11).

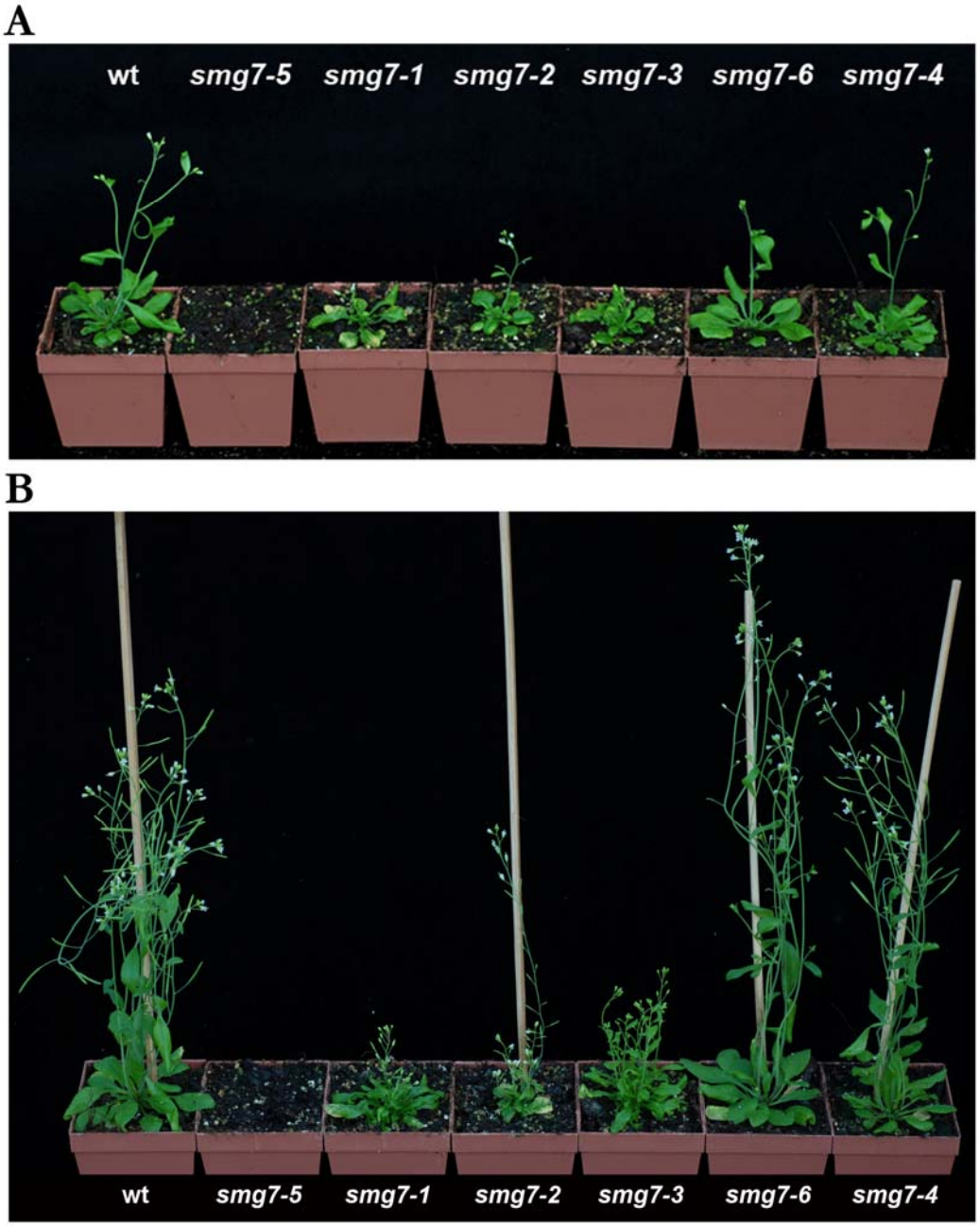

Figure 11. Homozygous *AtSMG7* T-DNA insertion lines after 4.5 weeks (A) and 6.5 weeks (B).

Since the *smg7-5* insertion is the only one that disrupts the EST1-TPR domain we concluded that this domain is vital for SMG7 function and that *smg7-5* fully disrupts SMG7 function. Northern analysis of RNA from mutants carrying different *smg7* alleles showed that mRNAs can be transcribed up to the insertion (figure 12). The truncated mRNAs possibly lead to truncated proteins that are partially functional, which indicates that the mutations in the viable *smg7* plants are of a hypomorphic nature.

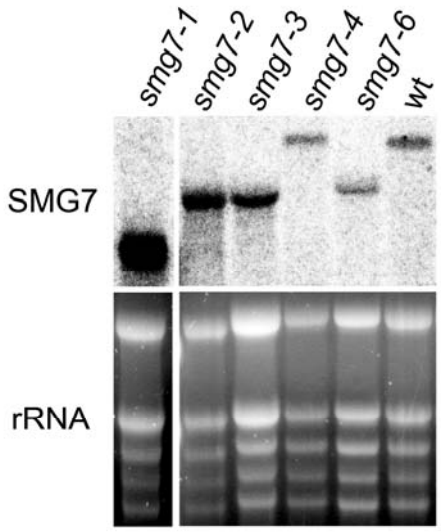

Figure 12. Expression of SMG7 by northern blot analysis of leaves of homozygous SMG7 mutant lines. Radioactively labeled probe corresponding to the 5´end of the SMG7 cDNA was used for hybridization. The rRNA bands of the ethidium bromide gel were used as loading controls.

A range of growth and developmental defects as well as necrotic lesions on leaves can be observed in *smg7-1*, *smg7-2* and *smg7-3* mutants. These plants show dwarfism and slow growth. They produce multiple shoots, which indicates a loss of shoot apical dominance. The inflorescence bolts are weak and slightly bent and they carry only few buds. The leaves are small and serrated and show multiple spots of necrosis.

Interestingly, the position of the T-DNA correlates with the severity of the phenotype. The closer the insertion is located to the 5´end of the gene the more severe the phenotype (figure 11A and 11B). Homozygous plants for the *smg7-1*, *smg7-2* and *smg7-3* allele display complete sterility and show a variety of defects in growth and development. Mutants with the *smg7-6* allele show only a sterility phenotype, and the *smg7-4* allele resembles wild-type. An interesting observation was that although the *smg7-2* T-DNA insertion is located further upstream then the *smg7-3* insertion, *smg7-2* mutant plants appear slightly healthier then in *smg7-3* mutants. For instance, the loss of shoot apical dominance seems to be less severe in *smg7-2*, and although the leaves still show necrotic lesions they are not serrated.

2.1.5 Characterization of *AtSMG7-like* T-DNA insertion lines

In order to gain insights of the function of the *AtSMG7-like* (or *AtSMG7L*) gene, I have obtained and characterized two *Arabidopsis* lines carrying two different T-DNA insertions in the *SMG7L* gene, called *smg7l-1* and *smg7l-2* (figure 13). *Arabidopsis* plants homozygous for either allele were viable and showed no visible defects in plant growth, development or fertility. The T-DNA insertion in the *smg7l-1* allele disrupts the region of the *SMG7L* gene that encodes for the EST1-TPR domain. A similar mutation in the *SMG7* gene (*smg7-5*) causes embryo lethality of the homozygous mutants, indicating that the EST1-TPR domain is vital for the protein function. However, *smg7l-1* mutants are viable and show no visible phenotype. This indicates that SMG7L is not essential and plays a less substantial role in the cell than SMG7.

According to the sequence data obtained through the NCBI (http://www.ncbi.nlm.nih.gov) and TAIR (http://www.arabidopsis.org) databases, alternative splice variants exist for the *SMG7L* gene (figure 13). Alternative splicing is a feature conserved with *SMG7* and suggests that *SMG7L* transcripts might be affected by NMD.

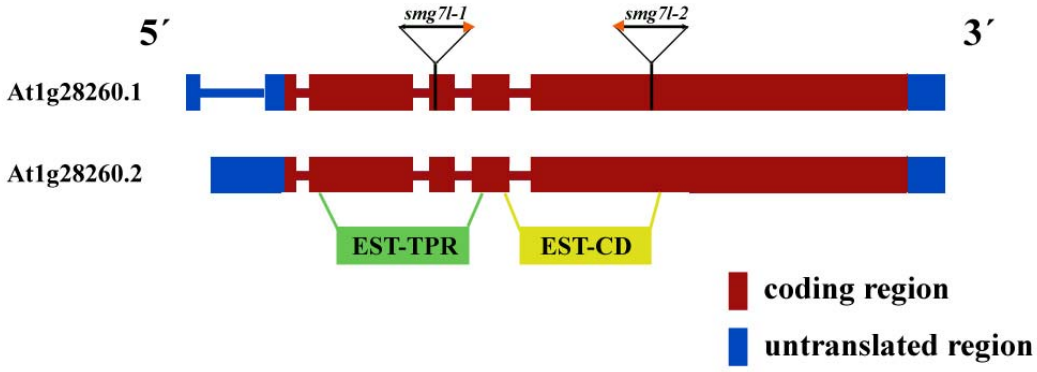

Figure 13. Schematic representation of the *AtSMG7L* gene with *smg7l-1* and *smg7l-2* insertions. Left borders of the insertions are indicated by orange arrowheads.

Since none of the *smg7l* mutant plants showed a visible phenotype I have focused my study on SMG7.

2.2 Generation of complementation lines

2.2.1 Complementation of *smg7-1* and *smg7-5*

2.2.1.1 Complementation of smg7-1 with ACT2::SMG7 and 35S::SMG7

Complementation of observed developmental defects by wild-type cDNA provides valuable evidence linking phenotypes and mutations within the gene. Therefore I generated two constructs containing the wild-type version of the *SMG7* full length cDNA cloned either behind the ACTIN2 or the 35S promoter. Both promoters are constitutively active in *Arabidopsis*. The two constructs were transformed in heterozygous *smg7-1* plants via *Agrobacterium tumefaciens* mediated gene transfer. The obtained T1 plants and the corresponding T2 progeny derived from self-fertilized T1 plants are listed in table 3.

I obtained three T2 plants where all phenotypes, the vegetative defects and the sterility, were completely complemented. Thus I showed that the *SMG7* wild-type cDNA introduced back in the *smg7-1* mutant plants could fully rescue the vegetative and fertility defects. These data suggest that the observed phenotypes in *smg7-1* are linked to the mutation in the *SMG7* gene. Additionally, I obtained in total eleven T2 plants that complemented all the vegetative phenotypes but were still sterile. The sterility was only complemented by the *ACT2:SMG7* construct but not by the construct that contained the 35S promoter. One possible reason for this observation is that the 35S promoter is not transcribed in meiotic cells or only at an insufficient level.

construct	**T1** (***smg7-1*** **+/-**)	**T2** (***smg7-1*** **-/-**)	**phenotype of T2**
35S::*SMG7*	#28	#45, #46, #47, #51	*smg7-1*
	#29	-	-
	#34	#66, #69	no vegetative defects, sterile
	#34	#70, #71	*smg7-1*
	#35	#73	no vegetative defects, sterile

ACT2:*SMG7*	#37	#98	no vegetative defects, sterile
	#39	-	-
	#42	#109, #110	fully complemented
	#44	#114	*smg7-1*
	#45	#115	fully complemented
	#51	-	-
	#52 (*smg7-1* -/-)	#121, #122, #124, #125, #126	no vegetative defects, sterile
	#52 (*smg7-1* -/-)	#123, #127	no vegetative defects, semi-sterile

Table 3. *SMG7* complementation lines.

2.2.1.2 Complementation of smg7-5 with SMG7::SMG7

In a second strategy I complemented the embryo lethal *smg7-5* allele with a construct that contained the whole *SMG7* gene and promoter region. Therefore I PCR-amplified the *SMG7* gene and the promoter and cloned the whole fragment into a pCB302 based binary vector. I transformed the construct into heterozygous *smg7-5* plants via *Agrobacterium tumefaciens* mediated gene transfer. I obtained 14 T1 plants that contained the construct and contained at least one allele of *smg7-5* T-DNA insertion. Two of the T1 plants gave rise to fully complemented *smg7-5* mutant T2 plants after self-fertilization.

2.2.2 Tagging of SMG7 protein with MYC

Generating a tagged version of the *SMG7* cDNA provides a useful tool for biochemical analysis and cytologic studies. Therefore I fused a 12x*MYC* tag to the C-terminal part of *SMG7* by cloning 12 *MYC* repeats in frame behind the *SMG7* cDNA. Using the unique restriction *Sal*I led to a small truncation of 9 amino acids of the full length protein. However since the T-DNA insertion in the *smg7-4* allele leads to truncation of 137aa and does not cause any visible phenotypes I concluded that the lack of 9aa at the C-terminus should not interfere with the protein function. Again both *SMG7* cDNA and

the *ACT2* promoter were cloned as described above. Then I transformed the construct into an *Arabidopsis* wild type suspension culture via *Agrobacterium* mediated gene transfer. An initial protein extraction using a protocol for soluble proteins was unsuccessful and did not yield sufficient amounts of the SMG7 tagged protein for detection (data not shown). A harsher protocol for protein extraction was required, indicating that the SMG7 protein is insoluble. The MYC tagged SMG7 protein was detected with an anti-MYC 9e10 antibody. I could detect a clear signal at the expected size of about 130kDa in the transformed cell suspension. The signal was absent in a cell suspension culture that was transformed with an *ACT2::GUS* control construct (figure 14, cell suspension).

Next, I generated stably transformed *smg7-1* mutant lines that contained the *ACT2::SMG7-MYC* construct. The complemented *smg7-1* mutants showed rescue of the vegetative defects but not of the sterility, indicating that the C-terminal tag or the removal of the last 9 amino acids influences the meiotic function of the SMG7 protein. Protein was extracted using a protocol for insoluble protein extraction and after western blotting, the tagged SMG7 protein was detected by anti-MYC 9e10 antibody in three *ACT2::SMG7-MYC* transformed T2 plants (#45, #49 and #55) at the expected size of ~130kDa. The SMG7 signal was not detectable in protein extracts of wild-type T2 plants that did not contain the construct.

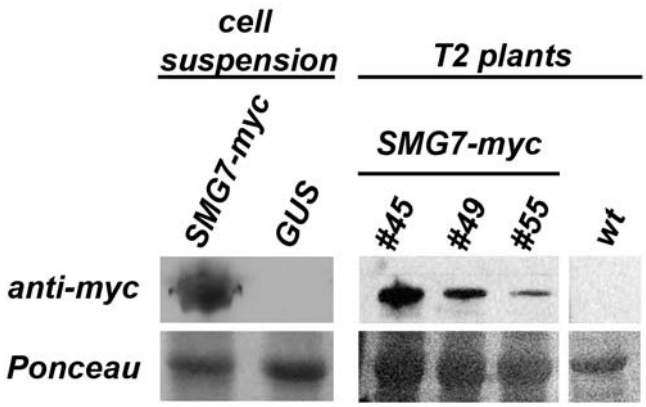

Figure 14. Western blot of transformed leave and cell suspension protein extracts. Anti-MYC (9e10 monoclonal Ig mouse) was used to detect the MYC tagged SMG7 protein. Ponceau staining of the western blots were used as loading control.

2.2.3 Subcellular localization of SMG7

The subcellular localization provides insights into protein function. Therefore I tagged the SMG7 protein with YFP. Using the same cloning strategy as for the *MYC* tagged *SMG7* construct I fused the *YFP* tag in frame to the 3´end of the *SMG7* cDNA. The construct encoded a fusion protein that had a 9aa truncation at the SMG7 C-terminus. I also cloned a control construct that contained the *YFP* tag directly behind the *ACT2* promoter.

I transformed the *ACT2::SMG7-YFP* construct into *smg7-5* heterozygous plants and the *ACT2::YFP* in wild-type plants. Complemented *smg7-5* mutant plants were viable and had no vegetative defects. However as in the case of the *MYC* tag, the complementation of the meiotic defect failed. I analyzed eight different T2 lines derived from self-fertilized T1 plants that were heterozygous for the *smg7-5* allele and contained the construct. Cytological preparations of the inflorescences in all eight T2 lines showed that SMG7-YFP signal concentrates in cytoplasmic foci (figure 15, SMG7-YFP). Since T2 plants of the *ACT2::YFP* control line showed diffuse YFP signal in the cytoplasm and the nucleus (figure 15, YFP) I concluded that the YFP tagged SMG7 signal in the cytoplasmic foci is SMG7 specific.

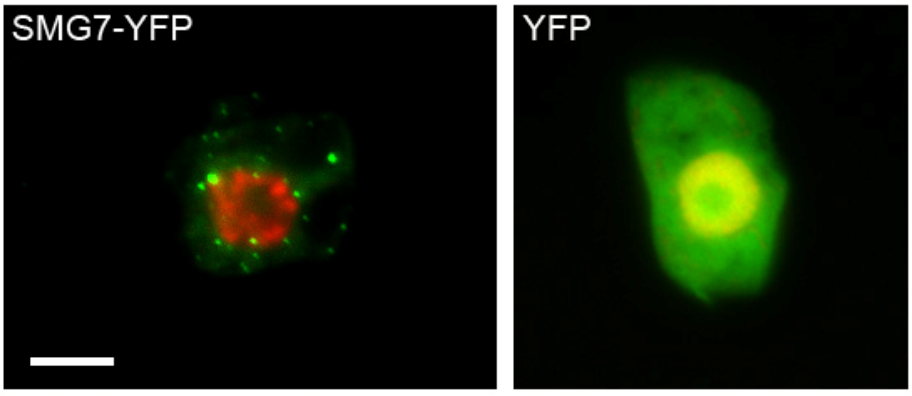

Figure 15. Subcellular localization of SMG7. YFP signal is shown in green. DNA is stained with DAPI (shown in red). Scale bar = 5µm.

The subcellular localization of the *Arabidopsis* SMG7 protein is consistent with data obtained from hSMG7 which has been shown to localize to P-bodies (Unterholzner and Izaurralde 2004). P-bodies are sites of mRNA degradation and are observed as cytoplasmic foci that are characterized by the co-localization of proteins of the mRNA deadenylation and degradation machinery such as DCP2, DCP1, and the exosome

(reviewed in Eulalio, Behm-Ansmant et al. 2007). It would be interesting to further test the co-localization of the *Arabidopsis* SMG7 protein with P-body marker proteins in order to clarify the nature of the cytoplasmic foci.

2.3 SMG7 is required for the Nonsense Mediated RNA decay

Animal and human SMG7 homologues are implicated in the nonsense-mediated RNA decay (NMD) pathway, which ensures the degradation of transcripts containing premature termination codons (PTC). Therefore I asked whether the *Arabidopsis* SMG7 protein has a function in NMD.

2.3.1 Upregulation of +PTC transcripts in *smg7* mutants

To test if the *Arabidopsis* SMG7 protein plays a conserved role in NMD I measured the abundance of naturally occurring transcripts containing premature stop codons (PTCs) in *smg7* mutants compared to wild-type plants. These naturally occurring PTC transcripts arise due to alternative splicing and have previously been described as natural NMD targets (Hori and Watanabe 2005) (figure 16). Total RNA extracts of wild type and *smg7-1* flowers and leaves were used for RT-PCR analysis with primers that can amplify both the normal (-PTC) and the nonsense transcript (+PTC) of the At5g62760, the At1g51340 and the At2g45670 gene.

The splice variants were distinguished by the size of the RT-PCR products and quantified. The +PTC/-PTC ratio was estimated for each individual sample. Since the splicing variants would only differ between 14-56bp I measured the cDNA levels using two different approaches.

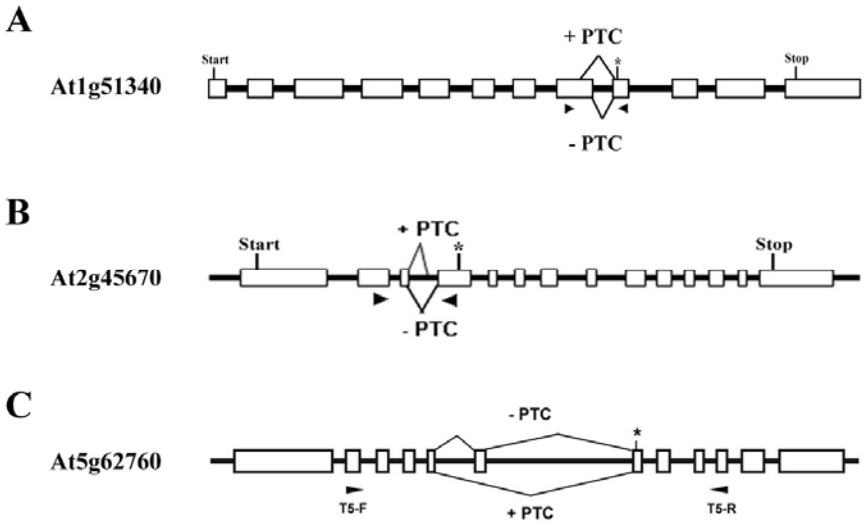

Figure 16. Alternative splicing of mRNAs derived from (A) the At1g51340, (B) the At2g45670 and (C) the At5g62760 locus. One splice variant contains a PTC (indicated by asterisks). Primers flanking the alternative splice site can amplify both transcripts in one reaction.

First, I directly sequenced the RT-PCR products of all three loci as described by Hori and colleagues (Hori and Watanabe 2005). The direct sequencing approach is based on the conclusion that higher or lower peaks in the sequencing chromatograms correspond proportionally to the relative amount of transcript fractions of the sequenced sample. Three independent plant samples were subjected to RT-PCR. The products were directly sequenced and the individual sequence peaks of the raw sequencing data, corresponding to the normal or the +PTC transcript were distinguished (figure 17). The peak heights were quantified and +PTC/-PTC ratios were calculated of each base pair. The average and standard deviation of all ratios were calculated and statistically evaluated (table 4). With this method I could detect a significant increase of the +PTC transcripts of At2g45670 and At1g51340 and a slight increase of the PTC-containing transcript corresponding to the At5g62760 locus in *smg7-1* mutants compared to wild type plants.

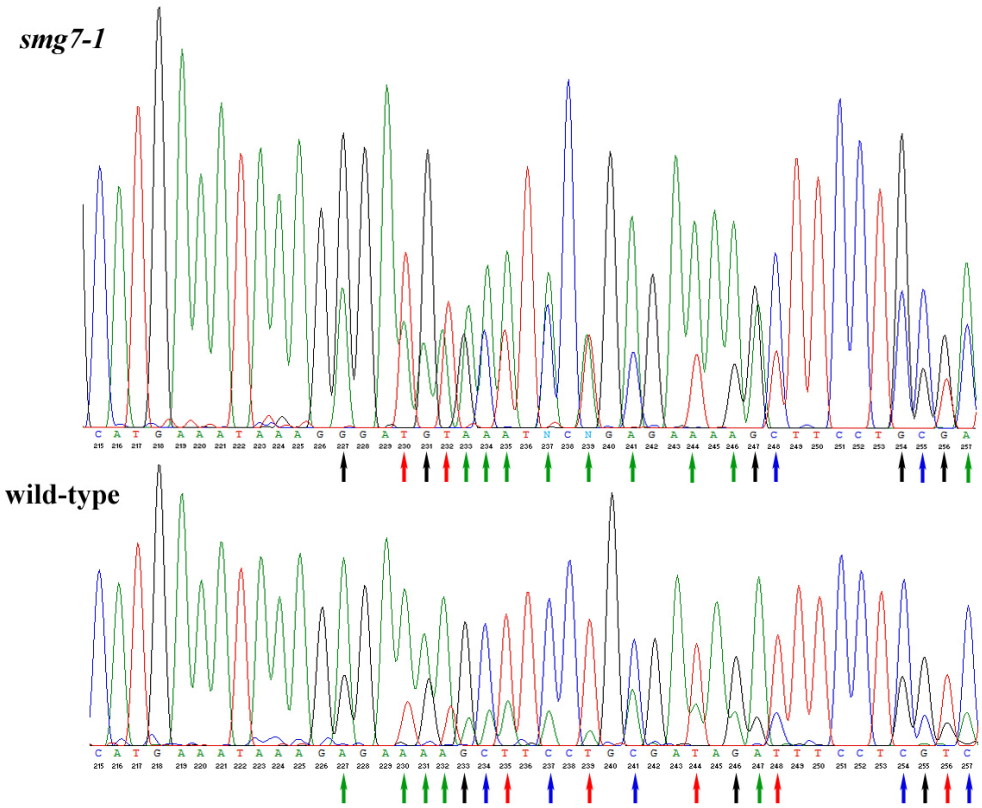

Figure 17. Raw sequence chromatogram of wild-type and *smg7-1* RT-PCR products derived from the At2g45670 locus. Arrows indicate the bases that differ in +PTC and +PTC transcripts.

Locus	Wild-type*	*smg7-1*	P**
At5g62760	1.92 ± 0.53 (n=12)	4.05 ± 0.99 (n=12)	
	1.42 ± 0.41 (n=12)	2.77 ± 0.82 (n=12)	0.061
		2.98 ± 0.88 (n=12)	
At2g45670	0.29±0.13 (n=15)	1.99±0.74 (n=15)	
	0.37±0.17 (n=15)	1.53±0.94 (n=15)	0.004
	0.26±0.15 (n=15)		
At1g51340	0.26±0.13 (n=17)	0.49±0.24 (n=17)	
	0.24±0.13 (n=17)	0.42±0.21 (n=17)	0.006
	0.21±0.11 (n=17)		

Table 4. Quantification of +PTC/-PTC ratio determined by direct sequencing. For each category, samples from two or three independent plants were quantified. *Values represent the average ratio of +PTC to -PTC transcripts. ± = standard deviation. n = number of quantified nucleotide positions for each transcript. **P indicates significance of the difference between wild-type and *smg7-1* mutants. Statistic evaluation was performed with repeated measures ANOVA.

In a second approach I separated the splice variants via gel electrophoresis. RT-PCR products derived from the At5g62760 locus showed the largest size difference, 56bp. Therefore I separated the products over a 3.5% agarose gel and performed southern blot analysis (figure 18). Five individual *smg7-1* homozygous plants showed upregulated levels of +PTC mRNAs (+PTC/-PTC ratio = 1.58±0.27) compared to the +PTC levels measured in five wild-type plants (+PTC/-PTC ratio = 1.05±0.05). Therefore this data confirms the results obtained by direct sequencing and shows a slight but statistically significant increase in the level of +PTC transcript derived from the At5g62760 locus.

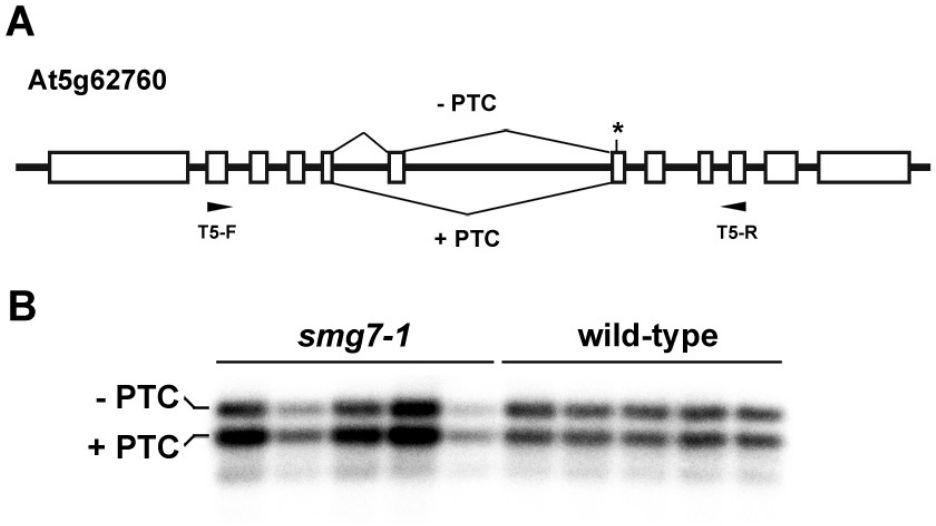

Figure 18. (A) Alternative splicing of the mRNA, derived from the At5g62760 locus, can yield a transcript containing a PTC (indicated by asterisk) (+PTC) besides the normal transcript (-PTC). Primer binding sites are indicated with arrows. (B) Southern blot analysis of the RT-PCR products.

The splice variants corresponding to the At2g45670 locus differ by 14bp and were separated by nondenaturating polyacrylamide gel electrophoresis (PAGE). Samples from four to five individual *smg7-1* and wild-type plants were analyzed. In all *smg7-1* mutants the +PTC transcripts were clearly elevated compared to wild-type (figure 19). Taken together I showed that +PTC transcripts are significantly increased in *smg7-1*.

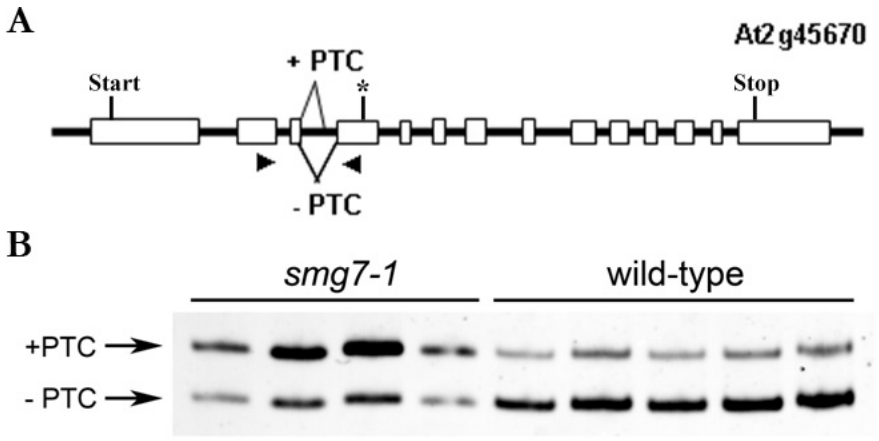

Figure 19. (A) Alternative splicing of At5g62760 leads to production of +PTC (premature stop codon is indicated by asterisk) and –PTC transcripts. Primer binding sites are indicated with arrows. (B) RT-PCR products were separated over a nondenaturating polyacrylamide gel.

2.3.2 Analysis of +PTC transcripts stability

Smg7-1 mutants showed a higher abundance of endogenous +PTC transcripts than normal transcripts compared to wild-type. However a higher abundance of aberrant splice products can occur not only from a defect in NMD but also from failures in the splicing machinery. To address if these transcripts are elevated due to an impaired degradation mechanism, I compared the stability of the PTC containing splice variant with the stability of the –PTC mRNA after in vivo inhibition of RNA Polymerase II transcription by cordycepin.

PTC containing transcripts are constantly produced. Therefore residual signals from the +PTC transcripts were detectable at the steady-state level even in wild-type samples (figure 19, wild-type +PTC transcripts). After inhibition of transcription, the remaining +PTC transcripts should become rapidly degraded by the NMD machinery and should not be detectable anymore in a wild-type situation. However, if the degradation machinery was impaired, nonsense transcripts would remain stable and detectable via RT-PCR.

In order to test the stability of the splice variants I treated *smg7-1* and wild-type leaves with cordycepin, an inhibitor of transcription. RNA was extracted at the following time points after treating leaves with cordycepin: 0h, 1h, 2h and 4h (figure 20A). The extracted RNA was used for RT-PCR, + and – PTC products were separated by

nondenaturating PAGE as shown in figure 19. In wild-type leaves +PTC transcripts were not detected 1 hour after cordycepin treatment , due to the active degradation via the NMD machinery, while the –PTC transcript remained stable even 4 hours after inhibition of transcription (figure 20B). These data demonstrate that the higher levels of nonsense transcripts that were detected in *smg7-1* mutants are indeed due to an impaired mRNA quality control or degradation machinery.

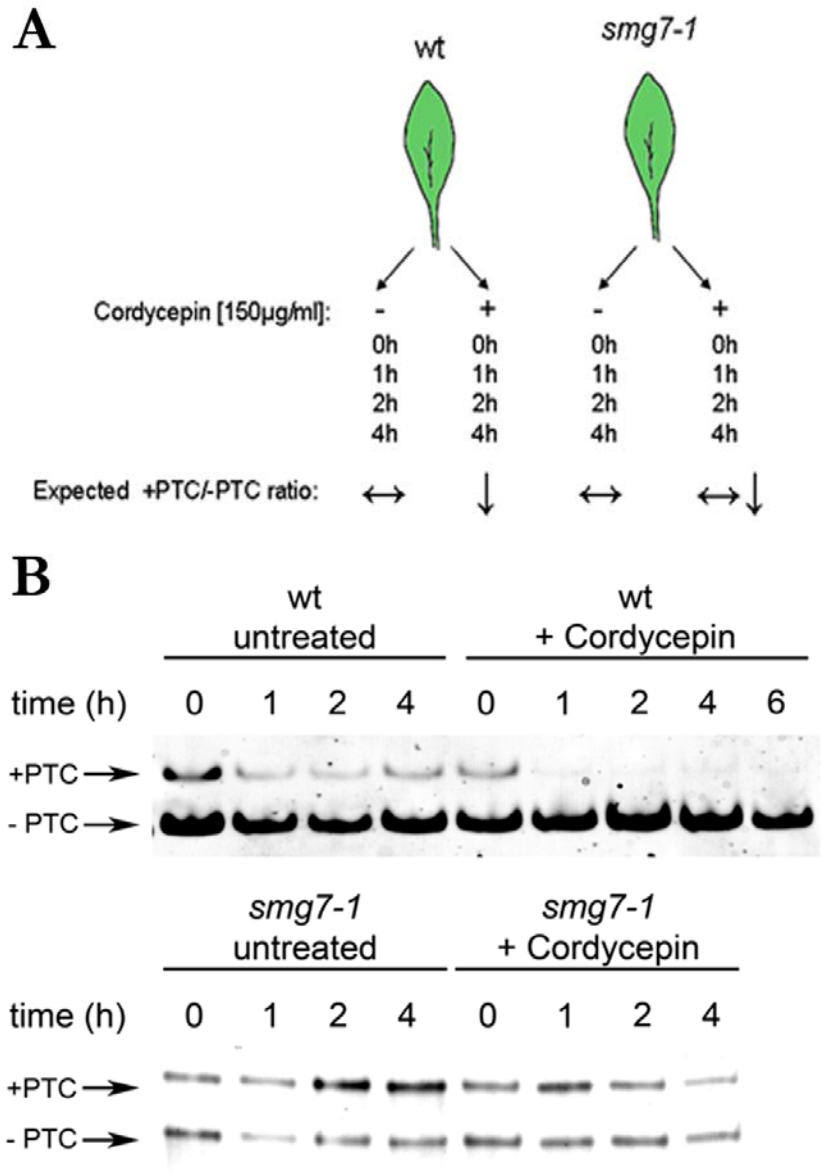

Figure 20. Stability of +PTC transcripts in *smg7* and wild-type leaves. (A) Cordycepin treatment was carried out as indicated. (B) RT-PCR products from each time point were analyzed over a nondenaturating polyacrylamide gel and stained with Sybr Green.

2.3.3 Translation dependent stabilization of +PTC transcripts

NMD targets are recognized in a pioneer round of translation (Ishigaki, Li et al. 2001). I asked whether the +PTC transcript derived from the At2g45670 locus is subjected to NMD and tested whether its stabilization is dependent on translation. Therefore I treated *smg7-1* and wild-type leaves with cycloheximide (figure 21A). This drug has been shown to block translation through inhibiting translation elongation. RNA was extracted and again used for RT-PCR analysis as described previously. A significant stabilization of the +PTC transcript was observed after 6 hours of drug treatment in wild-type leaves (figure 21B) and was comparable to the level of +PTC in *smg7-1* mutants. These data show that SMG7 is important for the downregulation of PTC-containing mRNAs and indicates that the SMG7 protein contributes to NMD in plants.

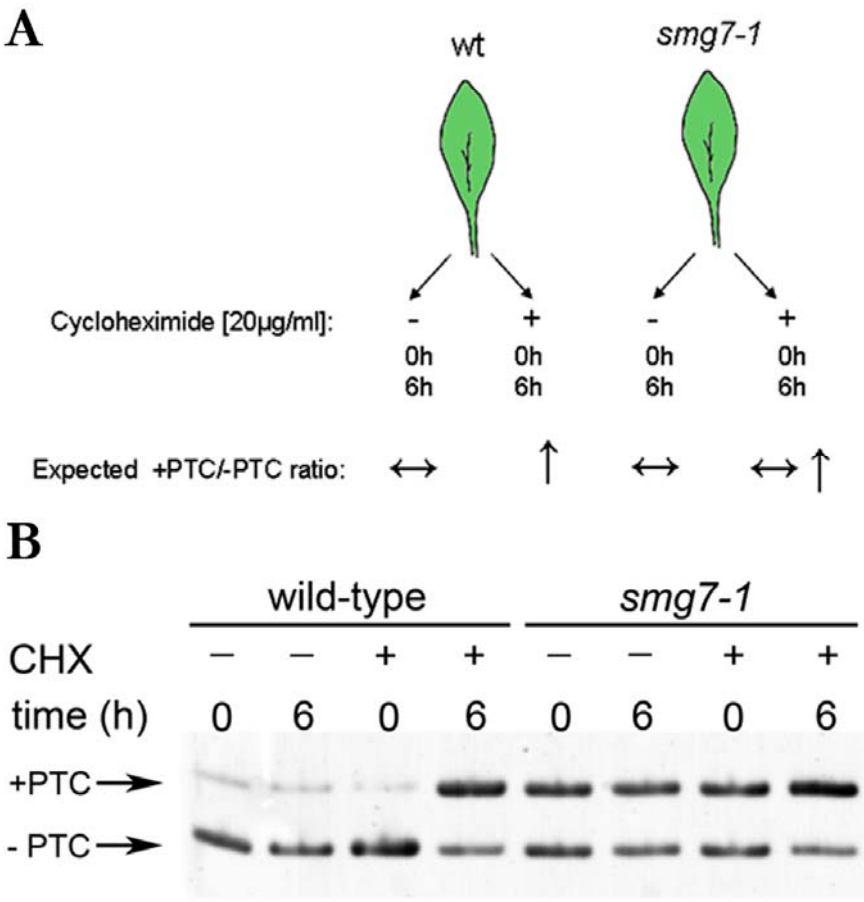

Figure 21. The stability of +PTC transcript derived from the At2g45670 locus depends on translation. (A) Experimental set up of the Cycloheximide treatment. (B) The splice variants were separated over nondenaturating polyacrylamide gel electrophoresis.

2.3.4 NMD defects in *smg7* alleles

My results showed that the degradation of the +PTC transcript of the At2g45670 locus, a naturally occurring NMD target, is impaired in *smg7-1*. I next asked if the other T-DNA insertion lines showed a defect in NMD and whether I can relate the defect with the position of the T-DNA insertion. I extracted RNA of homozygous mutants plants of all T-DNA insertion lines and wild-type and tested them for the abundance of the +PTC transcript compared to the –PTC transcripts (figure 22). Interestingly, I found a correlation of the vegetative pathogen response phenotype with the defect in NMD. The *smg7-1*, *smg7-2* and *smg7-3* mutants showed upregulation of the +PTC transcripts, whereas neither *smg7-4*, with a wild type phenotype, nor *smg7-6* mutation, which only causes sterility, show a defect in NMD.

Additionally I analyzed a T-DNA insertion line of SMG7L, the second EST1 domain containing protein in *Arabidopsis thaliana*. The +PTC transcript was slightly higher in *smg7like-1* mutants compared to wild-type but significantly lower than in *smg7-1*, indicating that SMG7L might only play a marginal role in NMD.

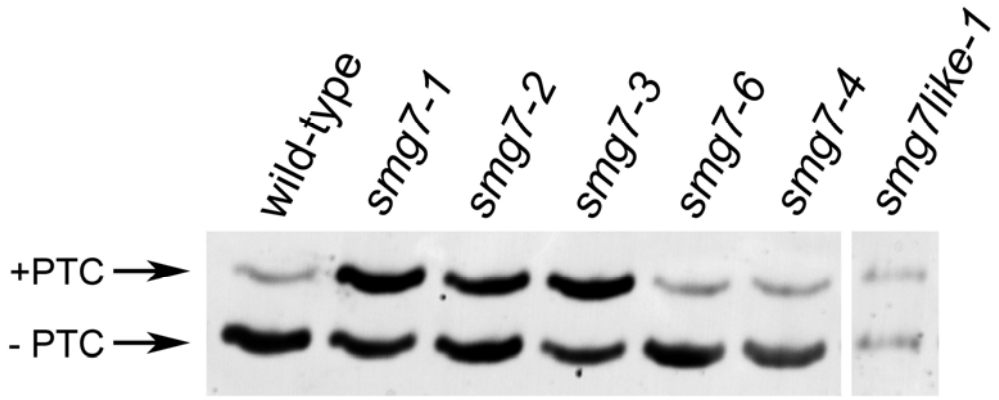

Figure 22. RT-PCR of the At2g45670 derived transcripts analyzed in a *smg7* mutant allelic series.

2.4 SMG7 is essential for exit from meiosis

So far I have shown that *Arabidopsis* SMG7 is an evolutionary conserved protein and plays a conserved function in NMD. *Smg7* T-DNA insertion lines display a wide range of vegetative defects and mutant plants are sterile. Up to now no other NMD factor has been shown to play a role in biological processes outside of NMD. Therefore investigation of the underlying cause of the sterility should give hints to the biological function of SMG7 within an organismal context.

2.4.1 Investigation of *smg7* gametogenesis

2.4.1.1 Investigation of smg7 microgametogenesis

Except for *smg7-4,* all *smg7* mutant lines do not produce seeds. I aimed to examine the cause of the sterility by investigating male gametogenesis. Therefore I stained anthers with Alexander´s stain which differentiates between viable and non-viable pollen (Alexander 1969). Viable pollen stained purple, while aborted pollen turned green. As shown in figure 23, *smg7-1* anthers contained only a few non-viable pollen, indicating that a severe defect in *smg7* male gametogenesis leads to abortion of the gametes.

Figure 23. Alexander staining of viable and non-viable wild-type and *smg7-1* pollen (Size bar = 0.1mm).

Smg7-6 mutant plants are also sterile but do not show any vegetative defect, indicating that s*mg7-6* is a separation of function mutation. Alexander staining of *smg7-6* anthers revealed a few viable pollen, indicating that the defect in gametogenesis is less severe in *smg7-6* compared to *smg7-1* (figure 24). These data indicate that SMG7 deficiency leads to the abortion of male gametogenesis.

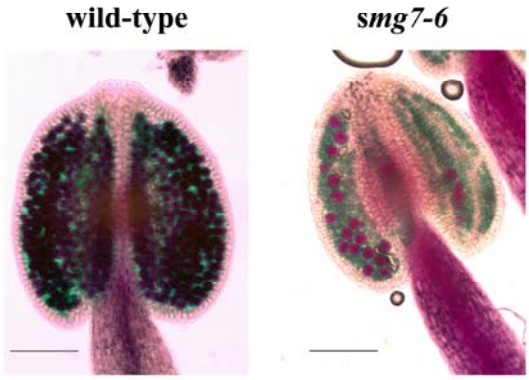

Figure 24. Alexander staining of wild-type and *smg7-6* anthers (Size bar = 0.1mm).

2.4.1.2 Investigation of macrogametogenesis

Some meiotic genes, for instance KATA/ATK1, show gender-specific functions (Chen, Marcus et al. 2002). Male gametogenesis of s*mg7-1* mutants is impaired. To analyze whether female gametogenesis is affected in the same manner, I fertilized *smg7-1* ovules with wild-type pollen and counted the number of seeds that were produced. In a control experiment I crossed wild-type plants. The wild-type cross yielded 25.3±9 (n=12) seeds per silique. In *smg7-1* I only obtained 1.7±1.9 (n=15) seeds, indicating that female fertility is dramatically decreased (~7%) but not completely abolished as is the case for pollen.

Furthermore, female fertility is also less affected in *smg7-6* compared to *smg7-1*. In a backcross using *smg7-6* ovules and wild-type pollen I obtained 13.48±4.06 (n=36) seeds per silique.

Complete male sterility and a severe reduction in the female fertility hint towards a severe defect in the *smg7* gamete formation. To investigate at which stage of gametogenesis the SMG7 protein becomes crucial I examined gametogenesis and, in particular, meiosis more carefully.

2.4.2 Introduction to meiosis

Meiosis is a specialized cell division that allows one diploid cell to produce four haploid gametes. During cell division, the most visible changes happen when the nuclei divide during M phase. In contrast to mitosis where in one M phase the sister

chromatids separate (figure 25A), in meiosis two subsequent M phases lead to the reduction of the chromosome number and results in haploid cells (figure 25B).

A mitotic M phase is usually divided into six stages: In prophase, chromosomes condense and the spindle assembles, which can then attach to the kinetochores of the chromosomes during prometaphase which occurs following nuclear envelope breakdown. In metaphase the chromosomes align at the equator of the spindle. After all chromosomes are properly attached to the spindle they are pulled apart during anaphase. During telophase the chromatids detach from the spindle, decondense and the nuclear envelope reassembles. Finally, the cytoplasm is seperated during cytokineses.

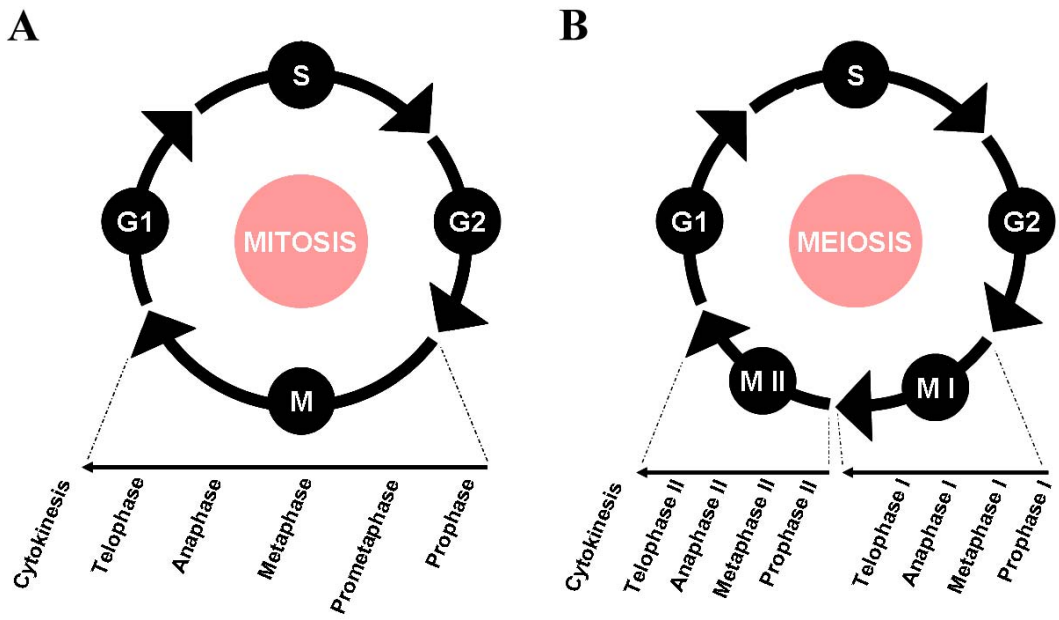

Figure 25. The phases of the mitotic (A) and meiotic (B) cell cycle. DNA is replicated during S phase. The gap phases (G1 and G2) allow the cell to grow and prepare the cell for the following stages. The mitotic M phase is sectioned into five nuclear divisions (Prophase, Prometaphase, Metaphase, Anaphase, Telophase) followed by cytoplasmic division (cytokineses). In meiosis two adjacent M phases follow the meiotic interphase. The figure does not represent the time duration of the individual stages.

The M phase of the first meiotic nuclear division (M I) differs from mitosis as homologous chromosomes and not sister chromatids segregate. To achieve this, the homologous chromosomes need to find each other and synapse. Then they exchange chromatid strands via homologues recombination. Following loss of sisterchromatid cohesion, which occurs only in the chromosome arms, they segregate to opposite spindle poles. During the second division the preserved cohesion at the centromeres is

removed at the metaphase II / anaphase II transition and the sister chromatids separate in a similar manner as in mitosis (figure 26). Not surprisingly while many mitotic factors are used to govern the second meiotic division, meiosis I requires many novel meiosis specific proteins to specify that homologues chromosomes recombine and divide (reviewed in Marston and Amon 2004).

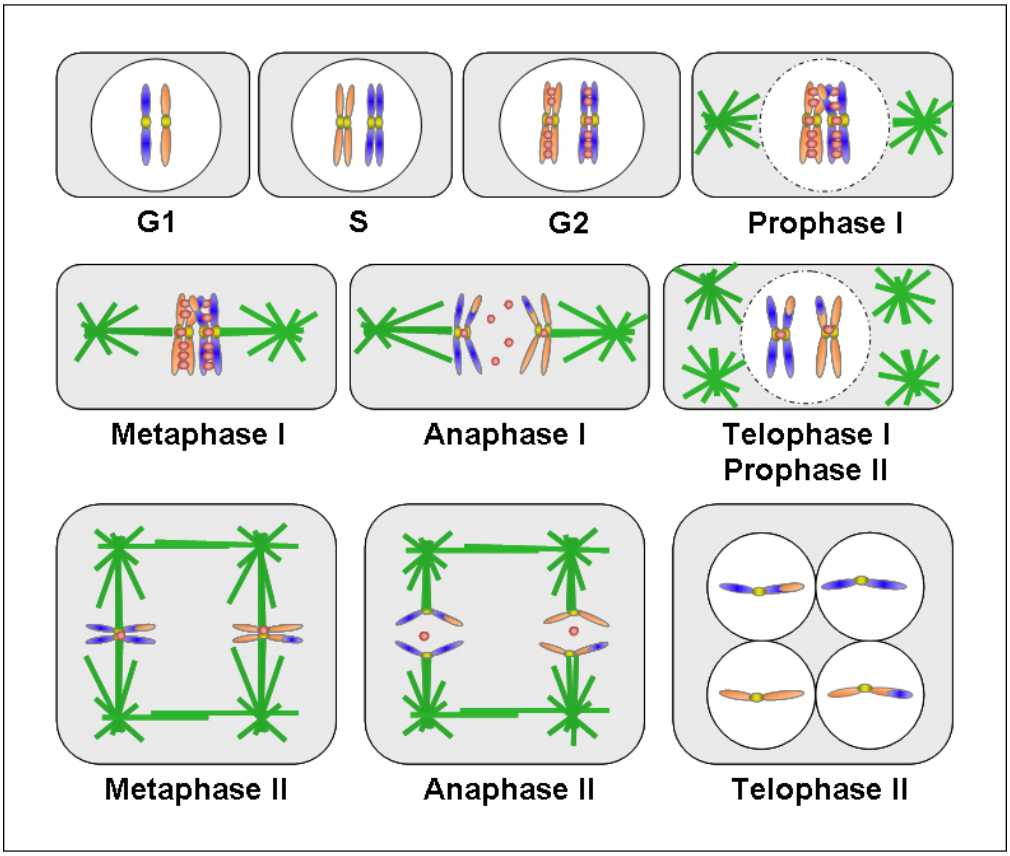

Figure 26. A schematic overview of the meiotic cell cycle is presented. Only one pair of homologous chromosomes is shown for simplicity. Homologous chromosomes, one from each parent, are depicted in orange and blue.

2.4.3 Analysis of smg7

Hypomorphic *smg7* mutant plants do not produce viable pollen. In order to understand the cause of the sterility I investigated meiosis.

2.4.3.1 Meiosis in SMG7 deficient pollen mother cells

Pollen mother cells are the precursor cells for the pollen sperm cells and the cells where male meiosis takes place. In order to investigate the meiotic cell cycle I

dissected anthers of the appropriate stages and cytologically examined the pollen mother cells (PMCs) (figure 27).

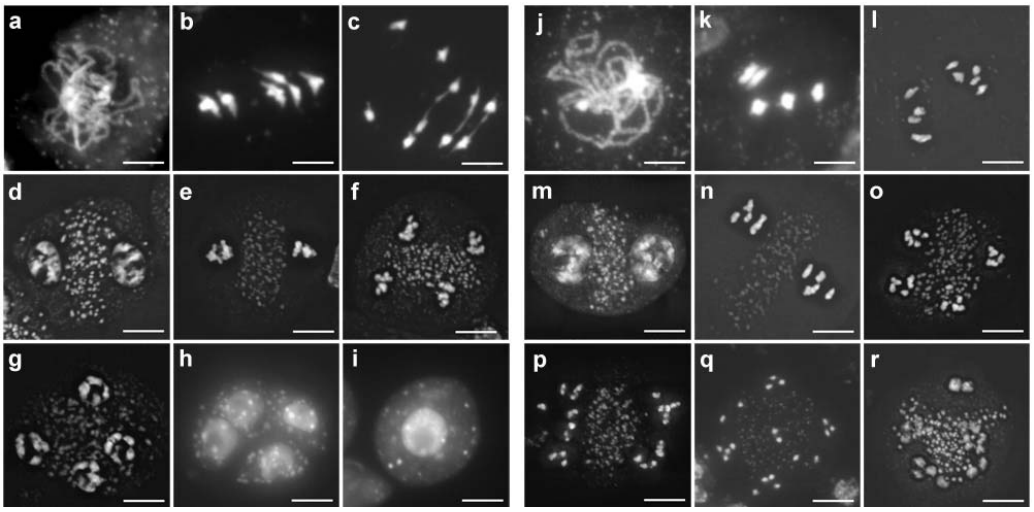

Figure 27. Meiosis in pollen mother cells (PMCs) of wild-type (a-i) and *smg7-1* (j-t) plants. Meiosis progresses normally through pachytene (a,j), metaphase I (b,k), anaphase I (c,l), telophase I (d,m), metaphase II (e,n). In wild-type anaphase II (f) is followed by telophase II (g) where chromosomes start to decondense and four haploid nuclei form. Cytokinesis follows and gives rise to tetrads (h) and microspores (i). In *smg7-1* mutants anaphase II like stages (o) are rarely observed. Chromosomes fail to decondense and scatter through the cell in an irregular anaphase II (p) and scattered chromatids (q) stage. Whereas PMCs shown in a-c and j-l were fixed in ethanol:acetic acid (3:1,v/v), the PMCs of later meiotic stages were fixed in 4% paraformaldehyde to preserve the 3D organization of the chromosomes. DNA is stained with DAPI. Scale bars: 5µm.

The progression of meiosis in wild-type pollen mother cells is shown in figure 27a-i. The first meiotic division (figure 27a-d) is characterized by the separation of the homologous chromosomes. During an extended prophase I, homologous chromosomes become synapsed and exchange chromatids via homologues recombination. Full synapsis is reached at the pachytene stage (figure 27a). Shortening and condensation of the chromosomes leads to the formation of five (*Arabidopsis thaliana* 2n=10) clearly distinguishably bivalents that are held together by chiasmata. The bivalents reach the state of the highest condensation at metaphase I (figure 27b) and align via attachment to the spindle at the metaphase plate. The homologous chromosomes become separated in anaphase I (figure 27c). The separated chromosomes decondense and form two nuclei at the telophase I stage (figure 27d). During the second meiotic division (figure 27e-g) the sister chromatids divide. At the metaphase II stage (figure 27e) chromosomes become highly condensed and align at the metaphase plate. The sister chromatids segregate to the opposite spindle poles in anaphase II (figure 27f). Four haploid nuclei with slightly decondensed chromatids form at the telophase II stage

(figure 27g). Chromatids become further decondensed and cytokinesis divides the cytoplasm at both axes simultaneously (figure 27h). The four fully separated microspores (figure 27i) will give rise to the four male gametophytes. For a more detailed description of meiosis in wild-type *Arabidopsis* see (Ross, Fransz et al. 1996; Armstrong and Jones 2003).

In *smg7* PMCs the first meiotic division completed normally resulting in the proper separation of the homologous chromosomes (figure 27j-m). Yet, *smg7* meiocytes showed aberrant progression through the second meiotic division (figure 27n-r). Although normal metaphase II (figure 27n) and sometimes normal anaphase II (figure 27o) stages were observed, regular telophase II or tetrad stages were never detected. However, very frequently, PMCs containing abnormally condensed and separated chromatids were found. Some meiocytes showed two clusters of separated chromatids that were still residing on opposite sides of the organelle band, reflecting an irregular anaphase II stage (figure 27p). In most of the abnormal meiocytes, chromatids were distributed randomly in a "scattered chromatids" stage throughout the cell (figure 27q). Some chromatids would slightly decondense and aggregate (figure 27r) to form polyads.

The fact that no single telophase II stage was found in *smg7* mutants indicates that the *smg7* meiocytes have a severe defect in anaphase II. Thus SMG7 is absolutely essential to progress through anaphase II and for exit from meiosis.

2.4.3.2 Meiosis in SMG7 deficient embryo-sac mother cells

Smg7-1 pollen mother cells fail to progress through anaphase II. To test whether female meiosis is affected in a similar manner, I investigated meiosis in embryo-sac mother cells (EMC), where female meiosis takes place and leads to the formation of the female haploid gametophyte. In contrast to wild-type telophase II where four nuclei are visible, *smg7* EMCs contained condensed chromatids that were distributed unequally in the cell (figure 28). I never detected similar cells in wild type plants. Thus the defect in female meiosis is similar to the anaphase II arrest observed in pollen mother cells, indicating that SMG7 is essential for the transition of anaphase II to telophase II in both male and female meiosis.

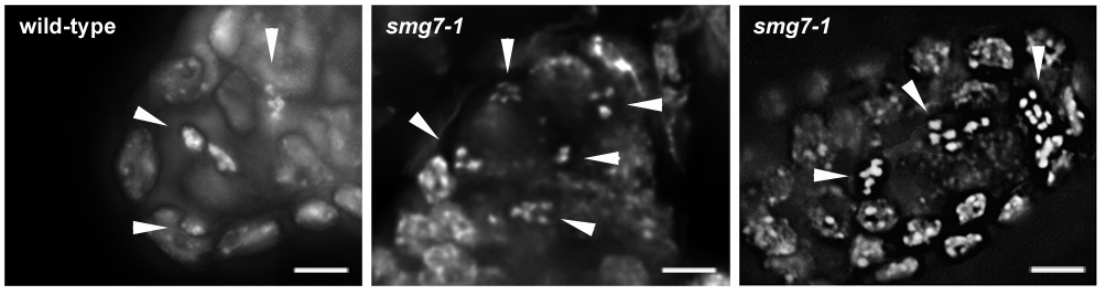

Figure 28. Macrogametogenesis of wild-type and *smg7-1* plants. White arrows highlight chromatids belonging to the embryo-sac mother cell (EMC). DNA is stained with DAPI. Size bar =5µm.

2.4.4 Mitosis progresses normally in *smg7* mutants

During the second meiotic division, sister chromatids separate in a manner similar to separation during mitosis. Therefore many mutants that affect the second meiotic division are also defective in mitosis. The *smg7-1*, *smg7-2* and *smg7-3* mutant plants show severe growth defects. A delay in mitosis or in cell proliferation could be an explanation for why the growth in *smg7* is inhibited. Therefore I tested whether there is a delay or arrest in the mitotic M phase in *smg7* mutants. If the progression through mitotic anaphase is slowed down, I would expect an increase in the frequency of anaphase cells in *smg7* mutants.

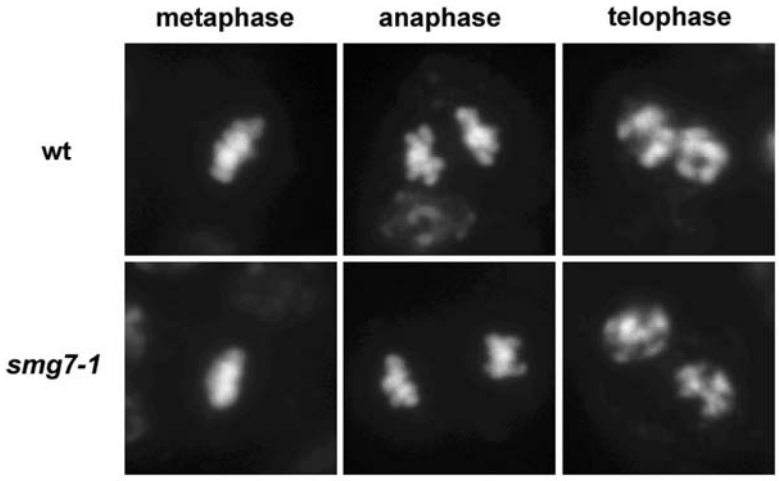

Figure 29. Pictures represent metaphase, anaphase and telophase in wild-type and s*mg7-1* mitosis in floral tissue. DNA is stained with DAPI.

I cytologically examined floral bud tissue and counted the abundance of metaphases (M), anaphases (A) and telophases (T) (figure 29). I then calculated the proportion of cells in M, A and T in *smg7-1* and compared it to wild type. As shown in table 5, I

could not detect a difference in the relative distribution of M, A and T in *smg7-1* compared to wild-type plants. This observation suggests that SMG7 is specifically required for meiosis and that SMG7 deficiency does not disrupt mitotic progression.

	Metaphase		**Anaphase**		**Telophase**		**Total**
	n	%	n	%	n	%	**n**
wt	168	39,6	213	50,2	43	10,2	424
smg7-1	218	41,8	252	48,4	51	9,8	521

Table 5. Mitotic index of metaphase, anaphase and telophase in wild-type and *smg7-1*.

Anaphase failures, like we see in *smg7* meiocytes, have not been described very often in the literature. In order to elaborate the possible mechanisms behind the SMG7 function in meiosis, I will briefly introduce the basic principles of meiotic cell cycle regulation in the following chapter.

2.4.5 Regulation of the meiotic cell cycle

During each cell division, chromosomes have to undergo tremendous changes. It is very important that these changes occur in a precise order and that they have to follow a tight schedule to ensure that each process happens only at the appropriate time point. Key players of the control system that coordinates the cell cycle are cyclins and cyclin-dependent kinases (CDK). The oscillating activity of certain cyclin-CDK complexes drives the cell cycle through the different cell cycle stages.

Disassembly of the spindle, chromosome decondensation and nuclear envelope reorganization are key events during the mitotic or meiotic exit. Here, additional factors are needed since CDK activity alone can only lead the cell as far as metaphase but not beyond. To successfully complete mitosis or meiosis, two main mechanisms need to occur: the CDK substrates need to become either dephosphorylated by phosphatases, and thus inactivated, or destroyed via the anaphase promoting complex (APC) (reviewed in Sullivan and Morgan 2007).

2.4.5.1 Cyclins and CDK

The oscillating activities of the different CDKs are regulated at the protein level for cyclins and by phosphorylation of the cyclin-CDK complexes. During M phase, the expression of A- and B-type cyclins peaks. Whereas cyclin A expression starts already at S phase, cyclin B levels start to rise in G2. The cyclin A-CDK complex contributes to chromosome condensation and nuclear envelope breakdown and is inactivated via cyclin A degradation prior to metaphase. Cyclin B-CDK acts together with cyclin A-CDK to complete chromosome condensation but is additionally needed to fulfill many M phase specific tasks, such as promoting spindle assembly until it becomes destroyed in metaphase (figure 30).

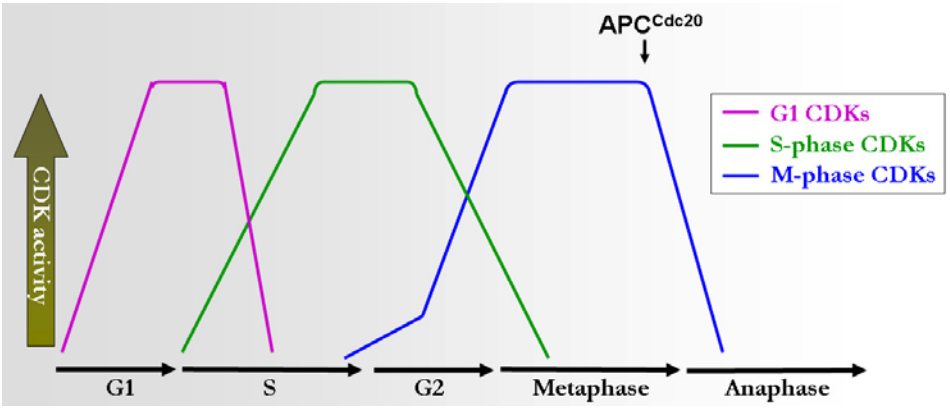

Figure 30. Levels of CDK activity during mitosis. The picture is adapted from Marston and Amon 2004.

The same basic principle also applies for the two meiotic M phases, but it is crucial that both M phase cyclins do not become completely destroyed during interkinesis in order to prevent the cell from entering another S phase (figure 31).

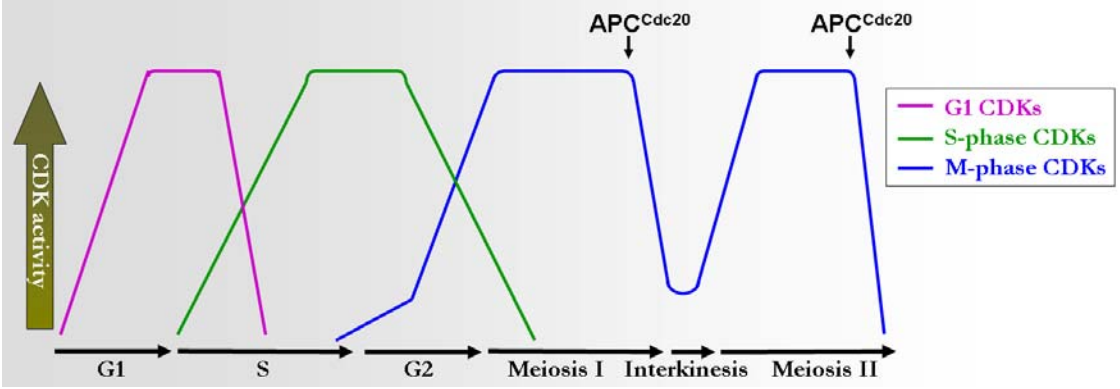

Figure 31. Activity of various CDKs oscillates during meiosis. The picture is adapted from Marston and Amon 2004.

2.4.5.2 The anaphase promoting complex (APC)

Besides cyclin-CDK complexes the activity of another key player, the so called anaphase promoting complex (APC), is crucial for cell cycle progression. The APC is essential for cell proliferation in all eukaryotes. It is a large protein complex, consisting of more than twelve subunits. The APC functions as an E3 ubiquitin ligase which covalently links polyubiquitin chains to substrate proteins leading to their destruction via the 26S proteasome. To ensure that APC degrades the right target at the right time, its enzymatic activity and substrate recognition is tightly regulated throughout the cell cycle.

The APC depends on cofactors to recognize its targets. The two major co-factors are Cdc20 and Cdh1. Cdc20 and APC form the APC^{Cdc20} complex which can then recognize and ubiquinate various targets at metaphase. The D- or KEN-box is a typical feature of APC substrates that can be recognized via the WD40 domain of the APC cofactors. One of the two most important substrates is securin, which is an inhibitor of separase. Cohesin is a ring shaped complex which holds sister chromatids together. In order to release this connection and separate the sister chromatids, separase can cleave a subunit of the cohesin complex and thus promote anaphase. During the first meiotic division, cohesin at the centromeric regions must be preserved. Sgo1 (also known as Shugoshin) binds to centromeric cohesion and protects it from cleavage.

Other important substrates of APC^{Cdc20} are the B-type cyclins. Proteolysis of B-type cyclins leads to CDK inactivation and thus to exit from M phase (figure 32). The APC^{Cdh1} complex is active in late M phase and keeps CDK activity low until the subsequent S phase (figure 32, reviewed in Peters 2006).

During meiosis the APC is activated in similar manner during both metaphase/anaphase transitions and in addition it needs to be kept inactive in between the two meiotic divisions. Thus additional factors are required to regulate the APC during meiosis. In several organisms meiosis specific APC regulators have been described (reviewed in Irniger 2006). In budding yeast Mnd2 inhibits APC activation in prophase I to prevent premature sister chromatid separation (Oelschlaegel, Schwickart et al. 2005; Penkner, Prinz et al. 2005). In fission yeast MES1 inhibits

complete destruction of cyclin B during anaphase I (Izawa, Goto et al. 2005). In higher eukaryotes, oocytes arrest in metaphase II, due to the activity of cytostatic factor (CSF), in order to prevent development without fertilization, also called parthogenesis. XErp1 has been identified as an important inhibitor of APC and is needed to maintain the metaphase II arrest (Schmidt, Duncan et al. 2005; Tung, Hansen et al. 2005).

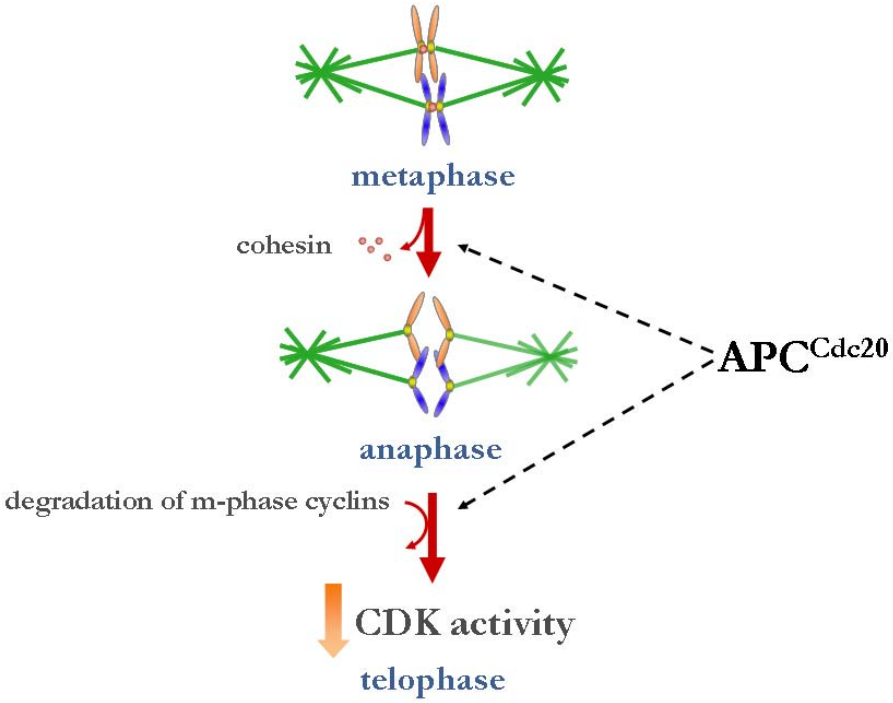

Figure 32. APC^{Cdc20} activity is required for mitotic and meiotic exit.

2.4.5.3 Phosphatases dephosphorylate CDK substrates

Downregulation of CDK activity alone is not sufficient to exit from M phase. Phosphatases need to reverse the phosphorylation status of CDK substrates. The best studied phosphatase is the Cdc14 phosphatase in budding yeast. Cdc14 phosphatase is a key player in at least two pathways, the cdc fourteen early anaphase release (FEAR) pathway and the mitotic exit network (MEN) (reviewed in Stegmeier and Amon 2004; Queralt and Uhlmann 2008). Budding yeast lacking Cdc14p arrest in a stage comparable to telophase showing an elongated mitotic spindle and bilobed anaphase nucleus (Culotti and Hartwell 1971). A similar phenotype can be observed in yeast that express undegradable mitotic cyclin (Surana, Amon et al. 1993). Dephosphorylation events in the exit from M phase in higher eukaryotes are much less well understood.

Although the dephosphorylation of certain CDK substrates is required for a successful completion of mitosis or meiosis, clear candidates for Cdc14 functional homologs in higher eukaryotes have not yet been identified (reviewed in Sullivan and Morgan 2007).

2.4.5.4 Spindle assembly checkpoint

As in every complex process, errors are likely to occur that can delay the completion of one step of the cell cycle. Therefore it is necessary to adjust the course of events so that no process can be initiated before the previous one is completed. For this purpose, the cell has evolved checkpoints that stop the cell cycle until the problems are resolved. For instance, the spindle assembly checkpoint (SAC) prevents chromosome segregation during metaphase until every chromosome is properly attached to the spindle. The spindle checkpoint protein Mad2 inhibits APC activation and thus progression into anaphase as along as it senses unattached kinetochores (reviewed in Marston and Amon 2004).

2.4.5.5 Possible explanations for anaphase arrests

Most genetic defects and errors that affect progression through mitosis lead to an arrest at the metaphase stage. This is mainly due to the fact that the spindle assembly checkpoint prevents the cell from progressing further through metaphase as long as all pre-requisites are not met. Upon deactivation of the spindle checkpoint, the APC^{Cdc20} complex becomes activated, which leads to the removal of sister chromatid cohesion as well as degradation of cyclin B. An anaphase arrest, as observed in *smg7*, would indicate that the activity of APC^{Cdc20} is uncoupled, meaning that sister chromatid cohesion is lost but cyclin B levels are maintained. In this scenario the chromosomes segregate but cell cycle progression to telophase is aborted.

In summary there are three possible scenarios leading to an anaphase arrest. First, an impaired degradation of cyclin B can lead to an arrest at the anaphase stage. Several studies have shown that the expression of non-degradable versions of cyclin B could hinder the completion of M phase (Holloway, Glotzer et al. 1993; Surana, Amon et al. 1993; Parry and O'Farrell 2001; Weingartner, Criqui et al. 2004; Potapova, Daum et al. 2006; Wolf, Wandke et al. 2006; Wolf, Sigl et al. 2007). Interestingly, Wolf and

colleagues showed that the stage of the arrest was dependent on the dosage of non-degradable cyclin B expressed in the system. A high amount of non-degradable cyclin B would arrest the cells in metaphase, whereas intermediate and lower amounts led the cell to arrest during anaphase or telophase.

A second possible scenario is that the CDK activity is decreased but the CDK substrates remain phosphorylated due to an inactive phosphatase. And finally, an anaphase-like arrest has been described in the *shugoshin* mutant. Shugoshin preserves sister chromatid cohesion on the centromeric regions as long as the spindle checkpoint remains active. Lack of Shugoshin leads to a premature loss of sister chromatid cohesion. Chromatids are separated prior to metaphase II and prior to the inactivation of the SAC. In this case the active SAC prevents the activation of APC and, as such, the progression of the cell cycle. The defect would appear as an anaphase arrest. Further experiments are required to address the question of whether pre-requisites for SAC inactivation exist, and if the arrest observed in *smg7* meiocytes occurs indeed at the anaphase stage.

2.4.6 Is sister chromatid cohesion lost prematurely in *smg7* meiocytes?

Premature loss of cohesion can impair SAC checkpoint deactivation and thus can lead to an arrest similar to what is observed in *smg7* meiocytes (Salic, Waters et al. 2004; Tang, Sun et al. 2004; Kitajima, Hauf et al. 2005; McGuinness, Hirota et al. 2005). Therefore I analyzed centromeric cohesion in *smg7* meiocytes via fluorescence *in situ* hybridization (FISH). I stained centromeric regions with a 180bp centromeric FISH probe and counted the number of foci in interkinesis. Cohesed centromeres appear as one signal, thus leading to 5 signals for each nuclei in interkinesis. Centromeres that are prematurely separated would result in 2 split signals. I found only 1 separated centromere in 48 analyzed interkinesis stages of *smg7*, compared to null from 40 analyzed wild-type stages (Figure 33A-C). Therefore no significant premature loss of cohesion was detected. Thus I conclude that cohesion is properly preserved in the interkinesis stages and premature loss of cohesion is unlikely to be the cause of the arrest seen in *smg7* meiocytes.

2.4.7 Are chromosomes properly bioriented at metaphase II in *smg7* meiocytes?

During metaphase II, all chromosomes attach to the spindle via their kinetochores and become bioriented. This is necessary to inactivate the spindle checkpoint and continue into anaphase II. In order to investigate if chromosomes are properly attached and bioriented in metaphase II stages of *smg7* I stained the centromeres with a FISH probe directed against the 180bp centromeric repeats. Tension arises due to the forces applied to the kinetochore. In this case, the spindle pulls the kinetochore towards the spindle pole while the sister chromatids remain cohesed, and thus the centromeric regions appear as stretched signals. In all 16 analyzed *smg7* as well as in the 15 wild-type control metaphase II stages the centromeric FISH signals were stretched, indicating that tension occurs and the chromosomes are properly bioriented (figure 33D-E). These data indicate that sister chromatid cohesion is maintained until metaphase II and that metaphase II chromosomes are properly attached to the spindle. This further indicates that *smg7* mutants normally enter anaphase II and that the observed arrest is not due to a premature loss of sister chromatid cohesion.

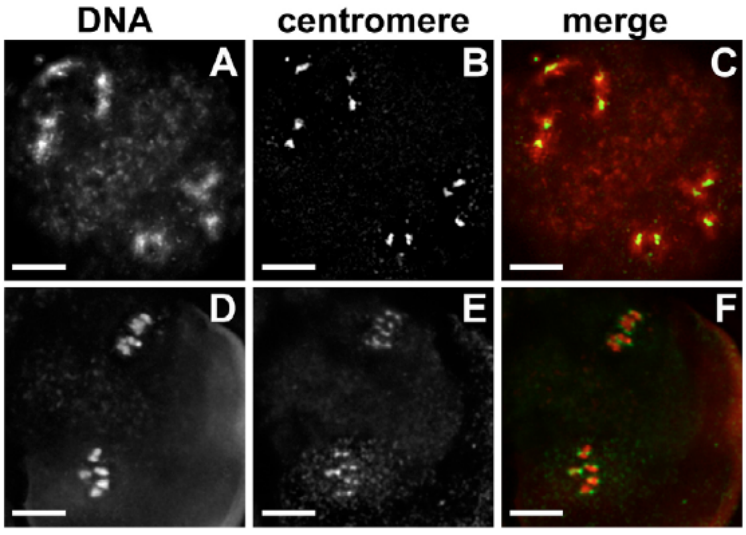

Figure 33. Pictures represent wild-type telophase I (A-C) and metaphase II (D-F) stages. Centromeres are stained by FISH (green). DNA is stained with DAPI (red). Size bar =5µm.

2.4.8 Investigation of meiotic cyclins in *smg7*

During the exit from meiosis, the chromosomes have to detach from the spindle and decondense. These processes can only occur at a stage of low CDK activity. This is strongly supported by the fact that non-degradable versions of cyclin B cannot finish M

phase (Holloway, Glotzer et al. 1993; Surana, Amon et al. 1993; Parry and O'Farrell 2001; Weingartner, Criqui et al. 2004; Potapova, Daum et al. 2006; Wolf, Wandke et al. 2006; Wolf, Sigl et al. 2007). The anaphase arrest in *smg7* can be due to a failure in degradation of cyclin B and thus downregulation of CDK activity. Therefore I wanted to analyze whether the cyclin B levels remain upregulated in the later stages of meiosis II in *smg7*.

2.4.8.1 Cyclin B1;1 expression

Plants seemed to have evolved a high degree of complexity in the regulation of CDK activity when compared to other organism. Based on bioinformatic searches, over 50 different cyclins have so far been identified (Wang, Kong et al. 2004). Among them, 11 different B-type and 10 different A-type cyclins were found as potential M phase cyclins. Only a few of them have been characterized so far, such as cyclin B1;1 (Ferreira, Hemerly et al. 1994), solo dancer (SDS) (Azumi, Liu et al. 2002) and cyclin A1;2 (Magnard, Yang et al. 2001; Wang, Magnard et al. 2004). Further investigation is needed to shed light on the function of the remaining cyclins; in particular, no meiotic cyclin B has been described so far.

The cyclin B1;1 protein has been characterized as a functional cyclin B (Ferreira, Hemerly et al. 1994). A cyclin::beta-glucuronidase reporter construct containing the *CYCB1;1* promoter and the *CYCB1;1* destruction box (CDB) fused in frame to the *GUS* reporter gene is available, which allowed us to study the cyclin B1;1 localization distribution in the cell. I performed anti-GUS immunostaining of wild-type mitosis to detect the distribution and localization of cyclin B1;1 (figure 34). GUS immunostaining was detected from G2/Prophase until telophase in mitotic cells. The cycB1;1-GUS signal was mainly cytoplasmic in G2 cells, while in prometaphase and metaphase it co-localized with chromosomes and started to dissociate from the DAPI staining in anaphase and telophase.

This distribution correlates with the expected behavior of cyclin B as was previously shown in other organisms, indicating that immunostaining of tagged cyclins can be used to detect cyclin behaviour and abundancy (Huang and Raff 1999). However, I failed to detect cyclin B1;1-GUS staining in pollen mother cells, which means that cyclin B1;1 is not expressed in meiosis.

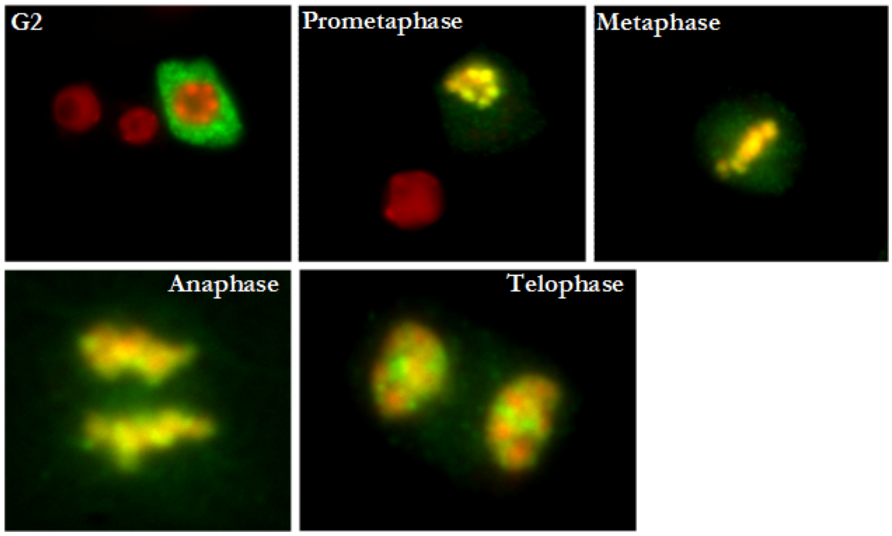

Figure 34. Cyclin B1;1-GUS expression in mitosis. DNA is stained with DAPI (shown in red). Cyclin B1;1-GUS is shown in green.

2.4.8.2 Genetic interaction of smg7 and tam

In Drosophila, the *cortex* gene encodes for a meiosis specific Cdc20 subunit of the APC. *Cortex* mutants show a defect in the meiotic cell cycle progression and a failure to exit from meiosis, similar to the phenotype observed in *smg7* mutants (Page and Orr-Weaver 1996; Chu, Henrion et al. 2001). Interestingly, decreased levels of cyclin A were sufficient to rescue the meiotic arrest in *cortex* mutants (Swan, Barcelo et al. 2005). In order to test whether the meiotic arrest in *smg7* meiocytes can be partially suppressed by decreasing the amount of M-type cyclin, I generated double mutants of *smg7* and *tam*. The *tardy asynchronous meiosis* (*tam*) is a temperature sensitive mutation that causes decreased levels of cyclin A1;2 at the restrictive temperature of 27°C. So far Cyclin A1;2 is the only A-type cyclin that has been shown to play a role in the *Arabidopsis* meiotic cell cycle. The meiotic interphase is prolonged in *tam* mutants and entry into the second meiotic division is delayed. This delay causes early cell wall formation after the first meiotic division, which is in contrast to wild-type cells where cytokineses happens only after completion of meiosis (figure 35) (Magnard, Yang et al. 2001; Wang, Magnard et al. 2004). Still, *tam* mutant plants are fertile.

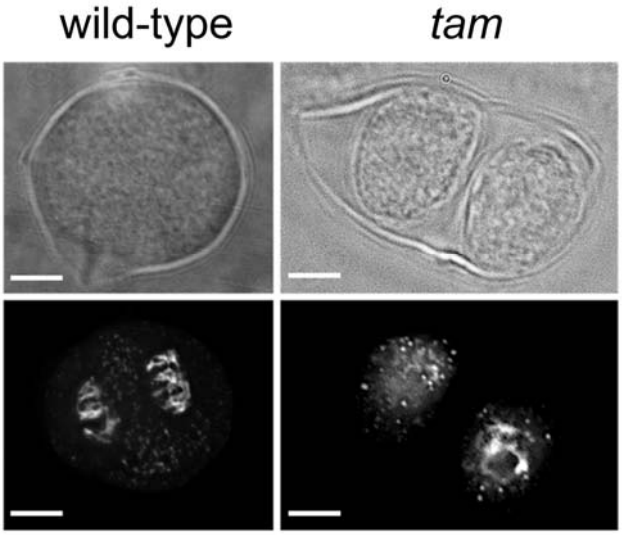

Figure 35. A cell wall forms during interkinesis in tardy asynchronous meiosis mutants between the two nuclei resulting from the first meiotic division. Wild-type meiocytes form cell walls only after the second meiotic division dividing the four haploid nuclei. DNA is stained with DAPI. Size bar =5µm.

The anaphase II arrest observed in *smg7* mutants could arise from a failure to inactivate CDK activity due to aberrant cyclin degradation. Thus, I tested whether a decrease in the level of the M phase cyclin A1;2 could rescue the defect in *smg7* meiocytes. I crossed heterozygous *smg7-1* with homozygous *tam* double mutants and analyzed double mutants in the F2 generation grown at the restrictive temperature. I found that *smg7-1 tam* double mutants still arrested at the anaphase/telophase II transition, similar to *smg7-1* (figure 36A, irregular anaphase II), indicating that the lower levels of cyclin A1;2 in the *smg7/tam* double mutants are not sufficient to rescue the anaphase II arrest caused by *smg7*. However, double mutants did not form a cell wall in interkineses as observed in *tam* mutants, indicating that *smg7* mutation rescues the cell cycle delay in *tam*.

I next questioned whether the cell wall formation in interkinesis in the *smg7 tam* double mutants is due to a defect in cell wall formation or whether the *smg7* mutation causes a change in the cell cycle progression through meiotic interphase. Therefore I scored the frequency of meiotic stages ranging from metaphase I until metaphase II (figure 36B).

In the wild-type situation the amount of the metaphase I, anaphase I, telophase I and metaphase II are relatively equally distributed, indicating that the duration of these individual cell cycle stages is similar (figure 36B, wild-type). However, in the *tam* mutant background around 50% of the total number of the meiotic stages belonged to interphase stages, resulting in interkineses stages in *tam* mutants being significantly more abundant than wild-type. This indicates that there is a significant delay in the cell cycle progression through meiotic interphases as was previously shown (figure 36B, *tam* and Magnard, Yang et al. 2001).

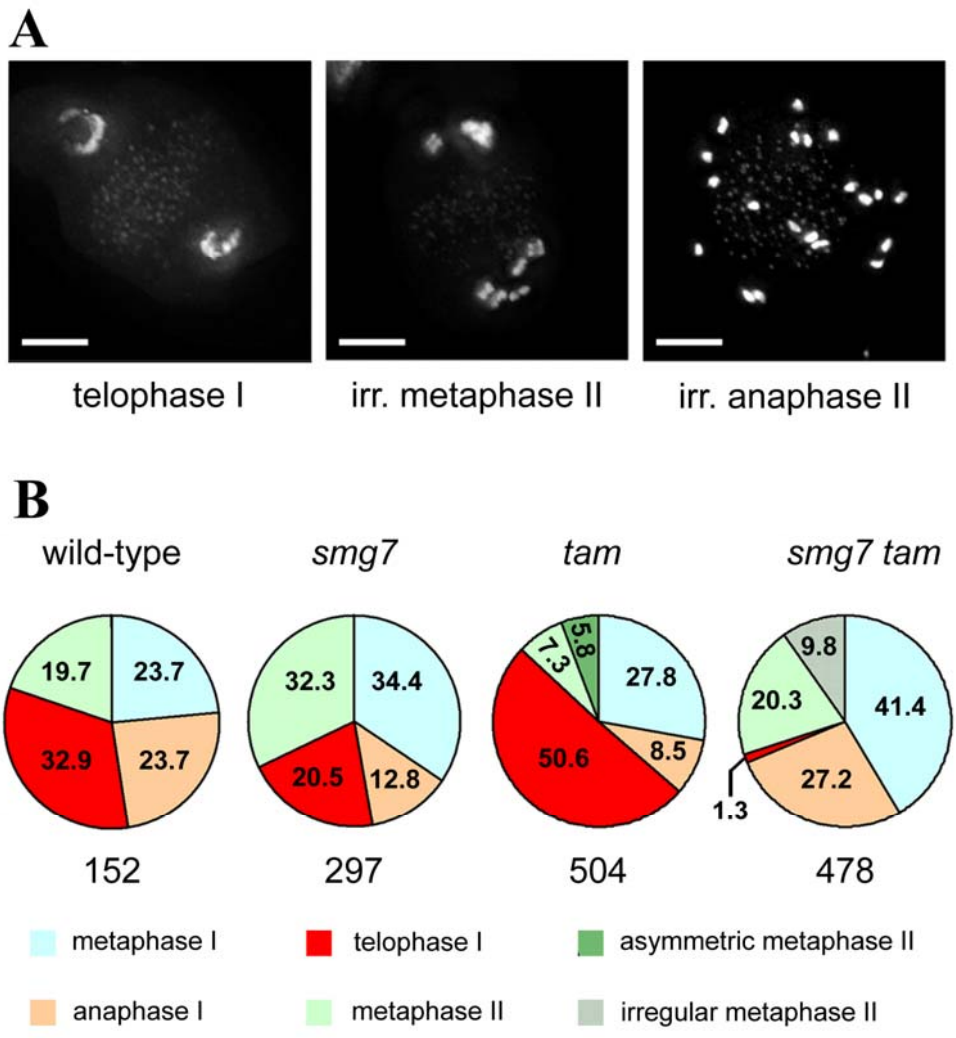

Figure 36. (A) Meiosis in *tam/smg7-1* mutant PMCs. DNA is stained with DAPI. Size bar = 5µm. (B) Score of meiotic cell cycle stages in the indicated mutant backgrounds.

In the *smg7 tam* double mutants I failed to observe any meiocytes of cytologically defined interphases. In a total of 478 analyzed meiocytes, only six possessed the characteristics of two clearly defined nuclei, but the chromosomes seemed unusually condensed (figure 36A, telophase I). Additionally, a fraction of meiocytes showed fully condensed metaphase II like chromosomes that were more than usually dispersed in the cell (figure 36A, irregular metaphase II). These data indicate that the cell cycle delay caused by *tam* is not only suppressed by *smg7* mutation but that the interkinesis stages are almost skipped (figure 36B, *smg7 tam*). Interestingly, already in *smg7* single mutants fewer anaphase I and telophase I stages were observed, which also suggests that these meiotic stages are shortened in *smg7* mutants (figure 36B, *smg7*). These results indicate that SMG7 is indeed regulating the meiotic cell cycle progression. Surprisingly, this experiment also demonstrates that SMG7 function is required not only at meiotic exit, but already during interkinesis.

2.5 SMG7 regulates the pathogen response

In order to gain more insights into the biological role of SMG7 in *Arabidopsis* I decided to investigate the vegetative phenotypes in *smg7* mutants.

2.5.1 *Smg7* mutants show similarities to lesion mimic mutants

As described before the *smg7-1*, *smg7-2* and *smg7-3* mutant plants display a range of growth and developmental defects. A peculiar observation was that leaves of mutant plants formed necrotic lesions. Another interesting observation was that the defects were modulated by different environmental conditions. Plants that were grown in vitro or under high humidity displayed weaker vegetative defects than plants grown on soil and under low humidity (figure 37).

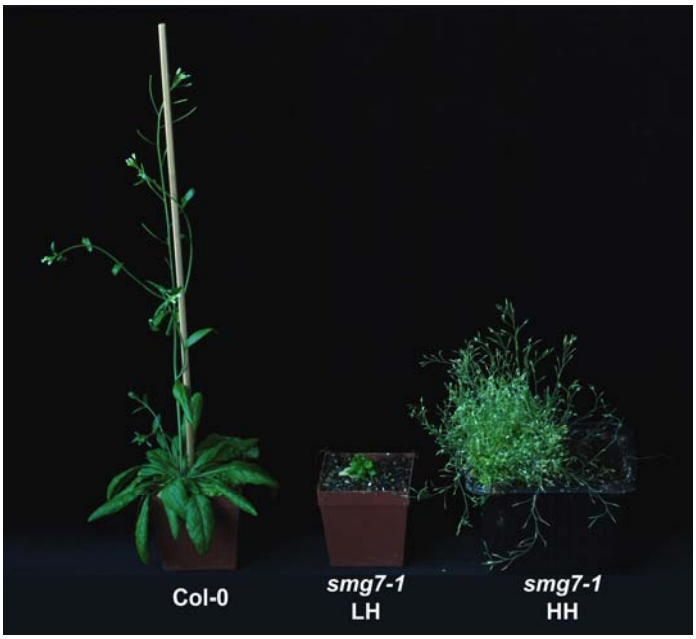

Figure 37. Different humidity conditions modulate the vegetative defects in *smg7-1* (LH = low humidity, HH = high humidity).

A humidity dependent growth defect with necrosis was also found on plants carrying mutations in the BON1/CPN1 gene (Jambunathan, Siani et al. 2001). BON1/CPN1 has been characterized as a regulator of the pathogen response in *Arabidopsis thaliana*. *Bon1/cpn1* mutants belong to the class of lesion mimic mutants (LMM) (Lorrain, Vailleau et al. 2003), a group of mutants that typically display necrotic lesions which

are caused by miss-regulation of the pathogen stress response and activation of the hypersensitive response (HR). We hypothesized that the necrotic lesions of *smg7* are due to activation of the hypersensitive response.

2.5.2 Introduction to plant pathogen response

Pathogens are a constant threat to plants. Therefore plants developed many different defense mechanisms. Microbes can penetrate the surfaces of leaves or roots directly, over wounds, or through natural openings such as stomata. On the host plasma membrane, extracellular surface receptor like kinases recognize pathogen-associated molecular patterns (PAMPs) and trigger an immune response that limits the extent of the disease but usually does not inhibit pathogen growth. Pathogenic microbes often produce avirulent effector molecules (Avr proteins), which can repress the immune response (reviewed in Akira, Uematsu et al. 2006; Jones and Dangl 2006; Zipfel 2008).

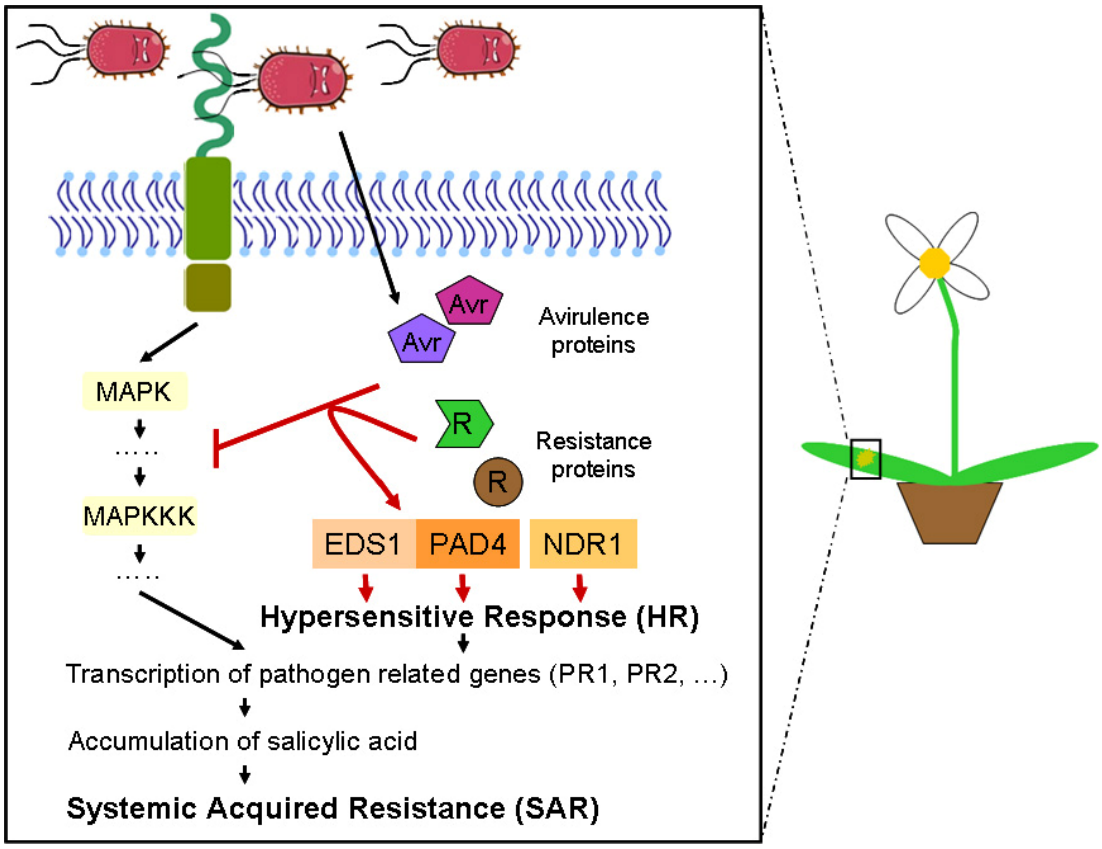

Figure 38. Plants that are challenged with pathogens respond in several different ways. (RLK = receptor-like kinase, PAMP = pathogen-associated molecular patterns).

Plant resistance (R) proteins detect the enzymatic activity of many effectors. If a response overcomes a certain threshold, the hypersensitive response (HR) is locally induced. This means that infected cells and cells in close proximity undergo a rapid programmed cell death which prevents the spread of the pathogen to the surrounding tissue. The *Arabidopsis* genome encodes around 200 genes which carry typical features of plant resistance proteins. Around 150 nucleotide-binding-site- (NBS) leucine-rich repeat (LRR) genes make up the largest class of R genes (Meyers, Kozik et al. 2003). The group of NBS-LRR genes can be further divided into CC-NBS-LRR and TIR-NBS-LRR. R proteins of the CC-NBS-LRR group contain a coiled-coiled domain in its N-terminal region, while the group of TIR-NBS-LRR proteins contain a domain that shows homology to the *Drosophila* Toll and mammalian interleukin (IL) receptors. To date only a few R genes have been characterized and very little is known about the downstream signaling events that they elicit. Some TIR-NBS-LRR R genes have been shown to require the major signaling proteins EDS1 and PAD4 to trigger the immune response. PAD4 is a lipase-like gene that is important for salicylic acid signaling (Zhou, Tootle et al. 1998; Jirage, Zhou et al. 2001). However, the molecular mechanism behind the signaling cascade has not yet been well characterized. Another important signaling factor is NDR1. It has been shown that at least some R genes of the leucine zipper subclass of NBS-LRR transmit the pathogen response signal over NDR1 (figure 38, reviewed in Heath 2000; Jones 2001).

Both basal defense and R gene mediated resistance lead to activation of SAR, which results in an increased broad spectrum resistance of the entire plant. Activation of SAR requires the accumulation of salicylic acid (SA) throughout the plant, which triggers a signaling cascade that leads to the expression of defense genes, such as PR1, PR2 and PR5 (reviewed in Ryals, Neuenschwander et al. 1996; Durrant and Dong 2004).

The pathogen stress response underlies a series of regulation steps. Miss-regulation of programmed cell death leads to mutant phenotypes that mimic the pathogen-induced hypersensitive response. These mutants are called lesion mimic mutants (LMM). The most typical feature of LMMs is spontaneous lesion formation in the absence of pathogens. Besides the appearance of lesions, the constitutive expression of marker genes (PR1, PR2, PR5,..) and the accumulation of salicylic acid has been associated with LMMs (reviewed in Lorrain, Vailleau et al. 2003).

2.5.3 Necrotic lesions are formed on leaves of SMG7 deficient plants

Necrotic lesions on leaves are a feature of programmed cell death and the hypersensitive response. Certainly, large necrotic spots are clearly visible on leaves of *smg7-1*, *smg7-2* and *smg7-3* homozygous mutants. In order to obtain a more detailed picture of the degree and the size of the lesions in all mutant lines, I stained the leaves with trypan blue, a dye that specifically stains dead cells (Koch and Slusarenko 1990). On the leaves of *smg7-1*, *smg7-2*, and *smg7-3* mutant plants, a large number of necrotic cells in a range of sizes are clearly detected (figure 39). Necrotic lesions are absent in *smg7-4* and *smg7-6* mutants. This result demonstrates that a large number of necrotic cells are present on the leaves of *smg7-1*, *smg7-2* and *smg7-3* mutant plants that have not been challenged by any type of biotic stress.

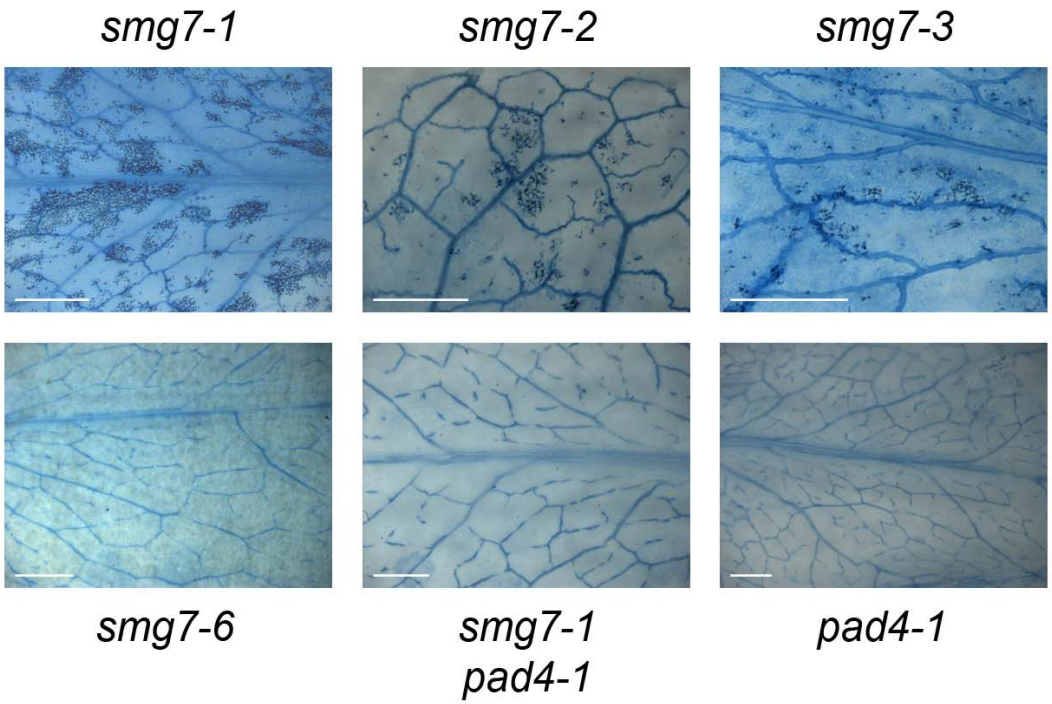

Figure 39. Necrotic Lesions. Visualization of necrotic lesions on *smg7* rosette leaves by trypan blue staining. Size bar = 2mm.

2.5.4 Genetic interaction of *PAD4* and *SMG7*

As described previously, PAD4, EDS1, and NDR1 are important factors in the signaling cascade of the pathogen response. I asked whether the necrotic lesions found on leaves in *smg7-1*, *smg7-2* and *smg7-3* mutant plants are due to miss-regulation of

the pathogen response. Therefore I chose to attenuate the pathogen response by mutating the PAD4, EDS1 or NDR1 genes. If the pathogen response pathway is up-regulated in *smg7* mutants I expected that double mutants of *smg7* and *pad4, eds1* or *ndr1* would show a clear decrease in necrotic lesions. Since two copies of EDS1 in a tandem array are present in the *Arabidopsis* genome, and EDS1 and PAD4 have been shown to interact and have overlapping functions (Feys, Moisan et al. 2001), I choose to use the *pad4-1* allele for my analysis. I obtained *pad4-1* mutant lines and crossed homozygous *pad4-1* with heterozygous *smg7-1* plants. In the F2 generation *pad4-1/smg7-1* double mutants were obtained. Surprisingly, not only the necrotic lesions (figure 39, *smg7-1/pad4-1* and *pad4-1*) but all vegetative growth and developmental defects were completely rescued in *smg7-1/pad4-1* double mutants (figure 40).

Figure 40. Rescue of all vegetative growth and developmental defects in *smg7-1* mutant plants via *pad4-1* mutation.

These data clearly demonstrate that the *pad4-1* mutation is able to suppress all the vegetative phenotypes in *smg7-1* mutants, thus I conclude that SMG7 is involved in the regulation of the pathogen response.

To confirm that the *pad4-1* mutation has no effect on NMD I analyzed the +PTC/-PTC ratio of the At2g45670 locus in *smg7-1/pad4-1* double mutants as described previously in section 2.3.4. As shown in figure 41, I could still detect high levels of +PTC transcripts indicating that *pad4* does not suppress the defect in NMD.

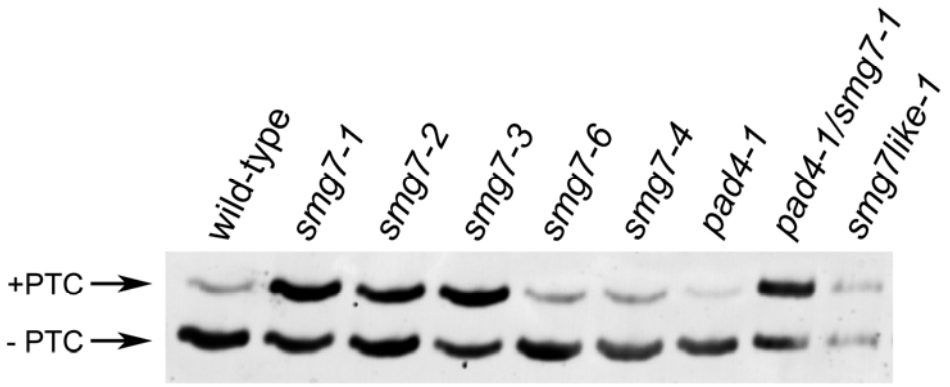

Figure 41. RT-PCR of the At2g45670 derived transcripts analyzed in a *smg7* allelic series. Part of the picture has been shown already in figure 22.

Further, I crossed *smg7-1* heterozygous plants with *ndr1-1* homozygous plants. However the *ndr1-1/smg7-1* double mutants did not show a significant suppression of the vegetative phenotypes (data not shown), indicating that the pathogen response caused by SMG7 deficiency is transmitted independently of NDR1.

Activation of the hypersensitive response can be triggered by R genes. For instance, a gain-of function allele of *SNC1*, an NBS-LRR resistance gene, has been shown to cause constitutive upregulation of the pathogen response (Zhang, Goritschnig et al. 2003). Interestingly, SNC1 levels were upregulated in the NMD mutant *upf1-5* (Yi and Richards 2007). To ask whether the *SNC1* gene is responsible for the *smg7* phenotype I generated *snc1-11/smg7-1* double mutants. However, necrotic lesions as well as vegetative growth defects were still visible in *snc1-11/smg7-1* double mutants (data not shown), indicating that *SNC1* is not responsible for the pathogen response defect in *smg7*.

2.5.5 *Pathogen related 1 (PR1)* gene expression

Up-regulation of the pathogen stress response can be determined by the analysis of the expression levels of pathogen related genes, such as *PR1*. Therefore I subjected all

smg7 mutants to quantitative analysis of *PR1* expression. Total RNA was extracted from leaves and used for northern blot analysis. Radioactively labeled probes corresponding to the full length *PR1* cDNA as well as to the 5´end of the *SMG7* cDNA and were used for hybridization (figure 42).

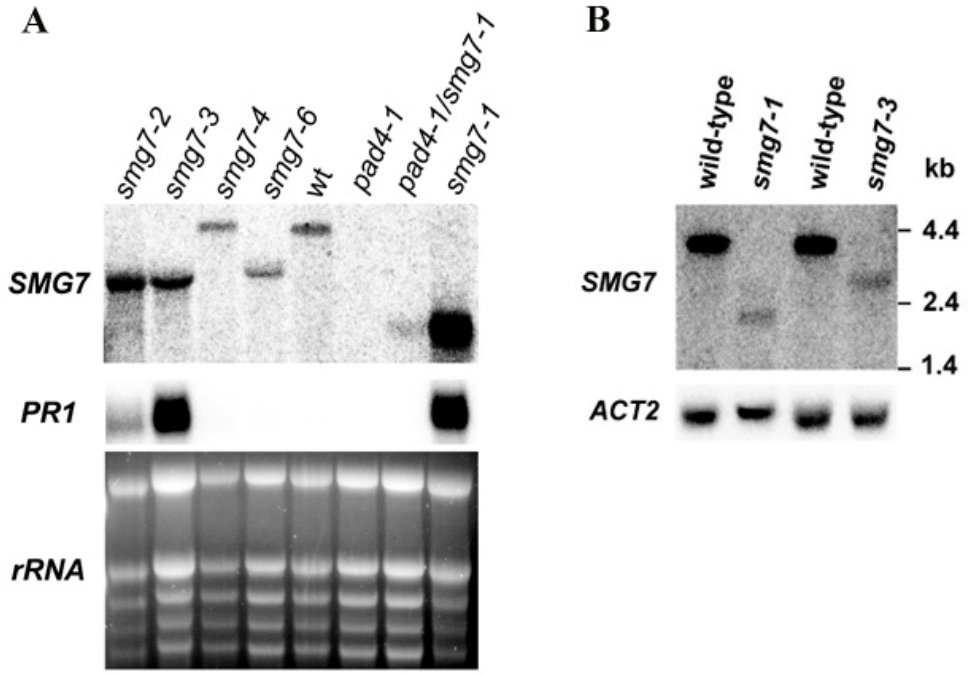

Figure 42. Quantitative expression analysis of *SMG7* and *PR1* expression. (A) *SMG7* and *PR1* expression analyzed by northern blot of leave tissue. Radioactively labeled probes corresponding to the 5´end of the *SMG7* cDNA and to the full length *PR1* cDNA were used for hybridization. The rRNA bands of the ethidium bromide gel were used as loading control. A portion of this picture was shown in figure 12. (B) SMG7 expression analysis in flowers. The northern blot was hybridized with a radioactively labeled probe corresponding to the 5´end of the *SMG7* cDNA in order to detect the SMG7 transcripts. The SMG7 probe was stripped and the blot was re-hybridized with a radioactively labeled ACT2 cDNA in order to detect the ACT2 transcript, which was used as loading control.

Smg7-1 and *smg7-3* mutants showed a large increase in *PR1* expression compared to wild-type, *smg7-4* and *smg7-6*. *PR1* transcripts were up-regulated in *smg7-2* but to a smaller degree than in *smg7-1* and *smg7-3*, which correlates with the less severe vegetative phenotype. Thus, I conclude that *PR1* expression is up-regulated and the pathogen response pathway is activated in the *smg7* mutants that also show necrotic lesions. In the *pad4-1*/*smg7-1* double mutants the *PR1* transcript level was drastically reduced and fell below the detection limit of the northern blot, which is consistent with the situation in wild-type, *pad4-1*, *smg7-4* and *smg7-6* plants. As *PR1* transcription is stimulated by an active pathogen response, these data suggest that the *pad4-1* mutation suppresses the vegetative phenotypes in *smg7-1* by interrupting the pathogen stress response.

The truncated transcripts of the various *SMG7* T-DNA insertion lines vary in their abundance in *Arabidopsis* leaves (figure 42A) and flowers (figure 42B). In flowers, the T-DNA truncated *SMG7* transcripts are significantly reduced compared to wild-type *SMG7*. However, in leaves of lines that show strong developmental defects I observed strong up-regulation of the truncated *SMG7* transcripts. Another interesting observation was that the wild-type *SMG7* transcript was not detectable in the *pad4* mutant background and the *smg7-1* truncated transcript was significantly reduced in the leaves of *pad4/smg7* double mutant. This indicates that *SMG7* itself might be regulated via the pathogen stress response. Further investigation is needed to clarify how *SMG7* expression is regulated and whether the pathogen stress response has indeed an affect on the regulation of *SMG7*.

2.5.6 Accumulation of salicylic acid (SA) in *smg7* mutant lines

Like necrotic lesions and *PR1* expression, accumulation of salicylic acid is a feature of systemic acquired resistance (SAR), a pathway that is often upregulated in lesion mimic mutants. Therefore we analyzed the level of salicylic acid (SA) in all *SMG7* T-DNA insertion lines and compared them with wild-type. All plants were grown under high humidity for 3 weeks in order to obtain enough material for analysis. Then the humidome was removed and low humidity conditions were induced for 2 weeks. In collaboration with Bettina Dekrout and Claudia Jonak (Gregor Mendel Institute of Molecular Plant Biology) the free and total salicylic acid levels were measured via HPLC (Rozhon, Petutschnig et al. 2005).

In *smg7-1* and *smg7-3* plants a ~10 fold increase in total SA as well as ~5 fold increase of free SA was observed (figure 43). Interestingly, *smg7-2* plants showed again a slightly lower increase compared to *smg7-1* which stands in accordance with a slightly milder vegetative phenotype and lower *PR1* expression. Salicylic acid levels in both *smg7-4* and *smg7-6* mutants are comparable to wild-type. Thus, these data show that salicylic acid, a signal molecule of systemic acquired resistance, is highly up-regulated in *smg7-1*, *smg7-2* and *smg7-3*, which correlates with necrosis and the elevated PR1 transcripts levels. In the *pad4-1*/*smg7-1* double mutants both total and free SA levels were at the range of wild-type plants and *pad4-1* single mutants. These data show that

salicylic acid, an important signaling molecule of the pathogen response, is highly up-regulated in *smg7-1*. The *pad4-1* mutation restores normal SA levels by blocking the pathogen stress response.

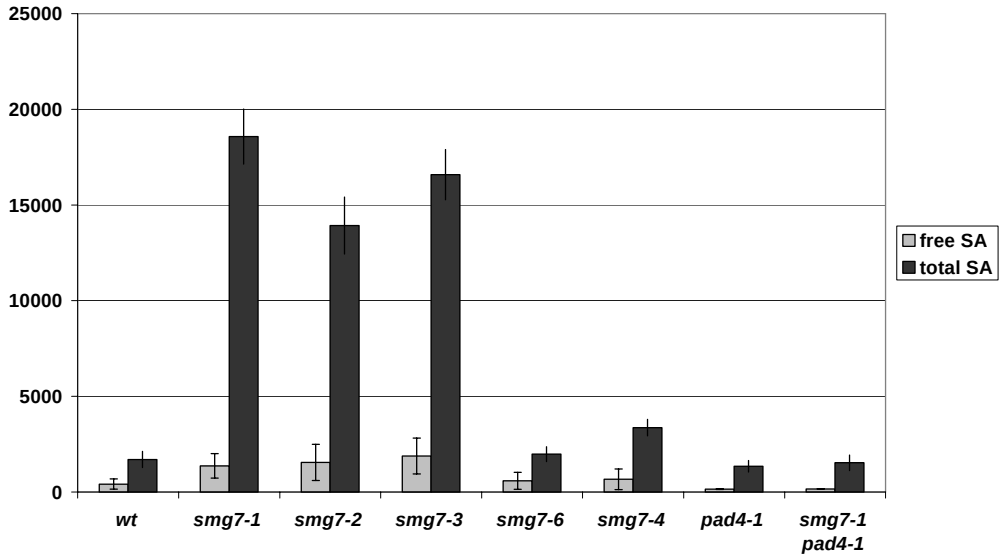

Figure 43. Free and total amounts of salicylic acid. Values on the y-axis show ng SA/fresh weight.

Taken together the elevated levels of *PR1* and salicylic acid as well as the genetic suppression of the vegetative phenotype in *smg7-1* mutants with the *pad4-1* mutation, I can conclude that SMG7 is involved in regulation of the pathogen response. These data indicate that *smg7* mutants show typical features of lesion mimic mutants and have constitutive activation of the pathogen response.

2.6 Comparison of NMD mutants with *smg7*

The characterization of *Arabidopsis* SMG7 so far showed that this protein is an evolutionarily conserved factor of the nonsense mediated RNA decay. In addition SMG7 deficient plants showed two distinctive defects affecting meiosis and the pathogen response. The question arose whether these specific defects observed in *smg7* mutants can be linked to NMD. Certain aberrant mRNAs that can not be removed by the impaired NMD machinery could cause the arrest in meiosis or the aberrant up-regulation of the pathogen response. Therefore I asked whether defects in either meiosis or the pathogen response can be observed in other mutants affecting NMD.

2.6.1 Phenotypic comparison of *smg7* with *upf1* and *upf3*

I asked whether the defect in NMD could be responsible for the miss-regulated pathogen response or meiotic arrest observed in *smg7* mutants. Therefore I examined all available mutant lines that have been shown to affect NMD in plants and compared their phenotypes with the defects observed in *smg7*. Homologs of UPF1 and UPF3 have been characterized in *Arabidopsis thaliana* and several reports have demonstrated that they function in NMD (Hori and Watanabe 2005; Arciga-Reyes, Wootton et al. 2006; Yoine, Ohto et al. 2006; Kerenyi, Merai et al. 2008).

I obtained five different homozygous mutant lines of *UPF* (*upf1-1/lba1*, *upf1-2*, *upf1-3*, *upf1-4* and *upf1-5)* as well as two different *UPF3* T-DNA insertion lines (*upf3-1* and *upf3-2)* and grew them under the same growth conditions as *smg7-1* and wild-type plants (figure 44, 45 and 46).

Figure 44. Comparison of 4 week old plants of *SMG7* with *UPF1* and *UPF3* homozygous T-DNA insertion lines.

Arabidopsis plants homozygous for the *upf1-3* allele are seedling lethal, but other *upf1* mutant plants (*lba1*, *upf1-2*, *upf1-4* and *upf1-5*) are viable (figure 44 and 45, (Arciga-Reyes, Wootton et al. 2006; Yoine, Nishii et al. 2006; Yoine, Ohto et al. 2006)).

The *low-beta-amylase1 (lba1)* mutant carries a pointmutation in the *UPF1* gene in a region that encodes the RNA helicase domain. Originally, the *lba1* allele was identified in a screen for *Arabidopsis* mutants that have a reduced beta-amylase activity in leaves (Mita, Murano et al. 1997). Additionally, *lba1* mutant plants bolted and flowered early under continuous light but grew slower under short day conditions (Yoine, Ohto et al. 2006). *Lba1* mutants grown under my standard conditions (16h light/ 8h dark) bolted and flowered earlier (figure 45, *lba1*) compared to wild-type but showed no additional phenotype.

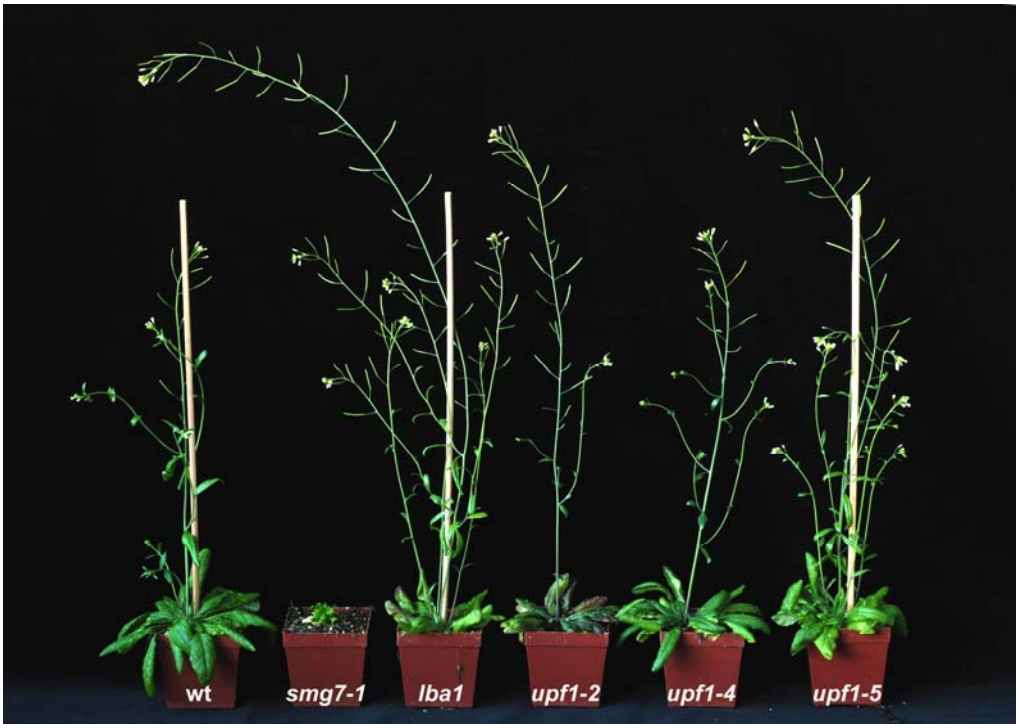

Figure 45. Comparison of 6.5 week old plants with *UPF1* homozygous T-DNA insertion lines.

Different observations regarding the phenotypic analysis of the other *upf1* mutant alleles have been reported in the literature. Yoine and colleagues (Yoine, Nishii et al. 2006) reported that homozygous mutant plants of the *upf1-2* and *upf1-4* alleles grew normally. Arciga-Reyes and colleagues (Arciga-Reyes, Wootton et al. 2006) found a weak phenotype of smaller and slightly indented leaves in *upf1-4* mutants. Additionally, they characterized the *upf1-5* allele where they observed stronger defects.

For instance *upf1-5* plants flowered later compared to wild-type, they showed narrow, jagged leaves and a floral phenotype in approximately 5% of all flowers. However *upf1-2*, *upf1-4* and *upf1-5* homozygous mutants grew normally under the growth conditions I used (figure 44 and 45).

Homozygous *upf3-1* and *upf3-2* mutant plants are viable (figure 44 and 46, (Hori and Watanabe 2005; Arciga-Reyes, Wootton et al. 2006). Whereas no visible phenotypes of *upf3-1* plants were reported from Hori and colleagues, Arciga-Reyes and colleagues found a delay in flowering, as well as reduced jagged leaves and floral phenotypes in some flowers in *upf3-1* plants and similar but milder defects in *upf3-2* mutants.
I grew UPF3 deficient plants under the same conditions as *smg7-1*, but neither of the *upf3* mutant plants showed an obvious growth or developmental defect (figure 44 and 46). Taken together, in none of the UPF1 or UPF3 deficient plants could I detect a phenotype that is similar to the defects observed in *smg7-1*.

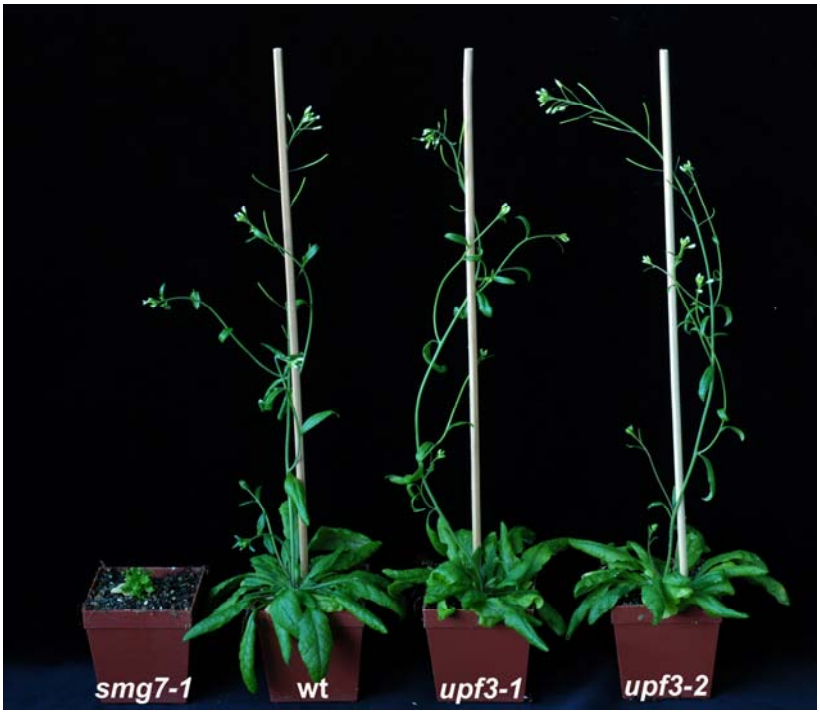

Figure 46. Comparison of 6.5 week old plants of *SMG7* with *UPF3* homozygous T-DNA insertion lines.

The growth or vegetative defects observed in *smg7* were absent in the analyzed UPF1 and UPF3 deficient plants, indicating that constitutive upregulation of the pathogen response is specific to the *smg7* mutation and unlikely due to NMD. Additionally all

upf1 and *upf3* mutants were fertile, therefore I concluded that the meiotic defect observed in *smg7* mutants is due to a meiosis specific role of SMG7 rather then NMD.

2.6.2 Comparison of the NMD defects of *smg7* with *upf1* and *upf3*

The *upf1-5* and *lba1* mutant alleles of the UPF1 gene as well as the *upf3-1* mutant have been shown to have impaired NMD function (Hori and Watanabe 2005; Arciga-Reyes, Wootton et al. 2006; Yoine, Ohto et al. 2006). In order to evaluate the severity of the analyzed NMD defect in the *smg7-1* mutant, I compared the ratio of +PTC to -PTC transcripts in *smg7-1* with the +PTC/-PTC ratio in *upf1-5* and *upf3-1*. I used the same assay as described previously in chapter 2.3.1, figure 19. RT-PCR was performed with primers that can amplify both splice variants derived from the At2g45670 gene. The RT-PCR products were separated over nondenaturating PAGE and the levels of +PTC and –PTC were compared in samples of three individual plants. The *upf1-5* mutants showed a significant increase in the level of +PTC transcript to a similar extent as observed in *smg7-1* mutants (figure 47A). These data indicate that the NMD defect in *upf1-5* is similar to *smg7-1*. However, the aberrant splice variant was only slightly increased in the *upf3-1* mutant (figure 47B), suggesting that, at least for the degradation of this particular transcript, UPF3 is not required.

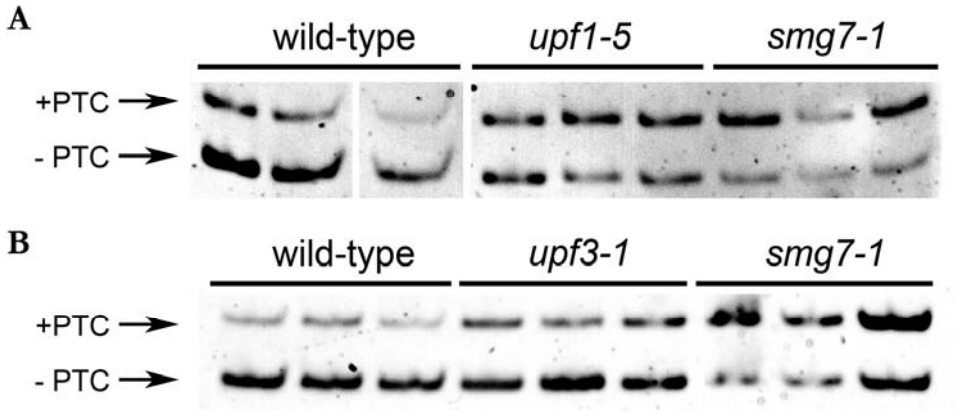

Figure 47. Analysis of +PTC/-PTC transcripts derived from the At2g45670 locus in *smg7-1* mutants compared to (A) *upf1-5* and (B) *upf3-1* mutants.

Although the NMD machinery seems affected in *smg7-1* mutants in a similar manner as in *upf1-5* mutants, the vegetative defects are much milder in *upf1-5* compared to *smg7-1*. These observations suggest that the impairment of the NMD machinery cannot

solely account for the defects in pathogen response or meiosis. Taken together these data show that SMG7 plays an additional function besides its role in NMD.

3 DISCUSSION

3.1 Identification and characterization of SMG7 and SMG7-like proteins in *Arabidopsis thaliana*

The *Arabidopsis* SMG7 and SMG7-like proteins belong to the EST1/SMG5-7 protein family, which all share protein homology over the EST1-TPR domain (figure 3). Based on the founding members, Est1p in *S. cerevisae* and SMG-5, SMG-6, and SMG-7 in *C. elegans*, the protein family was implicated in telomere biology and nonsense mediated RNA decay (Hodgkin, Papp et al. 1989; Lundblad and Szostak 1989; Cali, Kuchma et al. 1999). However, the characterization of these proteins in higher eukaryotes was limited to biochemical and functional studies. The aim of my PhD thesis was to characterize the EST1/SMG7 homologs in *Arabidopsis thaliana*. Both *Arabidopsis* proteins resembled the domain architecture of human SMG7 and thus were named AtSMG7 and AtSMG7-like (figure 4). Interestingly, SMG5 and SMG6 homologs, which are mainly characterized by the existence of a PIN domain, were not found in the plant kingdom. Whereas the SMG7 homolog is present in all plants, the presence of SMG7-like was restricted to dicots (figure 6), which suggests that the SMG7-like protein evolved later than SMG7. Additionally, characterization of the two different T-DNA insertion lines of the *AtSMG7-like* gene (figure 13) did not reveal obvious visible phenotypes, suggesting that the SMG7-like plays a less important role than SMG7.

Northern blot analysis of total RNA extracts showed that SMG7 is expressed ubiquitously in the plant (figure 8). Moreover, publically available microarray data showed a higher expression of SMG7 in pollen, which is consistent with SMG7 playing a role in gametogenesis. Additionally, high SMG7 expression was found in senescent leaves and xylem. I cloned and sequenced the full length cDNA of SMG7 and found an alternative splice variant. Within the sequenced cDNA, the end of the 7th exon shifted towards the 3`UTR, which results in a change of the stop codon, but does not lead to a change in the amino acid sequence (figure 7). Interestingly, the 3`UTR region of SMG7 has been shown to trigger NMD in a transient NMD assay in infiltrated tobacco leaves (Kerenyi, Merai et al. 2008). Additionally Kerenyi and colleagues found that the unusually long 3´UTR, as well as the presence of two introns

downstream of the stop codon, were conserved within flowering plants. The authors therefore speculate that SMG7 might act as a "sensor" for NMD and might "measure" NMD efficiency. Furthermore, microarray analysis of the *lba1* mutant showed a two-fold upregulation of *SMG7* transcripts, supporting the observation that SMG7 is regulated by NMD in *Arabidopsis* plants (Yoine, Ohto et al. 2006).

A major step in understanding the function of SMG7 is through the analysis of mutants. Therefore I characterized *SMG7* T-DNA insertion lines (figure 9, table 2). The *smg7-5* allele, which carries a T-DNA insertion in the conserved EST1-TPR domain, causes embryo lethality in homozygous mutant plants (figure 10). This indicates that the *Arabidopsis* SMG7 protein is essential, similar to its homologs in mammals. Complementation of the *smg7-5* allele with the full length *SMG7* gene and wild-type promoter gave rise to viable wild-type looking plants, indicating that the embryo lethality is caused by SMG7 deficiency.

All other mutant alleles (*smg7-1, smg7-2, smg7-3, smg7-6* and *smg7-4*) gave rise to viable homozygous mutant plants (figure 11). I could detect truncated SMG7 mRNAs in the mutant lines that correspond in size with the position of the T-DNA insertion (figure 12). These truncated mRNAs possibly lead to partially functional SMG7 proteins, thus the mutations are hypomorphic. Hence, the SMG7 hypomorphic mutant plants provide a good material to study, at least partially, the function of the essential SMG7 protein at the organismal level. Homozygous mutant plants for the *smg7-1, smg7-2,* and *smg7-3* alleles are completely sterile and show a variety of defects in vegetative growth and plant development. These phenotypes are clearly linked to the *smg7* mutation as I was able to fully complement the *smg7-1* allele with *SMG7* cDNA driven by the constitutively active ACTIN 2 promoter (table 3). The *smg7-4* allele contains a T-DNA insertion close to the end of the coding region and would lead to a truncation of 137aa. Homozygous *smg7-4* plants do not show a visible phenotype, which indicates that the last 137aa do not dramatically affect protein function, although a MYC-tag fused to the C-terminus of SMG7, leading to a loss of the last 9aa, did not complement the sterility of *smg7-1*. However, the *smg7-6* allele, in which the T-DNA insertion is located between the insertion sites of the *smg7-3* and the *smg7-4* alleles, does not show any vegetative defect but the fertility of the plant is affected, although the affect is less severe then in *smg7-1* (figure 24, chapter 2.4.1.2.). This indicates that

smg7-6 causes a separation of SMG7 function and that the region downstream of the *smg7-6* insertion is dispensable for the vegetative phenotype but still required for the meiotic function of SMG7.

3.2 SMG7 is a conserved factor of the Nonsense Mediated RNA decay

The SMG5, SMG6 and SMG7 proteins have been shown to be involved in nonsense mediated RNA decay in mammals (Ohnishi, Yamashita et al. 2003; Unterholzner and Izaurralde 2004) and invertebrates (Hodgkin, Papp et al. 1989; Cali, Kuchma et al. 1999; Gatfield, Unterholzner et al. 2003). Therefore I asked whether the *Arabidopsis* SMG7 protein is also involved in NMD. I analyzed three different naturally occurring NMD targets in *Arabidopsis* that arose due to alternative splicing (figure 16, Hori and Watanabe 2005). All three endogenous NMD targets were significantly upregulated in *smg7-1* mutants (table 4 and figure 18, 19). Upon inhibition of transcription, the +PTC transcript derived from the At2g45670 locus was rapidly degraded in wild-type plants, but stabilized in the *smg7-1* mutant (figure 20). These data indicate that degradation of the abnormal transcripts is impaired in the *smg7-1* mutant. PTC containing transcripts are recognized during a pioneer round of translation (reviewed in Maquat 2004). I showed that degradation of the PTC containing splice variants is dependent on translation (figure 21). Interestingly, NMD is impaired in *smg7-1*, *smg7-2* and *smg7-3* mutants but unaffected in *smg7-6* and *smg7-4* (figure 22), suggesting that the region upstream of the *smg7-6* insertion is essential for NMD. Taken together these data demonstrate that SMG7 is necessary for NMD, which indicates that the function of SMG7 is evolutionarily conserved.

A YFP tagged SMG7 protein localizes to cytoplasmic foci (figure 15). This is consistent with the localization of human SMG7, as it was shown to be located in cytoplasmic foci that co-localized with LSm4, a P-body marker (Unterholzner and Izaurralde 2004). P-bodies are the major site of mRNA degradation and contain many enzymes that participate in the degradation process, such as the exosome and decapping enzymes (reviewed in Eulalio, Behm-Ansmant et al. 2007). It would be interesting to test whether SMG7 co-localizes with P-body markers, such as the

decapping factors DCP1, DCP2 and VARICOUS which are currently the only proven plant P-body markers (Xu, Yang et al. 2006; Goeres, Van Norman et al. 2007; Iwasaki, Takeda et al. 2007). Another interesting observation was that a MYC-tagged SMG7 protein, which complemented the vegetative phenotype of *smg7-1,* was not soluble in standard protein extraction buffers (figure 14). This could indicate that the SMG7 protein binds to a large protein complex or membrane. Further analysis of the protein would be helpful to gain further insights into the function of SMG7.

3.3 SMG7 is important for meiotic cell cycle progression

Lack of SMG7 protein causes the complete sterility of mutant plants. Both male and female gametogenesis is severely affected (chapter 2.4.1). Examination of meiosis in pollen mother cells (figure 27) as well as embryosac mother cells (figure 28) of *smg7-1* revealed a severe delay at the anaphase II/telophase II transition, which resulted in the formation of an unusual anaphase II-like stage. These cells were characterized by separated chromatids that fail to aggregate in nuclei, disperse through the cell space and remain condensed (figure 27p-r). The second meiotic division is mechanistically similar to mitosis. However the anaphase defect in *smg7* was specific to meiosis and was not detected in mitotic cells (figure 29, table 5).

Cell cycle delays at the anaphase stage are very rare. Activation of the APC triggers the separation of the sister chromatids and subsequently the degradation of cyclin B (reviewed in Peters 2006). An anaphase arrest as observed in *smg7* would indicate that the activity of APC^{Cdc20} is uncoupled (figure 48).

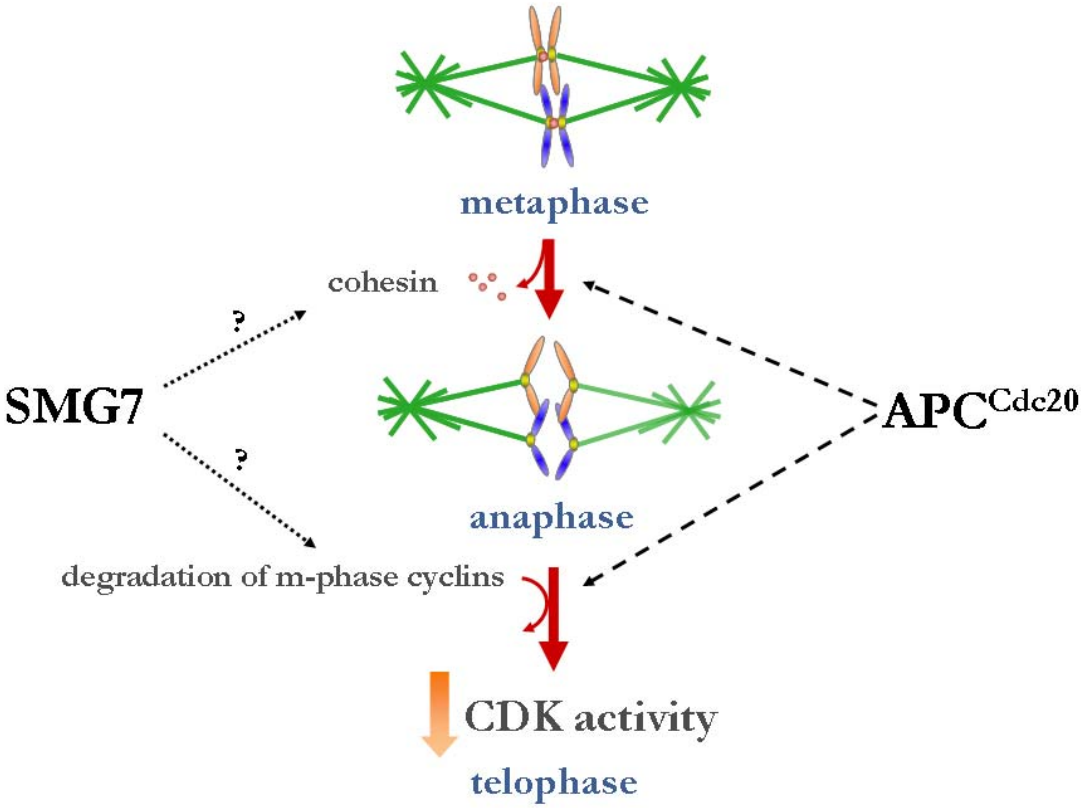

Figure 48. SMG7 uncouples APC^{Cdc20} activity.

Three likely scenarios can account for the anaphase II arrest that is observed in *smg7* mutants. The first hypothesis is that sister chromatid cohesion is lost before the spindle checkpoint becomes inactivated. A similar scenario has been shown to be the case in mitotic cells that were deficient for Shugoshin. These cells stalled in an anaphase-like arrest (Salic, Waters et al. 2004; Tang, Sun et al. 2004; Kitajima, Hauf et al. 2005; McGuinness, Hirota et al. 2005). To address this scenario I tested the preservation of centromeric cohesion prior to chromosome segregation. I found that centromeric cohesion is properly maintained in *smg7* mutants and that all chromosomes become properly bi-oriented at the metaphase II plate (figure 33). Hence, cohesion is not prematurely lost and prerequisites to deactivate the spindle checkpoint occur properly in *smg7* mutants. Therefore the cells should regularly enter into anaphase II. These data suggest that SMG7 acts downstream of APC^{Cdc20} activation.

A valuable hint as to how SMG7 protein might function came from crystal structure analysis. The EST1-TPR domain resembles a 14-3-3-like binding pocket (Fukuhara,

Ebert et al. 2005). It was shown that binding of human SMG7 to phosphorylated UPF1 is mediated by this domain. Additionally, the interaction of SMG5 and SMG7 with PP2A phosphatase is crucial for the dephosphorylation of UPF1 (Ohnishi, Yamashita et al. 2003). This suggests a second scenario where SMG7 could counteract CDK activity via facilitating the dephosphorylation of CDK substrates. Similar to its function in NMD, SMG7 could serve as an adapter molecule that recruits a phosphatase to the phosphorylated CDK substrates and promotes their dephosphorylation. In budding yeast it is well known that Cdc14 phosphatase is crucial for exit from M phase and *cdc14* mutants fail to progress through telophase (Culotti and Hartwell 1971), the responsible phosphatase in higher eukaryotes is not known (reviewed in Sullivan and Morgan 2007), which complicates further analysis of SMG7 function in this respect. Identification of proteins that interact with SMG7 could give further insights. However, a MYC-tagged SMG7 protein is insoluble in plant extracts, which hampers further protein studies, and a yeast two-hybrid screen of the N-terminal region of SMG7 against two different *Arabidopsis* cDNA library was unsuccessful (data not shown).

A third explanation for the anaphase arrest observed in *smg7* mutants is that cyclin B degradation is impaired. Cyclin B proteolysis is needed to decrease CDK activity so cells can exit meiosis or mitosis. Several reports showed that cells expressing a non-degradable cyclin B failed to exit the M phase (Holloway, Glotzer et al. 1993; Surana, Amon et al. 1993; Parry and O'Farrell 2001; Weingartner, Criqui et al. 2004; Potapova, Daum et al. 2006; Wolf, Wandke et al. 2006; Wolf, Sigl et al. 2007). A similar study showed that nondegradable cyclin B blocks mitotic exit and cytokinesis also in plants (Weingartner, Criqui et al. 2004). In mitotic cells that are stalled at anaphase by non-degradable cyclin B, an oscillating movement of the chromosomes between the spindle poles was observed by real-time imaging (Parry and O'Farrell 2001; Wolf, Wandke et al. 2006). Movement of chromosomes between the spindle poles could be the cause of the rearrangement of the chromosomes in *smg7* mutants. Moreover, in two studies it was shown that cyclin B dependent CDK activity is important for chromosome decondensation as well as spindle stability (Vagnarelli, Hudson et al. 2006; Woodbury and Morgan 2007). The rearrangement of chromosomes and the delayed chromatin decondensation observed in *smg7* mutants supports the hypothesis that SMG7 is important for down-regulation of cyclin B-dependent CDK activity.

To address this question I chose to analyze the distribution of cyclin B in *smg7* meiocytes. I tested the subcellular localization of cyclin B1;1 and showed that this cyclin resembles the expected spatial distribution of cyclin B in M phase (figure 34). However, I was unable to detect cyclin B1;1 in meiotic cells. Unfortunately, further investigation of this matter was limited as the *Arabidopsis* genome encodes at least ten other cyclin B-like proteins (Wang, Kong et al. 2004). It would be interesting to find out which cyclins are important for meiosis.

Drosophila cortex mutants show anaphase arrest in the second meiotic division that is caused by increased levels of cyclin A (Swan, Barcelo et al. 2005). Further characterization of the cortex gene showed that it encodes a meiotic Cdc20 subunit of APC (Page and Orr-Weaver 1996; Chu, Henrion et al. 2001). Therefore I tested whether SMG7 plays a role in the regulation of cyclin A and investigated the genetic interaction of *smg7-1* with *tam*, a temperature sensitive mutant of the meiotic cyclin A1;2 (Wang, Magnard et al. 2004). The characteristic feature of *tam* mutants is that at the restrictive temperature a cell wall is formed already after the first meiotic division leading to the formation of dyads (figure 35). In a wild-type situation, CDK activity between the two meiotic divisions is decreased but not completely abolished, therefore preventing the cell from progressing into cytokinesis (figure 49A). Due to the decreased cyclin A levels, CDK activity is lower in tam (figure 49B), allowing cell wall formation already at interkinesis. Additionally, lower cyclin A levels significantly delay the entrance to both M phases (Magnard, Yang et al. 2001).

Despite the decrease in cyclin A levels, s*mg7* / *tam* double mutants show the typical *smg7* anaphase II arrest (figure 36A) which indicates that cyclin A regulation is not affected by SMG7. However the *smg7* mutation abolished the cell wall formation in interkinesis that is typical for *tam* mutation. This surprising finding suggests that the meiotic role of SMG7 is not only restricted to anaphase II but that SMG7 contributes to the down-regulation of CDK activity already after the first meiotic division (figure 49C). Scoring of the meiotic cell cycle stages from anaphase I until metaphase II of wild-type, single and double mutants at the restrictive temperature showed that the delay in *tam* mutants is not only compensated by *smg7* mutation but interkinesis stages in the double mutant were very infrequently observed (figure 36B), suggesting that the duration of interkinesis stages was drastically shortened.

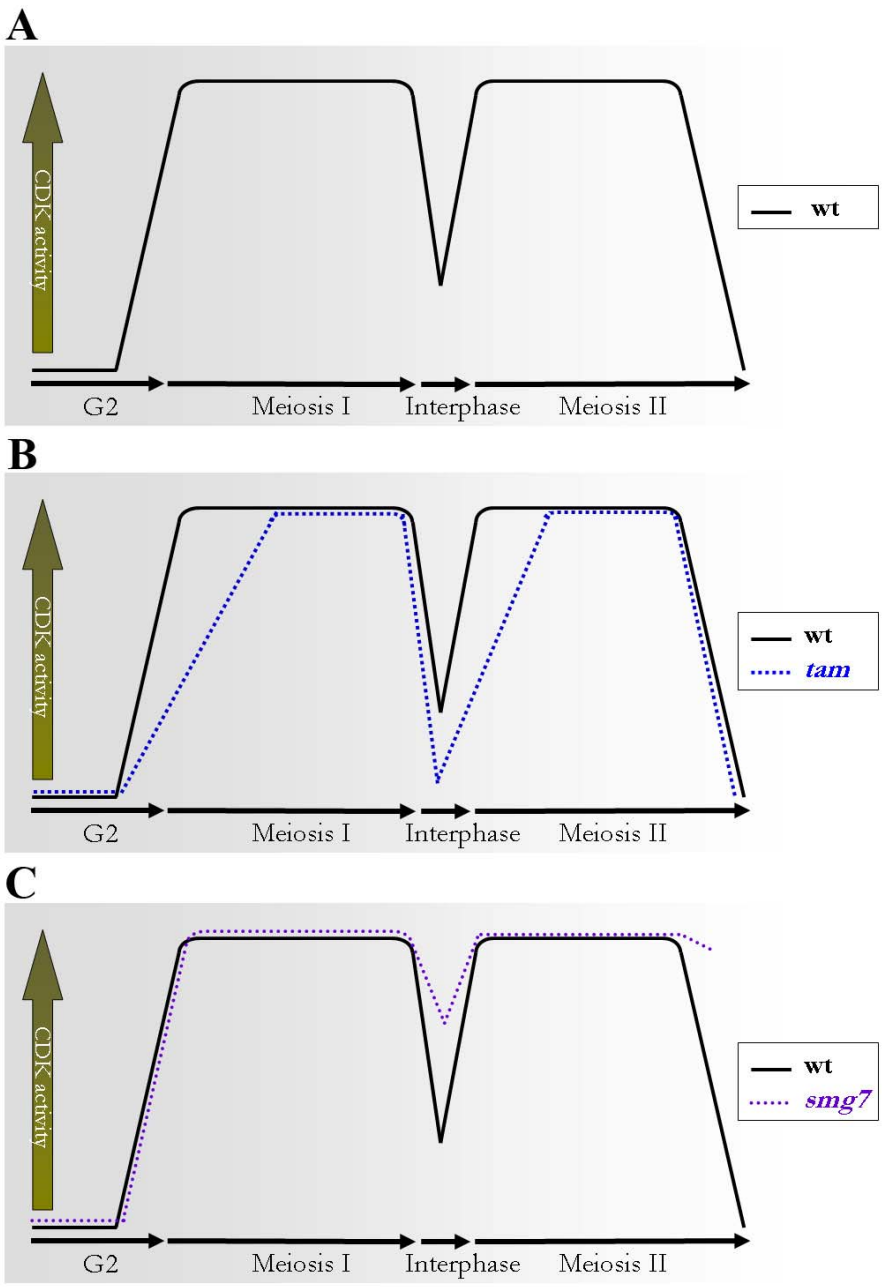

Figure 49. Hypothetical CDK activities in (A) wild-type, (B) *tam* and (C) *smg7*.

Additionally, chromosomes were highly condensed in *smg7 tam*, which suggests that SMG7 and cyclin A1;2 function synergistically during interkinesis and promote chromosome decondensation or suppress premature condensation. So far the exact role of cyclin A is not well understood (Yam, Fung et al. 2002; Fung and Poon 2005). Some studies suggest that cyclin A affects cyclin B. For instance, it has been reported that cyclin A contributes to the activation of cyclin B dependent CDK at the onset of mitosis (Fung, Ma et al. 2007). Furthermore, overexpression of cyclin A causes a cell

cycle delay in prometaphase, probably via affecting the stability of cyclin B (den Elzen and Pines 2001). Hence, a possible explanation for the effect of *smg7* mutation on the *tam* phenotype is, that the *Arabidopsis* cyclin A1;2 acts together with SMG7 and modulates cyclin B CDK activity during meiotic interphase.

How could SMG7 regulate CDK activity? Other NMD mutants such as UPF1 and UPF3 are fertile, indicating that the impaired NMD function is unlikely responsible for the *smg7* phenotype in meiosis. However SMG7 could play a broader role in RNA metabolism. For instance, SMG7 could regulate mRNA levels of cyclin B. Several studies showed that regulation of the level or processing of cyclin mRNA can be crucial for meiosis. Translational control of cyclins in budding yeast is important for the regulation of meiotic cell cycle (Jaillon, Bouhouche et al. 2008). Mes1p, an inhibitor of the APC is activated in meiosis due to alternative splicing (Kishida, Nagai et al. 1994). The budding yeast B-type cyclin *CLB3* mRNA has a feature of translational control in its 5´UTR region that restricts *CLB3* translation to meiosis II (Carlile and Amon 2008). It has also been shown in fission yeast that the meiosis specific RNA processing of the meiotic B-type cyclins *CRS1* and *REM1* is crucial for meiotic progression (Averbeck, Sunder et al. 2005; Malapeira, Moldon et al. 2005; McPheeters, Cremona et al. 2009).

Interestingly, the plant kingdom is lacking homologs of SMG5 and SMG6. Both proteins contain a PIN (PilT-amino-terminal) domain. In a recent study it was shown that PIN acts as an endonuclease and is important for the cleavage of targeted transcripts (Glavan, Behm-Ansmant et al. 2006). The absence of the PIN domain in plant homologs could indicate that the cleavage of mRNAs is not crucial for degradation or other endonucleases or PIN domain containing proteins are involved. The PIN domain containing protein AtPS1 has recently been found to play a role in meiosis (d'Erfurth, Jolivet et al. 2008). AtPS1 deficient plants show an abnormal orientation of the metaphase II spindle in male meiosis leading to a high frequency of diploid gamete formation. It will be interesting to find out whether AtPS1 plays a role in RNA decay and thus provides another link between RNA metabolism and meiosis.

A deeper comprehension of meiosis is important for fertility and reproduction, especially the understanding of plant meiosis can provide important knowledge useful

for crop production and plant breeding. Meiosis in plants is still poorly understood. Biochemical approaches to study meiotic functions are limited in *Arabidopsis* due to the small size of the anthers and the many important cell cycle players such as cyclins, CDK, and APC and its cofactors which have yet to be characterized for their role in meiosis. Besides SMG7, there are only very few factors that have been show to play a role in the exit from meiosis (reviewed in Hamant, Ma et al. 2006). Continuing investigations will be necessary to shed more light on the complex processes of meiosis.

3.4 Pathogen stress response is miss-regulated in *smg7* mutants

SMG7 deficient plants show a series of vegetative growth and developmental defects, which were modulated by humidity (figure 37). Strikingly, *smg7* mutants showed necrotic lesions on leaves that stained positive for dead cells (figure 39). Necrosis in the absence of biotic stress is a hallmark of lesion mimic mutants (reviewed in Lorrain, Vailleau et al. 2003). One example is the *bon1/cpn1* mutant. Mutations in the BON1/COPINE1 gene have been shown to cause dwarfism, necrotic lesions, and upregulation of PR transcripts (Jambunathan, Siani et al. 2001). Interestingly, like in *smg7* mutants, the penetrance of the phenotype of *bon1* mutant was humidity dependent. PR1 and salicylic acid levels were highly upregulated in *smg7* mutants (figure 42A and 43). PAD4 is a lipase like gene that has been shown to be important for salicylic acid signalling (Jirage, Tootle et al. 1999). Double mutants of *smg7-1* and *pad4-1* showed neither necrosis on leaves nor any of the vegetative defects that were observed in *smg7* single mutants (figure 40). Thus the attenuation of the pathogen signalling response in *smg7* mutants leads to a complete rescue of the *smg7* vegetative phenotype. Taken together these data indicate that the pathogen response is constitutively active in SMG7 deficient plants.

R gene mediated defense has been shown to cause the activation of the hypersensitive response, a specialized form of programmed cell death that leads to the formation of necrotic lesions (Jones and Dangl 2006). A suppressor of the *bon1* phenotype in the Wassiljewskia background turned out to be *SNC1*, an NBS-LRR type R gene (Yang

and Hua 2004). SNC1 requires PAD4 to activate the pathogen response (Zhang, Goritschnig et al. 2003). Furthermore, *SNC1* levels were upregulated in *upf1* mutants (Yi and Richards 2007). However double mutants of *snc1-11* and *smg7-1* did not restore the vegetative defects in *smg7*. Nevertheless R genes are good candidates for targets of SMG7, since many R genes are regulated on the post-transcriptional level (Zhang and Gassmann 2007).

Comparison of *smg7* mutants with other known NMD mutants such as *upf1* and *upf3* showed that both the vegetative phenotype and sterility are specific for *smg7*. This indicates that the defects in the pathogen response and meiosis are not caused by the impaired NMD machinery and that SMG7 has an additional function besides NMD. One possibility is that SMG7 plays a broader role in RNA metabolism than previously expected.

The *pad4-1* mutation restores all vegetative growth and developmental defects in *smg7-1* mutants but +PTC transcripts are still upregulated in *pad4-1* / *smg7-1* double mutants, indicating that the defect in NMD was unaffected by PAD4 deficiency (figure 41). Thus I was able to uncouple the vegetative phenotypes, caused by the activation of the pathogen response, with the defect in NMD. Interestingly, *pad4-1* / *smg7-1* double mutants do not show further visible defects indicating that further transcripts that might be miss-regulated by NMD do not cause an obvious phenotype. A strong mutant allele of UPF1, a conserved NMD factor, shows seedling lethality, but this does not imply that NMD is essential as UPF1 could be involved in other cellular processes. For instance, human UPF1 has also been implicated in other functions despite NMD such as SMD (staufen mediated RNA decay) or telomere maintenance (reviewed in Isken and Maquat 2008). Another study found that human UPF1 plays a role in genome stability during S phase in a non-NMD manner (Azzalin and Lingner 2006).

Besides NMD there exist more specialized mRNA degradation pathways such as nonstop mRNA decay (NSD), which degrades targets that lack a stop codon (Frischmeyer, van Hoof et al. 2002; van Hoof, Frischmeyer et al. 2002). Another mRNA surveillance pathway is the no-go decay (NGD), where secondary structures of the mRNA lead to a block of the translational elongation and thus to degradation of the mRNAs (Doma and Parker 2006) (reviewed in Isken and Maquat 2007). A model for

SMG7 action might be that it is involved in bridging several specialized mRNA degradation machineries with the general mRNA decay, or SMG7 might even play a role in general mRNA decay. Many mRNA degradation pathway mutants are embryo lethal. However weak alleles of some genes allow the study of viable plants and give hints towards some biological functions (reviewed in Chiba and Green 2009). For instance, a weak mutant allele of AtPARN, a poly(A) ribonuclease, has been implicated in abscisic acid (ABA), salicylic acid and stress responses (Nishimura, Kitahata et al. 2005). The CCR4/POP2 complex functions as deadenylase and degrades the poly(A) tail of mRNAs. CaCAF1, a POP2 homolog of chilli pepper (*Capsicum annuum*), has been implicated in pathogen response, since overexpression of CaCAF led to increased pathogen resistance in tomato (Sarowar, Oh et al. 2007). These are interesting observations which indicate that mutants affecting a major cell process can have specific effects on some developmental processes and stress responses.

A very interesting observation was that the *SMG7* transcript itself seems to underlay multi-facetted regulation. For instance, as discussed earlier, data from tobacco shows that *SMG7* itself is regulated via NMD (Kerenyi, Merai et al. 2008). Next *SMG7* transcripts were decreased in *pad4-1* mutant background (figure 42) suggesting that *SMG7* could be regulated by the pathogen response. The public microarray data queried with the Genevestigator tool (Hruz T 2008) showed an upregulation of *SMG7* in response to syringolin, a molecule that induces hypersensitive response in plants (Waspi, Schweizer et al. 2001). Taken together these data indicates that there is a feedback loop in the regulation of *SMG7*. It would be interesting to find out whether higher levels of *SMG7* transcript lead to a higher efficiency of NMD or the other unknown mechanism *SMG7* is involved in.

3.5 Conclusion and outlook

Taking together, I showed that SMG7 is involved in several biological processes. SMG7 is needed to complete the meiotic cell division, it plays an important role in the pathogen stress response, and it is an essential factor of nonsense mediated RNA decay. Other NMD mutants do not show phenotypes that implicate their involvement in the pathogen stress response or meiosis. This leads us to the hypothesis that SMG7 must play an NMD independent role in meiosis and pathogen response. One hypothesis is that the role of SMG7 in RNA metabolism has a wider spectrum then originally thought. One way to address this question is to compare the SMG7 and NMD mutants not only on the phenotypic but also on the transcriptome level. Differently regulated transcripts could provide hints as to the additional function of SMG7. It is puzzling that a protein that obviously plays a fundamental role in the cell can have specific defects in two specific biological processes, the meiotic cell cycle and the pathogen response. Further investigation of the miss-regulated molecules affecting these two pathways will be necessary to unravel the full function of SMG7.

4 MATERIAL AND METHODS

4.1 Arabidopsis protocols

4.1.1 Plant growth conditions

4.1.1.1 Arabidopsis thaliana cultivation on soil

Arabidopsis thaliana seeds were sown on a mixture of three parts soil and one part vermiculite. Plants were usually grown at 22°C under long day conditions (16h light / 8h dark). For analysis of the tam phenotype, *tam* / *smg7-1* double mutants, *smg7-1* single mutants and out-segregating wild-type control plants were grown for ~4-5 weeks under standard growth conditions until they were flowering, then they were switched to the restrictive temperature of 27°C. In low humidity (LH) experiments the humidome was removed 3-5 days after germination, whereas plants grown in high humidity (HH) the humidome was left on for up to 5 weeks. The difference in the relative humidity was ~60% for LH and ~90% for HH.

4.1.1.2 Arabidopsis thaliana cultivation on agar plates

Seeds were sterilized with bleaching solution (~ 6% sodium hypochloride + 0.1% Triton X-100) and plated on BM agar plates containing 4.33g/l MS complete salts (SIGMA), 20g/l sucrose, 0.5g/l MES (monohydrate (2-(N)-morpholino methansulfonic acid)) pH 5.8, Duchefa. Plates were sealed with leucopore tape and incubated at 4°C for 48h. Subsequently the plates were placed in a growth chamber at 22°C and plants were grown under long day (16h light /8h dark) conditions. After 2-3 weeks seedlings were transferred to soil.

4.1.2 *Arabidopsis thaliana* mutant lines

Table 6 represents a list of *Arabidopsis thaliana* mutant lines that were used during this project.

Name	Polymorphism	Type	Ecotype	AGI code	Reference
cycB1;1-GUS	cycB1;1-GUS	insertion	Col-0	AT4G37490	(Ferreira, Hemerly et al. 1994)
lba1	lba1	substitution	Col-0	AT5G47010	(Yoine, Nishii et al. 2006; Yoine, Ohto et al. 2006)
ndr1-1	ndr1-:PR1/GUS	deletion	Col-0	AT3G20600	(Century, Shapiro et al. 1997; Shapiro and Zhang 2001)
pad4-1	pad4-1	substitution	Col-0	AT3G52430	(Glazebrook, Zook et al. 1997; Nishimura, Stein et al. 2003)
smg7-1	SALK_073354	insertion	Col-0	AT5G19400	(Riehs, Akimcheva et al. 2008)
smg7-2	SALK_025699	insertion	Col-0	AT5G19400	(Riehs, Akimcheva et al. 2008)
smg7-3	SALK_112476	insertion	Col-0	AT5G19400	(Riehs, Akimcheva et al. 2008)
smg7-4	SAIL_63F08	insertion	Col-0	AT5G19400	
smg7-5	SALK_144162	insertion	Col-0	AT5G19400	
smg7-6	SALK_052532	insertion	Col-0	AT5G19400	
smg7l-1	SAIL_634H06	insertion	Col-0	AT1G28260	
smg7l-2	SALK_071725	insertion	Col-0	AT1G28260	
snc1-11	SALK_047058	insertion	Col-0	AT4G16890	(Yang and Hua 2004)
tam	-	substitution	Col-0	AT1G77390	(Magnard, Yang et al. 2001; Wang, Magnard et al. 2004)
upf1-2	SALK_004606	insertion	Col-0	AT5G47010	(Yoine, Nishii et al. 2006)

upf1-3	SALK_081178	insertion	Col-0	AT5G47010	(Arciga-Reyes, Wootton et al. 2006; Yoine, Nishii et al. 2006)
upf1-4	SALK_022721	insertion	Col-0	AT5G47010	(Arciga-Reyes, Wootton et al. 2006; Yoine, Nishii et al. 2006)
upf1-5	SALK_112922	insertion	Col-0	AT5G47010	(Arciga-Reyes, Wootton et al. 2006)
upf3-1	SALK_025175	insertion	Col-0	AT1G33980	(Hori and Watanabe 2005; Arciga-Reyes, Wootton et al. 2006)
upf3-2	SALK_097931	insertion	Col-0	AT1G33980	(Arciga-Reyes, Wootton et al. 2006)

Table 6. List of *Arabidopsis thaliana* mutant lines used for experiments.

4.1.3 Genotyping

4.1.3.1 Arabidopsis DNA extraction for genotyping

For DNA extraction, 1-2 rosette leaves or 3-4 inflorescences were ground in 400µl extraction buffer (200mM Tris-HCl pH7.5, 250mM NaCl, 25mM EDTA, 0.5% SDS). After a centrifugation step (13 000rpm, 5min, room temperature) the supernatant was transferred to a new reaction tube. In order to precipitate the DNA, 400µl isopropanol was added and mixed well. DNA was centrifuged at 13 000rpm for 10min at room temperature. The DNA pellet was washed with 70% ethanol, dried in the speed vacuum centrifuge and resuspended in 50µl water.

4.1.3.2 Genotyping PCR

The standard genotyping PCR condition for 1 reaction (20µl) contained 1µl template DNA, 1xPCR buffer (500mM KCl, 200mM Tris-HCl pH 8.3, 1.5mg/ml BSA), 0.2mM

dNTPs, 1.5mM $MgCl_2$, 0.5µM of each primer (table 7 and 8), 0.2µl home-made Taq polymerase. The standard cycling parameters were 94°C for 3 min, 40x (94°C for 15 sec, AT for 30 sec, 72°C for ET) and 72°C for 5 min. The primer combinations, the annealing temperature (AT) and the extension time (ET) for each allele are listed in table 7, the primer sequences are listed in table 8. In the case of dCAPS (Neff, Neff et al. 1998) genotyping (*lba1* and *pad4-1* alleles) the PCR products were digested with the enzyme listed in table 7. Fragments were mixed with 6x loading dye (60% glycerol, 10mM Tris-HCL pH 7.6, 0.03% Orange G, 60mM EDTA) and separated by agarose gel electrophoresis. 1-3% agarose gels were prepared in 1xTAE buffer (40mM Tris-acetate, 20mM EDTA pH 8.0) and stained with 0.5µg/ml ethidium bromide. To estimate the size of the products 5µl of GeneRuler™ 1 kb or 50bp DNA Ladder (Fermentas) was loaded on the gel. Electrophoresis was carried out at 90-120V. Bands were visualized with a GelDoc system (Biorad). The PCR products of the genotyping PCR for the *tam* allele were eluted from the gel with the Nucleospin Extract II kit (Macherey-Nagel) according to the manual and sequenced as described in section 5.5.2.5 using the cycA-Fnonspec primer.

Allele	Wild type allele	Mutant allele	AT (°C)	ET (sec)
cycB1;1-GUS	cyclinB-1 + GUS-1 (no product)	cyclinB-1 + GUS-1 (~1kbp)	60	60
lba1	lba1-dCAPS-F + lba1-dCAPS-R (+XbaI - 180bp)	lba1-dCAPS-F + lba1-dCAPS-R (+XbaI ~ 160bp)	55	30
ndr1-1	NDR-F + NDR-R2 (1575bp)	NDR-F + NDR-R2 (340bp)	60	90
pad4-1	pad4-1-PflmI-F + pad4-PflmI-R (+Van93I ~80bp)	pad4-1-PflmI-F + pad4- PflmI-R (+Van93I - 96bp)	55	30
pCBNR1	Est1b-1 + Est1b-2 (~560bp, cDNA ~460bp)	Est1b-1 + Lbc-1 (~300bp)	60	30
pCBNR2	Est1b-1 + Est1b-2 (~560bp, cDNA ~460bp)	Est1b-1 + Lbc-1 (~300bp)	60	30

pCBNR4	Est1b-1 + Est1b-2 (~560bp, cDNA ~460bp)	Est1b-1 + Lbc-1 (~300bp)	60	30
pCBNR5	Est1b-9 + Tnos-1 (vector ~667bp)	Est1b-2 + Lbc-1 (~700bp)	60	60
pCBNR6	Est1b-2 + Est1b-5 (~789bp, cDNA ~ 599bp)	Est1b-2 + Lbc-1 (~700bp)	60	60
pCBNR7	ACT2-1 + YFP-R (no product)	ACT2-1 + YFP-R (~1300kb)	55	90
smg7-1	Est1b-1 + Est1b-2 + Lbc-1 (~560bp)	Est1b-1 + Est1b-2 + Lbc1 (~300bp)	60	30
smg7-2 *smg7-3*	Est1b-14 + Est1b-7 + Lbc-1 (~1000bp)	Est1b-14 + Est1b-7 + Lbc-1 (~750bp)	60	60
smg7-4	Est1b-15 + Est1b-16 + SAIL-LB3 (~1kbp)	Est1b-15 + Est1b-16 + SAIL-LB3 (~600bp)	60	60
smg7-5	Est1b-2 + Est1b-5 (~800bp)	Est1b-2 + Lbc-1 (~750bp)	60	60
smg7-6	Est1b-7 + Est1b-14 + Lbc-1 (~1kbp)	Est1b-7 + Est1b-14 + Lbc-1 (~400bp)	60	60
smg7l-1	Smg7l-1 + Smg7l-2 + SAIL-LB3 (~480bp)	Smg7l-1 + Smg7l-2 + SAIL-LB3 (~100bp)	60	30
smg7l-2	Smg7l-3 + Smg7l-4 + Lbc-1 (~700bp)	Smg7l-3 + Smg7l-4 + Lbc-1 (~160bp)	60	60
snc1-11	SNC1F + SNC1R + Lbc-1 (~ 500bp)	SNC1F + SNC1R + Lbc-1 (~ 300bp)	60	30
tam	cycA-Fnonspec (sequencing: G at position 1455bp GI:186497660)	cycA-Rnonspec (sequencing: T at position 1455bp GI:186497660)	55	30
upf1-2	upf1-2F + upf1-2R + Lbc-1 (~800bp)	upf1-2F + upf1-2R + Lbc-1 (~500bp + 300bp)	55	60

upf1-3	upf1-3F + upf1-3R + Lbc-1 (~750bp)	upf1-3F + upf1-3R + Lbc-1 (~500bp)	55	60
upf1-4	upf1-4F + AtUPF1-1R + Lbc-1 (1073bp)	upf1-4F + AtUPF1-1R + Lbc-1 (~400bp)	55	60
upf1-5	AtUpf1-1F + AtUpf1-1R + Lbc-1 (~770bp)	AtUpf1-1F + AtUpf1-1R + Lbc-1 (~300 + ~500bp)	60	60
upf3-1	AtUpf3-1F + AtUpf3-6R + Lbc-1 (~1055bp)	AtUpf3-1F + AtUpf3-6R + Lbc-1 (~600bp)	60	60
upf3-2	AtUpf3-1F + AtUpf3-6R + Lbc-1 (~1055bp)	AtUpf3-1F + AtUpf3-6R + Lbc-1 (~300 + ~770bp)	60	60

Table 7. Primer combinations used for genotyping. AT = annealing temperature. ET = extenstion time.

Primer name	**Sequence in 5´to 3´ direction**
ACT2-1	CTG CCG CTG TTG TTT CTC CT
AtUPF1-1F	ACAATCCAAATCTTCAGTCTCA
AtUPF1-1R	CCCATAAGCCAATGATACCAAA
AtUPF3-1F	CCTGATTATCTTGAGTTTCTT
AtUPF3-6R	ATGCTGTTCCGGTTGTGGTGG
cycA f nonspec	TGTTACCTGCATGATGATAGCA
cycA r nonspec	GAACAGAAGACTCCATCTCCAA
cycB1-1	TTCTCGTTCGATTGTTCCTC
Est1b-1	GACCTTGGTAGCTGGTCCTGAG
Est1b-2	GGACAACAGGCCAACCATTCAAC
Est1b-5	GCCCGTGACAACTTGATTGTTGCTT
Est1b-7	GCAAACCCAGATAGGCTACTAGCA
Est1b-9	CACATAAGAGGAAAATGAAAATGT
Est1b-14	CGCTTGGACCTACGTTTATTGATG
Est1b-15	GCTGCTTCTCTTGCTAGTAGCCTA
Est1b-16	TGAGTGCCTACGCATGTGTAAACA
GUS-1	TCCCACCAACGCTGATCAAT
lba1-dCAPS-F	GTTGCCAGTGTTGATTCTTTTCTAG
lba1-dCAPS-R	TCCAACATTGATTTTCAGGAGA
LBc-1	TGGACCGCTTGCTGCAACTCT
NDR-F	GACGAGATTGCTCATTGCCATTGG

NDR-R2	CGAATAGCAAAGAATACGAGTAAA
pad4-1-PflmI-F	ATGAGTCGCATAAGACTAGCCAAG
pad4-1-PflmI-R	CCATTTCTTTCCTAAATGAAAATCA
SAIL-LB3	TAGCATCTGAATTTCATAACCAATCTCGATACAC
smg7l-1	TGCCGTTTCTGAGTGGTTTTCT
smg7l-2	GAGGAGATAATGTTGTACTTCA
smg7l-3	GAAGTCCTTGGCTCCTCTGGCT
smg7l-4	GATGGAGAGACTATCAAAGGCT
SNC1F	CTGGTGCCTGAATGAATTGGTGGA
SNC1R	GCGATGGTGGAACTGGATAGAGA
Tnos-1	GACGTTATTTATGAGATGGGT
upf1-2F	AATATGAAGGGAGGCTTTGGTG
upf1-2R	GCAGAACCACTTTCTACAAGAAGC
upf1-3F	GATGAGTCTACTCAAGCAACAG
upf1-3R	GAATCTCAAGACTCTCACCTG
upf1-4F	CGGGTGGATTTGCTGTTGAT
YFP-R	GAGCTCGACTGGTGATTTGCGGACT

Table 8. Sequences of genotyping primers.

4.1.4 Crossing

Plants were grown in soil for approximately 4-5 weeks until they were flowering. From the mother plant all siliques were cut off. From the top flower of the main stem, the shoot apical meristem, all small buds (<1mm) and opened flowers were snipped off and only the three to four largest closed buds were used for crossing. The buds were opened and anthers were carefully removed. Then anthers from just opened flowers were taken from the father plant and tapped on top of the pistils of the mother buds in order to cover them with yellow pollen. Seeds were harvested from the individual crossed siliques.

4.1.5 Agrobacter mediated gene transfer

4.1.5.1 Transforming a plasmid into Agrobacter tumefaciens

The pCB302 based binary vectors of interest were transformed in the *Agrobacterium tumefaciens* strain GV3101. The GV3101 strain contains the pMP90 helper plasmid that carries a gentamycin resistance marker. I used ~100ng of plasmid DNA and mixed it with 40µl of electrocompetent agrobacteria cells. The mixture was transferred to a

1mm pre-cooled cuvette and the transformation was performed with 400 Ω, 25 µF and 1.8kV. The length of the pulse was approximately 5-8ms. 1ml of LB liquid medium [1% tryptone, 0.5% yeast extract, 170mM NaCl] was added. Cells were transferred to a reaction tube and incubated at room temperature for 1h. 100µl of the cells were plated onto an LB agar plate (containing 50mg/l gentamycin and 50mg/l kanamycin (corresponding to the resistance marker of the binary vector)) and incubated for 2 days at 28°C. The selected agrobacteria clones were verified by colony PCR.

4.1.5.2 Transformation of Arabidopsis thaliana

A colony of a verified clone was plated on LB agar plates containing 50mg/l gentamycin and 50mg/l kanamycin. Plates were incubated at 28°C for 2 days. One large single colony was picked from the plate and mixed in 5ml LB medium with antibiotics. The inoculation was grown at 28° and 200rpm over night. The pre-culture was mixed with 500ml LB medium and again grown at 28°C over night. Then the agrobacteria were collected at 2800g and resuspended in 300ml of 5% sucrose solution + 200µl/l Silwet77. The siliques of young and freshly flowering *Arabidopsis* plants were removed. Then the flowers were dipped into the Agrobacterium suspension for 30 seconds. The plants were kept horizontally and under high humidity for two days to facilitate the transformation process. Seeds were harvested and transformed T1 plants were selected on 0.5 BM agar plates containing 10mg/l phosphinotricine (BASTA) and 250mg/l amoxycilin.

4.1.5.3 Transformation of Arabidopsis cell suspension culture

The transformation was performed according to Ferrando, Farras et al. 2000. A fresh culture of the *Agrobacterium* GV3101 strain containing the construct of interest was grown for 2-3 days at 28°C on selective LB plates containing 50mg/l gentamycin and 50mg/l kanamycin. 1-2 colonies were inoculated in 25ml liquid LB medium containing 50mg/l gentamycin and 50mg/l kanamycin and grown at 28°C under constant shaking at 130-180 rpm until the OD600 was 1. Then the bacteria cells were collected by centrifugation at 4000rpm for 10min at room temperature and the bacterial pellet was washed with suspension media (1x MS basal salts, 2x B5 Gamborg vitamins, 0.5g/l MES, 30g/l sucrose, pH 5.7-5.8 was adjusted with 1M KOH and sterile filtrated plant hormones (0.5 mg/l 2,4- dichlorophenoxyacetic acid, 2 mg/l indole-3-acetic acid

(IAA), 0.5 mg/l 6-(γ,γ-dimethylallylamino)-purine riboside (IPAR)) were added). The centrifugation step was repeated and the pellet was resuspended in 2.5ml suspension media in order to obtain a 10 fold concentration of the Agrobacterium culture.
The wild-type *Arabidopsis* cell suspension was cultured for four days following subculture. For the transformation of the cell suspension, 65µl of 0.2M acetosyringon was added to 25 ml of suspension culture. Then 1ml of the 10x concentrated *Agrobacterium* culture was added to the 25mls of acetosyringon-induced suspension. The suspension was further cultivated for 3 days. The cell suspension was centrifuged at 2600rpm for 5 min at room temperature without braking. Cells were washed four times with suspension media in order to remove the bacteria. After a final centrifugation step (2600rpm for 5min at room temperature without braking) 25ml of fresh suspension media was added. The transiently transformed culture was then subjected to protein extraction.

4.1.6 Trypan Blue staining

The trypan blue staining was carried out according to Koch and Slusarenko 1990. Mutant and wild-type control plants were grown on soil under high humidity for ~3 weeks to increase the size of *smg7* mutants in order to obtain comparable leaves. Then the humidome was removed and the plants were allowed to grow under low humidity conditions for 1-2 weeks. Rosette leaves of comparable age were snipped off and covered in lactophenol-trypan blue solution (10ml lactic acid (85%), 10ml glycerol, 10g phenol and 10mg trypan blue dissolved in 10ml distilled water). The leaves were boiled in the staining solution over a water bath for approximately 3min. The leaves were cleared in 2.5g/ml chloral hydrate solution for 2 days. The leaves were placed on slides and mounted in chloral hydrate solution. The preparation was covered with a cover slip, sealed with fixogum and examined under phase-contrast stereo microscope (Leica).

4.1.7 Salicylic acid measurement

Plants were grown for the first 2 weeks under high humidity then switched to low humidity and grown for another 2.5 weeks. Leaves of three plants were pooled and ground in liquid nitrogen to a fine powder. Free and total levels of salicylic acid were measured via HPLC by Bettina Dekrout according to Rozhon, Petutschnig et al. 2005.

4.1.8 Cordycepin and cycloheximide treatment

Plants were grown under the same conditions as described in section 4.1.7. For each experimental set up (with or without treatment) leaves of three *smg7-1* and three wild-type plants were cut in 0.5cm wide rectangular sections. The sections were infiltrated in incubation buffer under vacuum for 1h. The cordycepin treatment was carried out according to Gutierrez, Ewing et al. 2002 and Seeley, Byrne et al. 1992. The incubation buffer for the cordycepin treatment was comprised of 0.5M sucrose, 0.5M KCl, 0.1M sodium citrate pH 6.2. The cycloheximide treatment was performed as described in Hori and Watanabe 2005. For the cycloheximide treatment the incubation buffer contained 4,6g/l MS complete salts (SIGMA) and 10g/l sucrose. Two leaves of each set up were withdrawn (time point = 0h), immediately frozen in liquid nitrogen and used for total RNA extraction. The inhibitors were added to the incubation buffers to a final concentration of 150µg/ml for cordycepin and 20µg/ml for the cycloheximide treatment. At each time point (1h, 2h, 4h, 6h for cordycepin and 6h for cycloheximide) two leaves of each set up were sampled as described for time point zero.

4.2 RNA protocols

4.2.1 Total RNA extraction

4.2.1.1 RNA extraction

Around ~100 mg of fresh plant tissue (usually 2-3 leaves or 4-5 inflorescences) was ground to a fine powder in liquid nitrogen. 1ml of TRI REAGENT (Sigma) was added, gently mixed and incubated at room temperature for 10min. Then 0.2 ml chloroform was added, mixed and incubated at RT for 15min. After centrifugation at 13 000rpm at 4°C for 10min, the supernatant was transferred into a new 1.5ml reaction tube. Through mixing the supernatant with 0.4 volume of isopropanol the RNA was precipitated. The reaction tubes were left at room temperature for 15min before the RNA was centrifuged at 4°C at 13 000rpm for 10min. The pellet was washed with 70% ethanol, air dried and resuspended in 50 µL of nuclease free water. The RNA was stored at -70°C.

4.2.1.2 Measuring RNA concentration

The RNA concentration was determined by spectroscopy. RNA was diluted 250 times in nuclease free water, transferred to a quartz cuvette and the optical density (OD) was measured at 260nm. The concentration of the RNA sample was calculated using the following formula: Concentration [ng/µL] = OD(260nm) x 250 x 40

4.2.1.3 Testing RNA integrity

1 - 2µg of RNA (volume was adjusted to 5 µL with nuclease free water) was mixed with 5µL of 2x denaturing buffer (0,26g urea, 500µL 6x Loading Buffer III according to Sambrook J 2001, 200 µL of 5xTBE (445mM Tris, 445mM boric acid, 10mM EDTA) and 150µL sterile water). The mixture was incubated at 65°C for 3min and quickly cooled on ice for 1min before it was separated over a 1.5% agarose gel in 1xTBE buffer (89mM Tris, 89mM boric acid, 2mM EDTA). Intact RNA extracted from green tissues gave rise to five sharp bands whereas intact RNA from non-photosynthesizing tissues appeared as two sharp bands.

4.2.2 Two step RT-PCR

4.2.2.1 cDNA synthesis

For the cDNA synthesis reaction ~2µg RNA were mixed with 5pmol reverse primer (gene specific or Anchor dT) and incubated at 70°C for 5min. Then the mixture was quickly cooled on ice for 5min before adding components to the following final concentrations: 0.5mM dNTP, 30U M-MLV RT (h-) reverse transcriptase (MBI Fermentas) and 1x reaction buffer (supplied with M-MLV) in a total volume of 40µl. Reaction was incubated at 45°C for 1h. The enzyme was then inactivated by incubating the reaction at 70°C for 15min.

4.2.2.2 PCR amplification of +PTC/-PTC transcripts

For the analysis of NMD targets the standard protocol using home-made Taq polymerase was used. The reaction was set up similar to the PCR reaction described in "5.1.3.2. Genotyping PCR". The PCR cycling settings were 94°C – 3min, 30x (94°C - 15sec, 55°C - 30sec, 72°C - 2min 15sec) 72°C - 5min.

Because of the small size difference between the +PTC and –PTC amplified fragments, the PCR products were separated by nondenaturating polyacrylamide gel electrophoresis. For 30ml of polyacrylamid gels 8% acrylamide (29:1), 1x TBE (89mM Tris, 89mM boric acid, 2mM EDTA) and distilled water were mixed. After adding 140µl of 10% ammonium persulfate (APS) and 30µl TEMED (N,N,N´,N´Tetramethylethylenediamine) the mixture was poured between the glass plates (16.5cm x 22cm) with 0.5mm thick spacers and an appropriate well comb was added (Slab Gel chambers, C.B.S. Scientific). The gel was left to polymerize at room temperature for ~20min. The PCR samples were diluted 1:40 and mixed with 6x loading buffer III (0.25% (w/v) bromphenolblue, 0.25% (w/v) xylene cyanol FF, 30% glycerol, distilled water, according to Sambrook J 2001 and distilled water to a total volume of 20µl and loaded on the gel. 3µl of GeneRuler™ 50 bp DNA Ladder (Fermentas) was used for size estimation. The gel was run at 180V for 14h. DNA was stained with SYBR(R) Green I (SIGMA) and scanned with the Molecular Imager FX (Biorad). The images were analyzed with Quantity One (Biorad).

4.2.2.3 Generating PCR products for cloning

For cloning purposes I used a high fidelity enzyme such as KOD DNA polymerase (Novagen). One PCR reaction with total volume of 50µl was set up as followes: 1x buffer#1 (supplied by Novagen), 0.2mM dNTPs, 1mM $MgCl_2$, 0.4µM of each gene specific primer, 10U KOD HiFi DNA polymerase. Standard PCR cycling conditions were: 98°C for 1min, 25x (98°C for 20sec, 55°C for 30sec, 72°C for 90sec) 72°C for 2min. The KOD enzyme generates blunt ended PCR fragments. To obtain PCR products with 3`A overhangs for TOPO cloning, 0.4µl of home-made Taq polymerase was added to the reaction and incubated at 72°C for 15min.

4.2.3 3´Race

2-5µg of total RNA was mixed with 5pmol of Anchor dT primer and reverse transcribed to cDNA according to the procedure described in section 4.2.2.1. The first PCR reaction was carried out with a forward primer (Est1b-GSP1) binding ~500bp upstream of the expected transcription stop and the Anchor primer. For this reaction 5-10µl cDNA were mixed with 1x buffer Mg^{2+} free (supplied by Takara), 200µM dNTPs, 1.5mM $MgCl_2$, 0.5µM of each primer, 1.25U Ex Taq polymerase (Takara) in 50µl total

volume. The cycling parameters were: 94°C - 1min; 40x (94°C - 30sec, 55°C – 1min, 72°C -30sec) 72°C -2min. The first PCR reaction was diluted 1:100. 1µl of the dilution was used in a second round of PCR amplification with a nested gene specific forward primer (Est1b-GSP2) and the Anchor primer. PCR conditions were similar to before with 30 cycles instead of 40. After separating the PCR products by agarose gel electrophoresis, specific bands were excised, eluted and sequenced. All primer sequences are listed in table 9.

Primer name	Sequence in 5´to 3´ direction
Anchor dT	GACCACGCGTATCGATGTCGAC(T)16V
Anchor	GACCACGCGTATCGATGTCGAC
Est1b-GSP1	ATTACGCCACCTCTGGGAAACCAGAA
Est1b-GSP2	TCCAACTTCACAGGTCCAAGCAGATT

Table 9. Primers used for 3´RACE.

4.2.4 Formaldehyde agarose (FA) gel electrophoresis

For 100ml FA gel 1,6g agarose were heated in 1x FA gel buffer (20mM 3-[N-Morpholino] propanesulfonic acid, 5mM sodium acetate, 1mM EDTA pH 7.0) until it was melted. After cooling the mixture down to 65°C, 1.8ml of 37% formaldehyde and 2µl of 5mg/ml ethidium bromide were added and the gel was poured onto gel support. The solidified gel was equlibrated in 1xFA gel buffer for at least 30min before RNA samples were loaded. Around 20µg of the RNA was mixed with 1 volume of 5x loading buffer (4mM EDTA pH 8.0, 2.7% formaldehyde, 20% glycerol, 30% formamide, 4x FA gel buffer and a drop of a saturated aqueous bromphenolblue solution) and incubated at 65°C for 3-5min. The RNA was cooled on ice before it was loaded onto the FA gel. 5-7 V/cm were applied until the bromphenol blue front of the loading dye reached the bottom of the gel.

4.3 Nucleic acid blotting

4.3.1 Northern blot

The formaldehyde agarose gel with the separated RNA was soaked in water for 10-15min and then in 10x SSC (1.5M NaCl, 150mM Na-citrate pH 7.0) for an additional 10-15min. The "up to down" northern transfer was set up as followed: On top of a stack of cellulose paper towels were placed whatman filter paper and an uncharged nylon membrane (Hybond NX, Amersham), which were both soaked in 10x SSC. The gel was laid upon the membrane without trapping air bubbles in between. The gel was covered with another layer of pre-wet whatman paper and a sponge soaked with 10x SSC was applied on top in order to prevent drying. The blotting stack was left for 24h. The RNA was cross-linked to the membrane with a UV cross-linker.
Northern blots were usually kept wet and at-20°C. To reuse northern blots, radioactive signals can be stripped off. For mild treatment, the blots were soaked in 0.5% SDS at 60°C for 2h.

4.3.2 Southern blot

RT-PCR products were separated over a 3% agarose gel. Then the gel was soaked in 0.25M HCl for 10min in order to depurinate the DNA. After washing the gel with distilled water, it was submerged in denaturing solution (0.5 M NaOH, 1.5 M NaCl) for 30min, washed again with distilled water and incubated with neutralization solution (0.5 M TrisCl, 1.5 M NaCl pH 7.0) for 15min. The "up to down" transfer was set up in a manner similar to the northern transfer (described in 4.2.5).

4.3.3 Labeling of dsDNA probes

Fragments of interest were amplified from cDNA with primers listed in table 10. 25-50ng of the PCR product was mixed with 1µl of each gene specific primer (10µM) and 1µl random primers (125ng/µl) in a total volume of 30µl. Denaturation step was carried out at 95°C for 5min. Subsequently the reaction tube was cooled on ice for 5min. Then 10µl of 5x labeling buffer (250mM Tris HCl pH 8.0, 25mM $MgCl_2$, 5mM 2-mercaptoethanol, 2mM of each dCTP, dGTP and dTTP and 1M HEPES pH 6.6), 20µg BSA, 5U Klenow fragment (Fermentas) and 5µl [a32P] ATP (>3000Ci/mmol)

were added. The final volume of the reaction was 50µl. Then the reaction was incubated at 37°C for 1h. Purification of the labeled probe was performed with the nucleotide removal kit (QIAGEN) as described in the manual. The probe was boiled for 5min prior to hybridization.

Primer name	Sequence in 5´to 3´ direction
Est1b-6	CACCTTTCCCTCTTCCTTTACCAGT
AtEST1-1	GGATCCATGATGACTTTACAGATGGATAA
Act2-5	GTATTGTGCTCGATTCTGGTGATG
Act2-6	CTGTTGGAAGGTGCTGAGGGATG
PR1-F	ACAAGATTATCTAAGGGTTCACAA
PR1-R	TTAGTATGGCTTCTCGTTCACATA
NMD5-FP	GGAAGCAACATACAAGGACCCA
ATS2-R	TCCATGTCCATATCCACCTCC

Table 10. Primers used for generating probes.

4.3.4 Hybridization of dsDNA probes to northern and southern blots

The nylon membrane was incubated with 20ml hybridization buffer (7% SDS, 0.25M Na-phosphate buffer pH 7.0, 0.1 g/l BSA) for 2h at 65°C in order to pre-hybridize it. The labeled probe was added to the buffer and the membrane was hybridized over night at 65°C. The non-specific signal was washed off at 65°C during three washing steps with 2x SSC (300mM NaCl, 30mM Na-citrate pH 7.0), 0.1 % SDS for 2x 10min and with 1x SSC (150mM NaCl, 15mM Na-citrate pH 7.0), 0.1 % SDS for 1h. The membranes were wrapped in saran foil and exposed to a phosphor screen (Kodak). The images were taken with Molecular Imager FX (Biorad) and analyzed with the software Quantity One (Biorad).

4.4 Protein protocols

4.4.1 Protein extraction

4.4.1.1 Protein extraction with 2x extraction buffer

Plant tissue was homogenized in liquid nitrogen and the powder was resuspended 1:1 in 2 x extraction buffer (100mM Tris-HCl, 2mM EDTA, 1mM DTT, 20% glycerol,

0.2% NP-40) containing protease inhibitors (Complete Mini, Roche) and PMSF. Cell debris was removed by centrifugation for 10min at maximum speed at 4°C. Supernatant was transferred into a fresh tube. Protein extract was stored at -80°C.

Protein concentration was determined by Bradford assay. 1 or 2 µl fresh protein extract as well as BSA standards ranging from 1mg/ml to 30mg/ml were mixed with 1ml bradford-solution (RotiQuant, Carl Roth) and absorbance was measured at 595nm wavelength. Concentration was measured relative to the standard curve.

4.4.1.2 TCA protein extraction

The required plant tissue was frozen in liquid nitrogen and ground with a mortar and pestle. The homogenized material was transferred to a 50ml falcon tube. For each gram of material around 10ml precipitation solution (10% (w/v) TCA, 0.07% β-mercaptoethanol in acetone) was added immediately. The protein extract suspension was aliquoted in 1,5ml eppendorf tubes and dipped in liquid nitrogen for 30sec, followed by incubation at -20°C for 45min to 2h. Then the suspension was vortexed and centrifuged at maximum speed at 4°C for 15min. The supernatant was discarded and 1.5ml washing solution (0.07% 2-Mercaptoethanol in acetone) was added. The hard pellet was broken up with a 1ml pipette tip. The suspension was again dipped in liquid nitrogen, and incubated at -20°C for 30min. The washing step was repeated once more. Then the supernatant was removed and residual acetone was removed with the speed-vac centrifuge. Pellets were dissolve directly in ~ 200µl 2x SSB (100mM Tris-HCl pH 6.8, 20% glycerol, 10% β-mercaptoethanol, 5% SDS, 0.01% bromphenol blue) and 1M unbuffered Tris base was added until the color turned blue. The samples were boiled at 95°C for 5min prior to loading them on a SDS–polyacrylamide gel. The remaining aliquots were stored at -80°C.

4.4.2 SDS polyacrylamid gel electrophoresis

Protein SDS polyacrylamide gel electrophoresis was performed using the BIORAD mini gel appliance according to the discontinous system described by Laemmli 1970. A 10% polyacrylamide gel was used as this was suitable to separate proteins ranging from 30-120kDa in size. The 6ml running gel was prepared with 10% acrylamide (29:1) (Fluka), 0.375M Tris-HCl pH 8.7, 0.1% SDS, 0.1% ammonium persulfate

(APS) and distilled water. 6µl TEMED were added and the mixture poured between the glass plates, and covered with isopropanol. After the gel polymerized, isopropanol was washed off and 2ml of stacking gel mixture (5% acrylamid (29:1) (Fluka), 0.125M Tris-HCl pH 6.8, 0.1% SDS, 0.1% ammonium persulfate and 4µl TEMED) were prepared and poured on top of the running gel. The gel chamber was set up according to the manufacturer's instructions.

Protein extracts were mixed with 2x SSB and boiled for 5 min at 95°C before they were loaded onto the gel. 3µl pre-stained protein marker (Fermentas) was used for size estimation. Electrophoresis was carried out in electrophoresis buffer [200mM glycine, 0.1% SDS, 50mM Tris-HCl pH 8.3] at 150V at room temperature for 1h.

4.4.3 Western transfer and immunostaining

PVDF membranes were rinsed in methanol and placed in water for 2 min. To pre-equilibrate the membrane and the gel, they were soaked in transfer solution [200mM glycine, 25mM Tris-HCl, 20% methanol] for at least 15min prior to the blotting. Together the gel, membrane and wetted whatman filter paper were arranged in a blotting appliance according to the instruction manual. The transfer was carried out at 4°C at 380mA for 90min. To test the transfer quality the membrane was stained with ponceau solution [0.2% PonceauS, 5% acetic acid] and destained with distilled water.

The membrane was washed with 1x TBS (10mM Tris, 150mM NaCl) + 0.2 % Tween-20 three times for 10min. Then the membrane was incubated with blocking solution (5% low-fat milk powder in 1x TBS + 0.2% Tween-20) for 1h at room temperature. The primary antibody was diluted in blocking solution to the end concentration listed in table 11 and applied to the membrane at 4°C over night. To remove unbound antibodies the membrane was washed three times for 10min with 1x TBS + 0.2% Tween-20 at room temperature. The secondary antibody was diluted in 1x TBS + 0.2% Tween-20 (table 11). The membrane was incubated with the secondary antibody for 2h at room temperature, then washed again three times for 10min with 1x TBS + 0.2% Tween-20. Signals were detected with ECL Western Blotting substrate kit (Pierce #32209) and exposed on film (Kodak).

Primary antibodies	Working dilution
anti - C-myc, mouse monoclonal	1 : 20 000
Secondary antibodies	**Working dilution**
α – mouse conjugated to HRP (PIERCE #31444)	1 : 100 000

Table 11. Antibodies used for western blots.

4.5 Cloning

4.5.1 Generation of plasmids

4.5.1.1 Cloning of the SMG7 cDNA

According to section 4.2.2.1 RNA, which was extracted from suspension culture (kindly provided by Svetlana Akimcheva) was reverse transcribed with the AtEST1-2 primer. The cDNA was used as a template to amplify three overlapping ~1kbp fragments of the SMG7 cDNA. The AtEST1-1 and Est1b-2 primers were used to amplify the first fragment (SMG7-I), the Est1b-1 and Est1b-7 primers were used for SMG7-II amplification and SMG7-III was generated with SeqEst1-5-4 and AtEST1-2 primers (table 12). All PCR reactions were performed as described in section 4.2.2.2, cloned into pCR2.1-TOPO vector (invitrogen) according to the manual and transformed in Top10F´ cells. All constructs were verified by sequencing (see section 4.5.2.6). The full length cDNA was constructed by combining all three ~1kb fragments. The SMG7-I was digested with *Bam*HI and *Bsm*I, SMG7-II was digested with *Bsm*I and *Bst*EII and SMG7-III was digested with *Bst*EII and *Sac*I. The fragments were ligated together in pCR2.1-TOPO vector, which was cut with the *Bam*HI and *Sac*I restriction enzymes, and transformed in Top10F´ cells.

4.5.1.2 Cloning of the pCBNR1 construct (ACT2::SMG7)

The TOPO vector containing the SMG7 cDNA and the pCBK06 vector, that contained a 35S promoter, were digested with *Bam*HI and *Sac*I. The SMG7 cDNA was ligated with the vector backbone and transformed in Top10F´ chemical competent cells (figure 50).

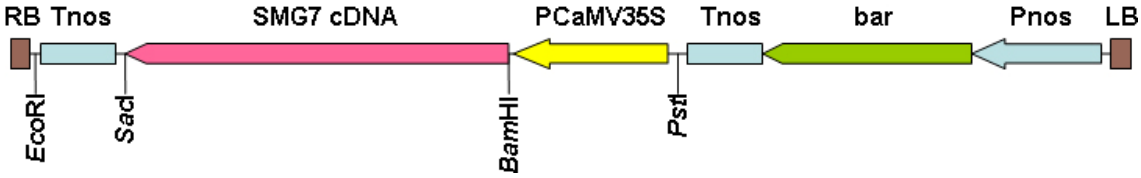

Figure 50. Schematic drawing of the pCBNR1 construct.

4.5.1.3 Cloning of the pCBNR2 construct (35S::SMG7)

The *SMG7* cDNA was cloned into the vector backbone of pCBM10 (containing the ACT2 promoter) giving rise to pCBNR2 construct (figure 51). The cloning procedure was performed in the same way as described in 4.5.1.2.

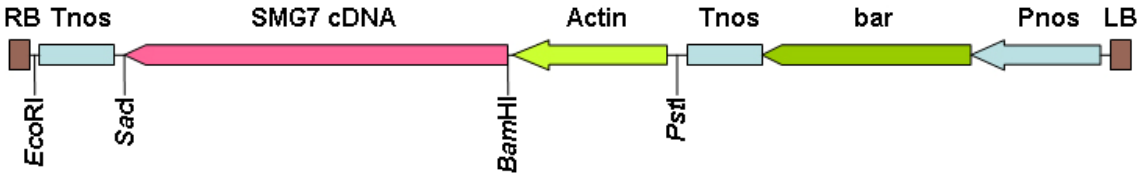

Figure 51. Schematic drawing of the pCBNR2 construct.

4.5.1.4 Cloning of the pCBNR4 construct (ACT2::SMG7-12xC-myc)

To generate the pCR-12-myc vector the 12xC-myc fragment was amplified out of the pCBS06 vector. In a total volume of 50µl around 0.5µg pCBS06 plasmid, 1x HF buffer (Biorad), 200µM of each dNTP, 0.5µM myc.R primer, 0.5µM SalI-myc.F primer and distilled water were mixed (for primer sequences see table 12). 1 unit of iProof High-Fidelity DNA Polymerase (Biorad) was added during the first denaturing step (hotstart). The cycling parameters were 98°C for 3min, 18x (98°C for 10sec, 55°C for 30sec, 72°C for 30sec) followed by a final extenstion step at 72°C for 5min. The 3´A overhangs were created by incubating the PCR reaction with 0.4µl home-made Taq polymerase at 72°C for 15min. The PCR product was cloned into pCR2.1-TOPO vector (invitrogen) according to the manual. The pCR-12myc vector was digested with *Sal*I, *Sac*I. The SMG7 cDNA was cut out of the pCR-cSMG7 with *Bam*HI, *Sal*I. Together the SMG7 cDNA and 12xmyc fragment was ligated with the vector backbone of pCBM10 which was digested before with *Bam*HI, *Sac*I giving rise to the pCBNR4 construct (figure 52). The ligation mixture was transformed in Top10F´ chemical competent cells.

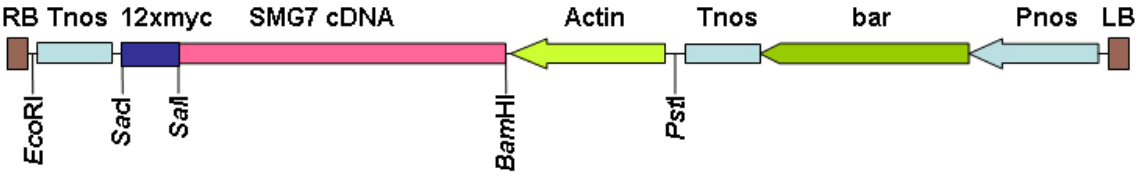

Figure 52. Schematic drawing of the pCBNR4 construct.

4.5.1.5 Cloning of the pCBNR5 construct (SMG7::SMG7)

The SMG7 promoter and gene was amplified from *Arabidopsis* wild-type DNA (kindly provided by Barbara Zellinger). The 50µl reaction was comprised of 0.1µg DNA, 1x HF buffer (Biorad), 200µM of each dNTP, 0.5µM pEST1b-1(*Sbf*I) primer, 0.5µM SacI-Est1b-R primer and distilled water (for primer sequences see table 12). 1 unit of iProof High-Fidelity DNA Polymerase (Biorad) was added hotstart. The PCR settings were 98°C for 3min, 25x (98°C for 10sec, 60°C for 30sec, 72°C for 3min) and 72°C for 10min. The 3´A overhangs were added with 0.4µl home-made Taq polymerase at 72°C for 15min. The PCR fragment was cloned into pCR2.1-TOPO vector (invitrogen) according to the manufacturer's instructions. The vector, now called pCR-pgSMG7, was digested with *Sbf*I, *Sac*I and ligated with the vector backbone that was cut out of the pCBK06 vector with *Pst*I and *Sac*I (figure 53).

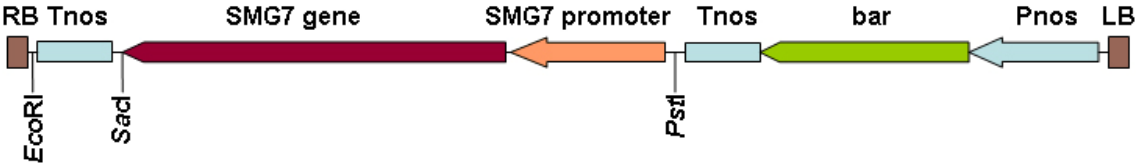

Figure 53. Schematic drawing of the pCBNR5 construct.

4.5.1.6 Cloning of the pCBNR6 construct (ACT2::SMG7-YFP)

The YFP cDNA was amplified from the pGWR8-ASKkappa-YFP vector (kindly provided by Wilfried Rozhon). The 50µl PCR reaction contained: 1x buffer#1 (supplied by Novagen), 0.2mM dNTPs, 1mM $MgCl_2$, 0.4µM of *Bam*HI-*Sal*I-YFP-F primer, 0.4µM *Sac*I-YFP-R primer (for primer sequences see table 12). 10 units KOD HiFi DNA polymerase (Novagen) was added hot start. PCR cycling conditions were

set up as follows: 98°C for 3min, 15x (98°C for 30sec, 60°C for 30sec, 72°C for 1min) 72°C for 2min. To generate PCR products with 3`A overhangs, 0.4µl of home-made Taq polymerase was added to the reaction and incubated at 72°C for 15min. YFP fragment was cloned into the pCR2.1-TOPO vector (invitrogen) according to the manual and transformed in Top10F´. The *SMG7* cDNA was cut out of the TOPO vector with *Bam*HI and *Sal*I restriction enzymes. The pCBM10 vector was digested with *Bam*HI, *Sac*I and the pCR-YFP vector was digested with *Sal*I and *Sac*I. Together the SMG7 cDNA, the pCBM10 vector backbone and the YFP cDNA was ligated together and transformed into Top10F´ (figure 54).

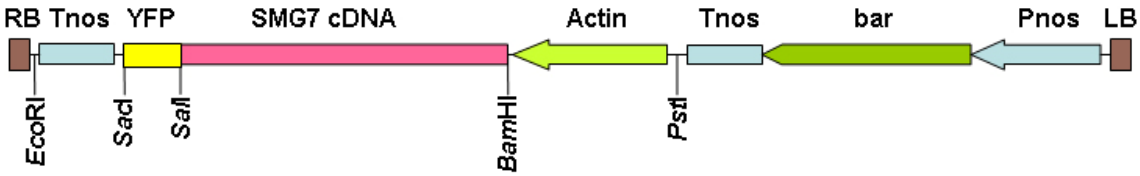

Figure 54. Schematic drawing of the pCBNR6 construct.

4.5.1.7 Cloning of the pCBNR7construct (ACT2::YFP)

The pCR-YFP construct described in 5.5.1.6 was digested with *Bam*HI and *Sac*I. The YFP fragment was ligated with the backbone of the pCBM10 vector, which was digested with *Bam*HI and *Sac*I as well. The ligation was transformed in Top10F´ (figure 55).

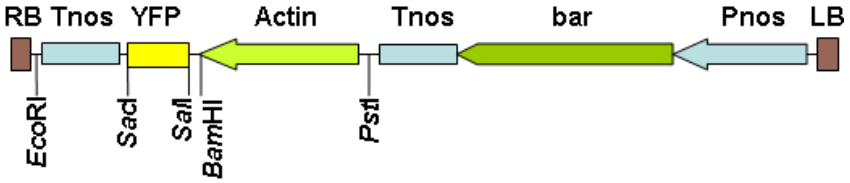

Figure 55. Schematic drawing of the pCBNR7 construct.

Primer name	Sequence in 5´to 3´ direction
AtEST1-1	GGATCCATGATGACTTTACAGATGGATAA
AtEST1-2	GGATCCATGATGACTTTACAGATGGATAA
BamHI-SalI-YFP-F	GGATCCGTCGACTATGGTGAGCAAGG
Est1b-2	GGACAACAGGCCAACCATTCAAC
Est1b-7	GCAAACCCAGATAGGCTACTAGCA

myc.R	TTGCCAAATGTTTGAACGAT
pEST1b-1(SbfI)	CCTGCAGGAAGCCAATTACAACTGAAAGT
SacI-Est1b-R	GAGCTCGTTGAAGGAGAGAGGGCT
SacI-YFP-R	GAGCTCGACTGGTGATTTGCGGACT
SalI_myc.F	GTCGACTGGTTCTGCTGCTAGTGGTGAA
SeqEst1-5-4	AATCACAGGTCGCACAACCA

Table 12. Primers used for cloning.

4.5.2 Standard cloning techniques

4.5.2.1 Restriction enzyme digest

For one 20µl standard restriction enzyme digest reaction 1µg of DNA was mixed with 1x reaction buffer (supplied with the restriction enzyme), 1U of restriction enzyme and distilled water. The reaction was incubated at 37°C (or at the recommended temperature) for 2h. Restriction fragments were separated over agarose gel electrophoresis. The specific bands were excised and eluted with the Nucleospin Extract II kit (Macherey-Nagel) according to the manufacturer's instruction.

4.5.2.2 Ligation

For a standard ligation reaction ~20ng vector DNA was mixed with insert DNA to achieve a molar ratio of 1 mole vector to 5 moles insert. Then 1x ligation buffer and 1 Weiss unit of T4 DNA ligase (both MBI Fermentas) were added. The reaction was diluted to a total volume of 10µl with distilled water and incubated at room temperature for 2h or at 4°C over night.

4.5.2.3 Preparation of chemical competent E. coli

To prepare chemical competent cells 5ml LB was inoculated with the Top10F´ strain and grown at 37°C, 200rpm over night. 1ml of the pre-culture was added to 250ml LB + 10mM MgSO4 liquid media and incubated at 37°C until the OD[590nm] reached 0.4 - 0.6. The cells were collected at 4000rpm for 5min at 4°C and resuspended in 100ml pre-cooled TFB1 buffer [100mM RbCl, 30mM potassium acetate, 10mM $CaCl_2$, 50mM $MnCl_2$, 6.7% glycerol, pH 5.8 was adjusted with acetic acid]. The suspension

was incubated on ice for 5min then centrifuged at 4000rpm, 4°C for 5min. The pellet was resuspended in 10ml ice cold TFB2 buffer [10mM PIPES pH 6.5, 75mM $CaCl_2$, 10mM RbCl, 6.7% glycerol, pH6.5 was adjusted with KOH] and incubated on ice for 15-60min. 100µl aliquotes were quickly frozen in liquid nitrogen and stored at -80°C.

4.5.2.4 Transformation of chemical competent E. coli

For transformation, aliquots were thawed on ice and 1ng plasmid or 10µl ligation mixture was added. The reaction tube was placed on ice for 5min. Cells were heat shocked at 42°C for 45sec and afterwards immediately placed on ice. 0.9ml LB liquid media was added and incubated at 37°C and slowly shaken for 1h. The transformed cells were plated on an LB plate + 50mg/l of an appropriate antibiotic. For IPTG/X-Gal - blue white selection 40µl of 100mM IPTG and 40µl of X-gal (40mg/ml) were spread on the plate prior to plating the cells. The plate was incubated at 37°C over night. White colonies were screened for the insert DNA with colony PCR.

4.5.2.5 Plasmid extraction from E.coli

A single colony of a positive clone was used to inoculate 5ml LB [1% tryptone, 0.5% yeast extract, 170mM NaCl] + 50mg/l antibiotic and incubated at 37°C over night. Cells were collected at 11000rpm for 1min. Pellet was dissolved in 250µl resuspension buffer [50mM Tris.HCl pH 8.0, 10mM EDTA, 200µg/ml RNase A]. Then 250µl lysis buffer [200mM NaOH, 1% SDS] and 300µl neutralization buffer [3M potassium acetate pH 5.5] were added and gently mixed. The mixture was centrifuged at 13000rpm for 10min. The supernatant was transferred into a fresh reaction tube and plasmid DNA was precipitated by adding 600µl isopropanol and centrifuged at 13000rpm for 10min. The DNA was washed with 70% ethanol. The air-dried pellet was resuspended in 20-50µl water.

4.5.2.6 Sequencing

Plasmids were purified with polyethylenglycol (PEG), thus 30µl of PEG solution (20% PEG(6000), 2.5mM NaCl) was added to 50µl plasmid (see above) and incubated for 1h on ice. DNA was spun down at 13000rpm, 4°C for 15min. The pellet was washed with 70% ethanol, air-dried and resuspended in 20µl distilled water. PCR products were

purified over agarose gel electrophoresis and eluted with the Nucleospin Extract II kit (Macherey Nagel).

For one sequencing reaction with 10µl total volume 0.2 – 1µg of the plasmid or PCR product were mixed with 0.4µM primer (table 13). 0.75x sequencing buffer and 1 µl BigDye (both from Applied Biosystems) were added. PCR settings were 96°C-2min, 25x (96°C - 30sec, 45°C- 15sec, 60°C- 4min). Sequencing reaction was analyzed by the sequencing service of VBC-GENOMICS. The chromatograms were analyzed with Vector NTI Advance 10 (Invitrogen).

Primer name	Sequence in 5´to 3´ direction
T7	TAATACGACTCACTATAGGG
M13-R	CAGGAAACAGCTATGACCAT

Table 13. Primers used for sequencing.

4.6 Cytology

4.6.1 Slide pre-preparation

The slides were acid-cleaned as follows: Slides were treated with sulfochromic acid for at least 3 h at room temperature. For the sulfochromic acid solution 100g kaliumdichromat in 800ml distilled water was boiled and after the solution cooled, 100ml sulfuric acid was slowly added. Slides were washed in running tap water for 5 min and rinsed thoroughly in distilled water. After the slides were air-dried they were placed in 96% ethanol for 10 min to 2 days.

For 3D preparations, slides were additionally coated with gelatin. 10µl of 1% fresh gelatin solution was applied on the washed slides and dispensed with a pasteur pipet.

4.6.2 Preparation of pollen mother cells (PMCs) for immunostaining

Young inflorescence were harvested and covered with fixative (4% paraformaldehyde in 1x PBS (137mM NaCl, 2.7mM KCl, 10mM Na_2HPO_4, 1.8mM KH_2HPO_4, pH 7.4) + 0.1% Triton X). Samples were infiltrated under vacuum and kept at room temperature for 1h. Inflorescences were washed 3x10 min in 1x PBS + 0.1% Triton X. Floral buds

were digested with enzymatic mixture of 2.5% pectinase (v/v; Sigma #P-4716), 2.5% cellulase "Onozuka R-10" (w/v; Serva #16419) and 2.5% pectolyase (w/v; Sigma #P-3026) in PBS at 37°C for 30min in a wet chamber. Enzymatic mixture was replaced and washed 3x 10 min in PBS. 4 to 6 floral buds smaller than 0.5mm were placed in 10µL of PBS buffer on a clean Poly-lysine slide. Anthers were dissected with needles and carefully squashed. A cover slip was placed on top and the anthers very gently tapped with the rubber end of the pencil to release the PMCs. Then the slide was carefully squashed and the cover slip removed with a razor blade after dipping the slide into liquid nitrogen. Slides were transferred into PBS buffer and immunostaining was performed.

4.6.3 Fluorescence immunolocalization

Slides were washed 3x5 min in 1xPBS + 0.1% Triton solution. To block non-specific antibody binding, 20µl of blocking buffer (1xPBS, 0.1% Triton, 3% BSA) were applied on the slides and incubated at room temperature for 60 min. 20µl of primary antibody (table 14), diluted in 1x PBS + 0.1% Triton + 1% BSA were added on the slides and incubated overnight at 4°C in a moisture chamber. Slides were washed 3x 5min in 1x PBS. 20µl of the secondary antibody (table 14) diluted in 1x PBS + 0.1% Triton + 1% BSA were applied on the slide and incubated for at least 120 min at room temperature. Finally the slides were washed for 3x5 min and stained with DAPI (10µg/ml). Slides were mounted in Vectashield antifade mounting medium (Vector Labs) with DAPI (2µg/ml). The slides were examined under Axio Imager.Z1 epifluorescence microscope (Zeiss). Pictures were taken with a cooled CCD camera (Visitron) and MetaMorph (Molecular Devices Corporation) software. Deconvolution was performed with AutoQuantX (AutoQuant Imaging).

Primary antibodies	**Working dilution**
anti-GUS (Molecular Probes #A-5790)	1 : 500
Secondary antibodies	**Working dilution**
cy3-conjugated anti-rabbit (Amersham # PA43004)	1 : 1 000

Table 14. Antibodies used for immunostaining.

4.6.4 Preparation of pollen mother cells (PMCs) for FISH

Whole inflorescence were fixed in freshly made Carnoy´s fixative (ethanol: acetic acid (3:1)) and incubated at room temperature for at least 30min. Inflorescences were transferred into watch glass containing distilled water and washed two three times for 10min with 1x citrate buffer (4 parts of 0.01M citric acid and 6 parts of 0.01M tri-sodium citrate, pH 4.6-4.8). Floral buds larger than 0.5mm were discarded. ~20µl of enzymatic mixture (0.25% cellulase (Sigma), 0.25% pectolyase (Sigma) in 1x citrate buffer) was applied and incubated at 37°C for 30min in a wet chamber. The enzymatic mixture was washed off three times for 10 min in 1x citrate buffer. The buds were placed on pre-treated slides onto one drop of 1x citrate buffer and anthers were dissected with forcipes and needles. A cover slip was placed on top and the anthers very gently tapped with the rubber end of the pencil and carefully squashed. Slides were dipped into liquid nitrogen and the cover slip was quickly removed with a razor blade. The slides were air dried. 8µl of Vectashield (Vector Labs) + DAPI (2µg/ml) was added and the slide covered with a cover slip. Slides were examined as described in 4.6.3.

4.6.5 Fluorescence *in situ* hybridization (FISH)

After the immersion oil was removed with diethylether, slides were washed in 2x SSC (300mM NaCl, 30mM Na-citrate pH 7.0) at room temperature for 10 min or until the cover slips fells off. The washing was repeated twice for 5 min. Slides were incubated with 100 µl RNAse A (100 µg/ml) covered with plastic cover slips for 1h at 37°C in a humid chamber. RNAse was washed off 3x5 min in 2x SSC at room temperature. Then 100µl of pepsin (50µg/ml in 0.01N HCl) was applied on the slides and incubated 2-4min at room temperature. Slides were washed again 3x5 min in 2x SSC. The cells were re-fixed by dipping the slides in 4% paraformaldehyde in 1xPBS + 0.01% TritonX100 for 10min. Then slides were washed again 3x5 min in 2x SSC. The material was then dehydrated by incubating the slides in a series of ethanol (50%, 70% and 96%) for 2 min each. Slides were air dried before hybridization mix was applied. For one slide the hybridization mixture was prepared as followed: 15µl formamide, 10% dextran sulphate (50%), 1x SSC (150mM NaCl, 15mM Na-citrate pH 7.0), 60 - 100ng/l labeled probe and distilled water up to a total volume of 30 µl. Prior to applying the hybridization mix on the slides it was denaturated at 75°C for 10 min and

cooled on ice for 5 min. The probe was applied on the slide. For DNA denaturation probe hybridisation the slides were incubated at different temperatures using a thermal cycler equipped with flat plate. The temperature was programmed as followed: 75°C for 5 min, 65°C for 2 min, 55°C for 2 min, 45°C for 2 min. When the temperature reached 37°C, slides were transferred into a pre-warmed moist chamber. Slides covered with plastic cover slips and incubated at 37C over night. The next day the unspecific and unbound probe was washed off with following washing steps:

2 x 5 min in 2x SSC at 42°C

2 x 5 min in 0.1x SSC (15mM NaCl, 1.5mM Na-citrate pH 7.0) at 42°C

2 x 5 min in 2x SSC at 42°C and cooled down to room temperature

5 min in 2x SSC

7 min in 4x SSC (600mM NaCl, 60mM Na-citrate pH 7.0) + 0.1% Tween 20

5 min in 1x PBS

Slides were mounted in Vectashield (Vector Labs) and DAPI (2µg/ml) and analyzed in fluorescence microscope.

4.6.6 Preparation of embryo-sac mother cells (EMCs)

Pistils ranging from 0.5-0.9mm were fixed in freshly made Carnoy´s fixative (ethanol: acetic acid (3:1)). Slides were prepares as described in 4.6.5. Ovules were dissected in 1x citrate buffer and gently squashed. Slides were mounted with Vectashield (Vector labs) and DAPI (2µg/ml).

4.6.7 Alexander Staining

Alexander staining solution was prepared according to Alexander et al.(Alexander 1969). 4% acetic acid was added freshly before usage. One drop of the staining solution with 4% acetic acid was put on one slide. From three opened flowers the buds that have only just opened and were only the tips of the white petals are visible were put on the slide. Anthers were dissected and then slides were covered with a cover slip and sealed. The slides were left at room temperature for at least 2hr before the staining was observed under light microscope.

5 REFERENCES

Akira, S., S. Uematsu, et al. (2006). "Pathogen recognition and innate immunity." Cell **124**(4): 783-801.

Alexander, M. P. (1969). "Differential staining of aborted and nonaborted pollen." Stain Technol **44**(3): 117-22.

Amrani, N., R. Ganesan, et al. (2004). "A faux 3'-UTR promotes aberrant termination and triggers nonsense-mediated mRNA decay." Nature **432**(7013): 112-8.

Anders, K. R., A. Grimson, et al. (2003). "SMG-5, required for C.elegans nonsense-mediated mRNA decay, associates with SMG-2 and protein phosphatase 2A." Embo J **22**(3): 641-50.

Arciga-Reyes, L., L. Wootton, et al. (2006). "UPF1 is required for nonsense-mediated mRNA decay (NMD) and RNAi in Arabidopsis." Plant J **47**(3): 480-9.

Armstrong, S. J. and G. H. Jones (2003). "Meiotic cytology and chromosome behaviour in wild-type Arabidopsis thaliana." J Exp Bot **54**(380): 1-10.

Averbeck, N., S. Sunder, et al. (2005). "Negative control contributes to an extensive program of meiotic splicing in fission yeast." Mol Cell **18**(4): 491-8.

Azumi, Y., D. Liu, et al. (2002). "Homolog interaction during meiotic prophase I in Arabidopsis requires the SOLO DANCERS gene encoding a novel cyclin-like protein." Embo J **21**(12): 3081-95.

Azzalin, C. M. and J. Lingner (2006). "The human RNA surveillance factor UPF1 is required for S phase progression and genome stability." Curr Biol **16**(4): 433-9.

Azzalin, C. M., P. Reichenbach, et al. (2007). "Telomeric repeat containing RNA and RNA surveillance factors at mammalian chromosome ends." Science **318**(5851): 798-801.

Beernink, H. T., K. Miller, et al. (2003). "Telomere maintenance in fission yeast requires an Est1 ortholog." Curr Biol **13**(7): 575-80.

Behm-Ansmant, I., I. Kashima, et al. (2007). "mRNA quality control: an ancient machinery recognizes and degrades mRNAs with nonsense codons." FEBS Lett **581**(15): 2845-53.

Cali, B. M., S. L. Kuchma, et al. (1999). "smg-7 is required for mRNA surveillance in Caenorhabditis elegans." Genetics **151**(2): 605-16.

Carlile, T. M. and A. Amon (2008). "Meiosis I is established through division-specific translational control of a cyclin." Cell **133**(2): 280-91.

Century, K. S., A. D. Shapiro, et al. (1997). "NDR1, a pathogen-induced component required for Arabidopsis disease resistance." Science **278**(5345): 1963-5.

Chang, Y. F., J. S. Imam, et al. (2007). "The nonsense-mediated decay RNA surveillance pathway." Annu Rev Biochem **76**: 51-74.

Chen, C., A. Marcus, et al. (2002). "The Arabidopsis ATK1 gene is required for spindle morphogenesis in male meiosis." Development **129**(10): 2401-9.

Chiba, Y. and P. J. Green (2009). "mRNA Degradation Machinery in Plants." Journal of Plant Biology **52**(2): 114-124.

Chiu, S. Y., G. Serin, et al. (2003). "Characterization of human Smg5/7a: a protein with similarities to Caenorhabditis elegans SMG5 and SMG7 that functions in the dephosphorylation of Upf1." Rna **9**(1): 77-87.

Chu, T., G. Henrion, et al. (2001). "Cortex, a Drosophila gene required to complete oocyte meiosis, is a member of the Cdc20/fizzy protein family." Genesis **29**(3): 141-52.

Conti, E. and E. Izaurralde (2005). "Nonsense-mediated mRNA decay: molecular insights and mechanistic variations across species." Curr Opin Cell Biol **17**(3): 316-25.

Culbertson, M. R., K. M. Underbrink, et al. (1980). "Frameshift suppression Saccharomyces cerevisiae. II. Genetic properties of group II suppressors." Genetics **95**(4): 833-53.

Culotti, J. and L. H. Hartwell (1971). "Genetic control of the cell division cycle in yeast. 3. Seven genes controlling nuclear division." Exp Cell Res **67**(2): 389-401.

d'Erfurth, I., S. Jolivet, et al. (2008). "Mutations in AtPS1 (Arabidopsis thaliana parallel spindle 1) lead to the production of diploid pollen grains." PLoS Genet **4**(11): e1000274.

den Elzen, N. and J. Pines (2001). "Cyclin A is destroyed in prometaphase and can delay chromosome alignment and anaphase." J Cell Biol **153**(1): 121-36.

Do, C. B., M. S. Mahabhashyam, et al. (2005). "ProbCons: Probabilistic consistency-based multiple sequence alignment." Genome Res **15**(2): 330-40.

Doma, M. K. and R. Parker (2006). "Endonucleolytic cleavage of eukaryotic mRNAs with stalls in translation elongation." Nature **440**(7083): 561-4.

Durrant, W. E. and X. Dong (2004). "Systemic acquired resistance." Annu Rev Phytopathol **42**: 185-209.

Eulalio, A., I. Behm-Ansmant, et al. (2007). "P bodies: at the crossroads of post-transcriptional pathways." Nat Rev Mol Cell Biol **8**(1): 9-22.

Evans, S. K. and V. Lundblad (1999). "Est1 and Cdc13 as comediators of telomerase access." Science **286**(5437): 117-20.

Ferrando, A., R. Farras, et al. (2000). "Intron-tagged epitope: a tool for facile detection and purification of proteins expressed in Agrobacterium-transformed plant cells." Plant J **22**(6): 553-60.

Ferreira, P. C., A. S. Hemerly, et al. (1994). "Developmental expression of the arabidopsis cyclin gene cyc1At." Plant Cell **6**(12): 1763-74.

Feys, B. J., L. J. Moisan, et al. (2001). "Direct interaction between the Arabidopsis disease resistance signaling proteins, EDS1 and PAD4." Embo J **20**(19): 5400-11.

Ford, A. S., Q. Guan, et al. (2006). "Ebs1p, a negative regulator of gene expression controlled by the Upf proteins in the yeast Saccharomyces cerevisiae." Eukaryot Cell **5**(2): 301-12.

Fribourg, S., D. Gatfield, et al. (2003). "A novel mode of RBD-protein recognition in the Y14-Mago complex." Nat Struct Biol **10**(6): 433-9.

Frischmeyer, P. A. and H. C. Dietz (1999). "Nonsense-mediated mRNA decay in health and disease." Hum Mol Genet **8**(10): 1893-900.

Frischmeyer, P. A., A. van Hoof, et al. (2002). "An mRNA surveillance mechanism that eliminates transcripts lacking termination codons." Science **295**(5563): 2258-61.

Fukuhara, N., J. Ebert, et al. (2005). "SMG7 is a 14-3-3-like adaptor in the nonsense-mediated mRNA decay pathway." Mol Cell **17**(4): 537-47.

Fung, T. K., H. T. Ma, et al. (2007). "Specialized roles of the two mitotic cyclins in somatic cells: cyclin A as an activator of M phase-promoting factor." Mol Biol Cell **18**(5): 1861-73.

Fung, T. K. and R. Y. Poon (2005). "A roller coaster ride with the mitotic cyclins." Semin Cell Dev Biol **16**(3): 335-42.

Galtier, N., M. Gouy, et al. (1996). "SEAVIEW and PHYLO_WIN: two graphic tools for sequence alignment and molecular phylogeny." Comput Appl Biosci **12**(6): 543-8.

Gatfield, D., L. Unterholzner, et al. (2003). "Nonsense-mediated mRNA decay in Drosophila: at the intersection of the yeast and mammalian pathways." Embo J **22**(15): 3960-70.

Gehring, N. H., G. Neu-Yilik, et al. (2003). "Y14 and hUpf3b form an NMD-activating complex." Mol Cell **11**(4): 939-49.

Glavan, F., I. Behm-Ansmant, et al. (2006). "Structures of the PIN domains of SMG6 and SMG5 reveal a nuclease within the mRNA surveillance complex." Embo J **25**(21): 5117-25.

Glazebrook, J., M. Zook, et al. (1997). "Phytoalexin-deficient mutants of Arabidopsis reveal that PAD4 encodes a regulatory factor and that four PAD genes contribute to downy mildew resistance." Genetics **146**(1): 381-92.

Goeres, D. C., J. M. Van Norman, et al. (2007). "Components of the Arabidopsis mRNA decapping complex are required for early seedling development." Plant Cell **19**(5): 1549-64.

Gutierrez, R. A., R. M. Ewing, et al. (2002). "Identification of unstable transcripts in Arabidopsis by cDNA microarray analysis: rapid decay is associated with a group of touch- and specific clock-controlled genes." Proc Natl Acad Sci U S A **99**(17): 11513-8.

Hall, T. A. (1999). "Bioedit: a user-friendly biological sequence alignment editor and analysis program for windows 95/98/nt." Nucleic Acids Symposium Series **41** 95-98.

Hamant, O., H. Ma, et al. (2006). "Genetics of meiotic prophase I in plants." Annu Rev Plant Biol **57**: 267-302.

He, F. and A. Jacobson (1995). "Identification of a novel component of the nonsense-mediated mRNA decay pathway by use of an interacting protein screen." Genes Dev **9**(4): 437-54.

Heath, M. C. (2000). "Hypersensitive response-related death." Plant Mol Biol **44**(3): 321-34.

Hodgkin, J., A. Papp, et al. (1989). "A new kind of informational suppression in the nematode Caenorhabditis elegans." Genetics **123**(2): 301-13.

Holbrook, J. A., G. Neu-Yilik, et al. (2004). "Nonsense-mediated decay approaches the clinic." Nat Genet **36**(8): 801-8.

Holloway, S. L., M. Glotzer, et al. (1993). "Anaphase is initiated by proteolysis rather than by the inactivation of maturation-promoting factor." Cell **73**(7): 1393-402.

Hori, K. and Y. Watanabe (2005). "UPF3 suppresses aberrant spliced mRNA in Arabidopsis." Plant J **43**(4): 530-40.

Hori, K. and Y. Watanabe (2007). "Context analysis of termination codons in mRNA that are recognized by plant NMD." Plant Cell Physiol **48**(7): 1072-8.

Hruz T, L. O., Szabo G, Wessendorp F, Bleuler S, Oertle L, Widmayer P, Gruissem W and P Zimmermann (2008). "Genevestigator V3: a reference expression database for the meta-analysis of transcriptomes." Advances in Bioinformatics 2008 **420747**.

Huang, J. and J. W. Raff (1999). "The disappearance of cyclin B at the end of mitosis is regulated spatially in Drosophila cells." Embo J **18**(8): 2184-95.

Irniger, S. (2006). "Preventing fatal destruction: inhibitors of the anaphase-promoting complex in meiosis." Cell Cycle **5**(4): 405-15.

Ishigaki, Y., X. Li, et al. (2001). "Evidence for a pioneer round of mRNA translation: mRNAs subject to nonsense-mediated decay in mammalian cells are bound by CBP80 and CBP20." Cell **106**(5): 607-17.

Isken, O. and L. E. Maquat (2007). "Quality control of eukaryotic mRNA: safeguarding cells from abnormal mRNA function." Genes Dev **21**(15): 1833-56.

Isken, O. and L. E. Maquat (2008). "The multiple lives of NMD factors: balancing roles in gene and genome regulation." Nat Rev Genet.

Iwasaki, S., A. Takeda, et al. (2007). "Characterization of Arabidopsis decapping proteins AtDCP1 and AtDCP2, which are essential for post-embryonic development." FEBS Lett **581**(13): 2455-9.

Izawa, D., M. Goto, et al. (2005). "Fission yeast Mes1p ensures the onset of meiosis II by blocking degradation of cyclin Cdc13p." Nature **434**(7032): 529-33.

Jaillon, O., K. Bouhouche, et al. (2008). "Translational control of intron splicing in eukaryotes." Nature **451**(7176): 359-62.

Jambunathan, N., J. M. Siani, et al. (2001). "A humidity-sensitive Arabidopsis copine mutant exhibits precocious cell death and increased disease resistance." Plant Cell **13**(10): 2225-40.

Jirage, D., T. L. Tootle, et al. (1999). "Arabidopsis thaliana PAD4 encodes a lipase-like gene that is important for salicylic acid signaling." Proc Natl Acad Sci U S A **96**(23): 13583-8.

Jirage, D., N. Zhou, et al. (2001). "Constitutive salicylic acid-dependent signaling in cpr1 and cpr6 mutants requires PAD4." Plant J **26**(4): 395-407.

Jones, J. D. (2001). "Putting knowledge of plant disease resistance genes to work." Curr Opin Plant Biol **4**(4): 281-7.

Jones, J. D. and J. L. Dangl (2006). "The plant immune system." Nature **444**(7117): 323-9.

Kerenyi, Z., Z. Merai, et al. (2008). "Inter-kingdom conservation of mechanism of nonsense-mediated mRNA decay." Embo J **27**(11): 1585-95.

Kertesz, S., Z. Kerenyi, et al. (2006). "Both introns and long 3'-UTRs operate as cis-acting elements to trigger nonsense-mediated decay in plants." Nucleic Acids Res **34**(21): 6147-57.

Kishida, M., T. Nagai, et al. (1994). "Meiosis-dependent mRNA splicing of the fission yeast Schizosaccharomyces pombe mes1+ gene." Curr Genet **25**(6): 497-503.

Kitajima, T. S., S. Hauf, et al. (2005). "Human Bub1 defines the persistent cohesion site along the mitotic chromosome by affecting Shugoshin localization." Curr Biol **15**(4): 353-9.

Koch, E. and A. Slusarenko (1990). "Arabidopsis is susceptible to infection by a downy mildew fungus." Plant Cell **2**(5): 437-45.

Kurihara, Y., A. Matsui, et al. (2009). "Genome-wide suppression of aberrant mRNA-like noncoding RNAs by NMD in Arabidopsis." Proc Natl Acad Sci U S A **106**(7): 2453-8.

Laemmli, U. K. (1970). "Cleavage of structural proteins during the assembly of the head of bacteriophage T4." Nature **227**(5259): 680-5.

Larkin, M. A., G. Blackshields, et al. (2007). "Clustal W and Clustal X version 2.0." Bioinformatics **23**(21): 2947-8.

Leeds, P., S. W. Peltz, et al. (1991). "The product of the yeast UPF1 gene is required for rapid turnover of mRNAs containing a premature translational termination codon." Genes Dev **5**(12A): 2303-14.

Leonardi, J., J. A. Box, et al. (2008). "TER1, the RNA subunit of fission yeast telomerase." Nat Struct Mol Biol **15**(1): 26-33.
Lewis, B. P., R. E. Green, et al. (2003). "Evidence for the widespread coupling of alternative splicing and nonsense-mediated mRNA decay in humans." Proc Natl Acad Sci U S A **100**(1): 189-92.
Linde, L. and B. Kerem (2008). "Introducing sense into nonsense in treatments of human genetic diseases." Trends Genet **24**(11): 552-63.
Lorrain, S., F. Vailleau, et al. (2003). "Lesion mimic mutants: keys for deciphering cell death and defense pathways in plants?" Trends Plant Sci **8**(6): 263-71.
Losson, R. and F. Lacroute (1979). "Interference of nonsense mutations with eukaryotic messenger RNA stability." Proc Natl Acad Sci U S A **76**(10): 5134-7.
Luke, B., C. M. Azzalin, et al. (2007). "Saccharomyces cerevisiae Ebs1p is a putative ortholog of human Smg7 and promotes nonsense-mediated mRNA decay." Nucleic Acids Res **35**(22): 7688-97.
Lundblad, V. and J. W. Szostak (1989). "A mutant with a defect in telomere elongation leads to senescence in yeast." Cell **57**(4): 633-43.
Magnard, J. L., M. Yang, et al. (2001). "The Arabidopsis gene tardy asynchronous meiosis is required for the normal pace and synchrony of cell division during male meiosis." Plant Physiol **127**(3): 1157-66.
Malapeira, J., A. Moldon, et al. (2005). "A meiosis-specific cyclin regulated by splicing is required for proper progression through meiosis." Mol Cell Biol **25**(15): 6330-7.
Maquat, L. E. (2004). "Nonsense-mediated mRNA decay: splicing, translation and mRNP dynamics." Nat Rev Mol Cell Biol **5**(2): 89-99.
Marston, A. L. and A. Amon (2004). "Meiosis: cell-cycle controls shuffle and deal." Nat Rev Mol Cell Biol **5**(12): 983-97.
McGuinness, B. E., T. Hirota, et al. (2005). "Shugoshin prevents dissociation of cohesin from centromeres during mitosis in vertebrate cells." PLoS Biol **3**(3): e86.
McPheeters, D. S., N. Cremona, et al. (2009). "A complex gene regulatory mechanism that operates at the nexus of multiple RNA processing decisions." Nat Struct Mol Biol **16**(3): 255-64.
Metzstein, M. M. and M. A. Krasnow (2006). "Functions of the nonsense-mediated mRNA decay pathway in Drosophila development." PLoS Genet **2**(12): e180.
Meyers, B. C., A. Kozik, et al. (2003). "Genome-wide analysis of NBS-LRR-encoding genes in Arabidopsis." Plant Cell **15**(4): 809-34.
Mita, S., N. Murano, et al. (1997). "Mutants of Arabidopsis thaliana with pleiotropic effects on the expression of the gene for beta-amylase and on the accumulation of anthocyanin that are inducible by sugars." Plant J **11**(4): 841-51.
Mitrovich, Q. M. and P. Anderson (2000). "Unproductively spliced ribosomal protein mRNAs are natural targets of mRNA surveillance in C. elegans." Genes Dev **14**(17): 2173-84.
Morrison, M., K. S. Harris, et al. (1997). "smg mutants affect the expression of alternatively spliced SR protein mRNAs in Caenorhabditis elegans." Proc Natl Acad Sci U S A **94**(18): 9782-5.
Neff, M. M., J. D. Neff, et al. (1998). "dCAPS, a simple technique for the genetic analysis of single nucleotide polymorphisms: experimental applications in Arabidopsis thaliana genetics." Plant J **14**(3): 387-92.

Nishimura, M. T., M. Stein, et al. (2003). "Loss of a callose synthase results in salicylic acid-dependent disease resistance." Science **301**(5635): 969-72.
Nishimura, N., N. Kitahata, et al. (2005). "Analysis of ABA hypersensitive germination2 revealed the pivotal functions of PARN in stress response in Arabidopsis." Plant J **44**(6): 972-84.
Oelschlaegel, T., M. Schwickart, et al. (2005). "The yeast APC/C subunit Mnd2 prevents premature sister chromatid separation triggered by the meiosis-specific APC/C-Ama1." Cell **120**(6): 773-88.
Ohnishi, T., A. Yamashita, et al. (2003). "Phosphorylation of hUPF1 induces formation of mRNA surveillance complexes containing hSMG-5 and hSMG-7." Mol Cell **12**(5): 1187-200.
Page, A. W. and T. L. Orr-Weaver (1996). "The Drosophila genes grauzone and cortex are necessary for proper female meiosis." J Cell Sci **109 (Pt 7)**: 1707-15.
Page, M. F., B. Carr, et al. (1999). "SMG-2 is a phosphorylated protein required for mRNA surveillance in Caenorhabditis elegans and related to Upf1p of yeast." Mol Cell Biol **19**(9): 5943-51.
Page, R. D. (1996). "TreeView: an application to display phylogenetic trees on personal computers." Comput Appl Biosci **12**(4): 357-8.
Parry, D. H. and P. H. O'Farrell (2001). "The schedule of destruction of three mitotic cyclins can dictate the timing of events during exit from mitosis." Curr Biol **11**(9): 671-83.
Pendle, A. F., G. P. Clark, et al. (2005). "Proteomic analysis of the Arabidopsis nucleolus suggests novel nucleolar functions." Mol Biol Cell **16**(1): 260-9.
Penkner, A. M., S. Prinz, et al. (2005). "Mnd2, an essential antagonist of the anaphase-promoting complex during meiotic prophase." Cell **120**(6): 789-801.
Pennock, E., K. Buckley, et al. (2001). "Cdc13 delivers separate complexes to the telomere for end protection and replication." Cell **104**(3): 387-96.
Peters, J. M. (2006). "The anaphase promoting complex/cyclosome: a machine designed to destroy." Nat Rev Mol Cell Biol **7**(9): 644-56.
Pinto, I., J. G. Na, et al. (1992). "cis- and trans-acting suppressors of a translation initiation defect at the cyc1 locus of Saccharomyces cerevisiae." Genetics **132**(1): 97-112.
Potapova, T. A., J. R. Daum, et al. (2006). "The reversibility of mitotic exit in vertebrate cells." Nature **440**(7086): 954-8.
Qi, H. and V. A. Zakian (2000). "The Saccharomyces telomere-binding protein Cdc13p interacts with both the catalytic subunit of DNA polymerase alpha and the telomerase-associated est1 protein." Genes Dev **14**(14): 1777-88.
Queralt, E. and F. Uhlmann (2008). "Cdk-counteracting phosphatases unlock mitotic exit." Curr Opin Cell Biol **20**(6): 661-8.
Rehwinkel, J., I. Letunic, et al. (2005). "Nonsense-mediated mRNA decay factors act in concert to regulate common mRNA targets." Rna **11**(10): 1530-44.
Reichenbach, P., M. Hoss, et al. (2003). "A human homolog of yeast Est1 associates with telomerase and uncaps chromosome ends when overexpressed." Curr Biol **13**(7): 568-74.
Riehs, N., S. Akimcheva, et al. (2008). "Arabidopsis SMG7 protein is required for exit from meiosis." J Cell Sci **121**(Pt 13): 2208-16.
Ross, K. J., P. Fransz, et al. (1996). "A light microscopic atlas of meiosis in Arabidopsis thaliana." Chromosome Res **4**(7): 507-16.

Rozhon, W., E. Petutschnig, et al. (2005). "Quantification of free and total salicylic acid in plants by solid-phase extraction and isocratic high-performance anion-exchange chromatography." Anal Bioanal Chem **382**(7): 1620-7.
Ryals, J. A., U. H. Neuenschwander, et al. (1996). "Systemic Acquired Resistance." Plant Cell **8**(10): 1809-1819.
Salic, A., J. C. Waters, et al. (2004). "Vertebrate shugoshin links sister centromere cohesion and kinetochore microtubule stability in mitosis." Cell **118**(5): 567-78.
Sambrook J, R. D. (2001). "Molecular Cloning: A Laboratory Manual. 3rd Ed. ." Cold Spring Harbor Laboratory Press.
Sarowar, S., H. W. Oh, et al. (2007). "Capsicum annuum CCR4-associated factor CaCAF1 is necessary for plant development and defence response." Plant Journal **51**(5): 792-802.
Schmidt, A., P. I. Duncan, et al. (2005). "Xenopus polo-like kinase Plx1 regulates XErp1, a novel inhibitor of APC/C activity." Genes Dev **19**(4): 502-13.
Seeley, K. A., D. H. Byrne, et al. (1992). "Red Light-Independent Instability of Oat Phytochrome mRNA in Vivo." Plant Cell **4**(1): 29-38.
Seto, A. G., A. J. Livengood, et al. (2002). "A bulged stem tethers Est1p to telomerase RNA in budding yeast." Genes Dev **16**(21): 2800-12.
Shapiro, A. D. and C. Zhang (2001). "The role of NDR1 in avirulence gene-directed signaling and control of programmed cell death in Arabidopsis." Plant Physiol **127**(3): 1089-101.
Snow, B. E., N. Erdmann, et al. (2003). "Functional conservation of the telomerase protein Est1p in humans." Curr Biol **13**(8): 698-704.
Stegmeier, F. and A. Amon (2004). "Closing mitosis: the functions of the Cdc14 phosphatase and its regulation." Annu Rev Genet **38**: 203-32.
Sullivan, M. and D. O. Morgan (2007). "Finishing mitosis, one step at a time." Nat Rev Mol Cell Biol **8**(11): 894-903.
Surana, U., A. Amon, et al. (1993). "Destruction of the CDC28/CLB mitotic kinase is not required for the metaphase to anaphase transition in budding yeast." Embo J **12**(5): 1969-78.
Swan, A., G. Barcelo, et al. (2005). "Drosophila Cks30A interacts with Cdk1 to target Cyclin A for destruction in the female germline." Development **132**(16): 3669-78.
Tang, Z., Y. Sun, et al. (2004). "Human Bub1 protects centromeric sister-chromatid cohesion through Shugoshin during mitosis." Proc Natl Acad Sci U S A **101**(52): 18012-7.
Tung, J. J., D. V. Hansen, et al. (2005). "A role for the anaphase-promoting complex inhibitor Emi2/XErp1, a homolog of early mitotic inhibitor 1, in cytostatic factor arrest of Xenopus eggs." Proc Natl Acad Sci U S A **102**(12): 4318-23.
Unterholzner, L. and E. Izaurralde (2004). "SMG7 acts as a molecular link between mRNA surveillance and mRNA decay." Mol Cell **16**(4): 587-96.
Vagnarelli, P., D. F. Hudson, et al. (2006). "Condensin and Repo-Man-PP1 co-operate in the regulation of chromosome architecture during mitosis." Nat Cell Biol **8**(10): 1133-42.
van Hoof, A., P. A. Frischmeyer, et al. (2002). "Exosome-mediated recognition and degradation of mRNAs lacking a termination codon." Science **295**(5563): 2262-4.
Wang, G., H. Kong, et al. (2004). "Genome-wide analysis of the cyclin family in Arabidopsis and comparative phylogenetic analysis of plant cyclin-like proteins." Plant Physiol **135**(2): 1084-99.

Wang, W., I. J. Cajigas, et al. (2006). "Role for Upf2p phosphorylation in Saccharomyces cerevisiae nonsense-mediated mRNA decay." Mol Cell Biol **26**(9): 3390-400.

Wang, Y., J. L. Magnard, et al. (2004). "Progression through meiosis I and meiosis II in Arabidopsis anthers is regulated by an A-type cyclin predominately expressed in prophase I." Plant Physiol **136**(4): 4127-35.

Waspi, U., P. Schweizer, et al. (2001). "Syringolin reprograms wheat to undergo hypersensitive cell death in a compatible interaction with powdery mildew." Plant Cell **13**(1): 153-161.

Weingartner, M., M. C. Criqui, et al. (2004). "Expression of a nondegradable cyclin B1 affects plant development and leads to endomitosis by inhibiting the formation of a phragmoplast." Plant Cell **16**(3): 643-57.

Wolf, F., R. Sigl, et al. (2007). "'... The end of the beginning': cdk1 thresholds and exit from mitosis." Cell Cycle **6**(12): 1408-11.

Wolf, F., C. Wandke, et al. (2006). "Dose-dependent effects of stable cyclin B1 on progression through mitosis in human cells." Embo J **25**(12): 2802-13.

Woodbury, E. L. and D. O. Morgan (2007). "Cdk and APC activities limit the spindle-stabilizing function of Fin1 to anaphase." Nat Cell Biol **9**(1): 106-12.

Xu, J., J. Y. Yang, et al. (2006). "Arabidopsis DCP2, DCP1, and VARICOSE form a decapping complex required for postembryonic development." Plant Cell **18**(12): 3386-98.

Yam, C. H., T. K. Fung, et al. (2002). "Cyclin A in cell cycle control and cancer." Cell Mol Life Sci **59**(8): 1317-26.

Yang, S. and J. Hua (2004). "A haplotype-specific Resistance gene regulated by BONZAI1 mediates temperature-dependent growth control in Arabidopsis." Plant Cell **16**(4): 1060-71.

Yi, H. and E. J. Richards (2007). "A cluster of disease resistance genes in Arabidopsis is coordinately regulated by transcriptional activation and RNA silencing." Plant Cell **19**(9): 2929-39.

Yoine, M., T. Nishii, et al. (2006). "Arabidopsis UPF1 RNA helicase for nonsense-mediated mRNA decay is involved in seed size control and is essential for growth." Plant Cell Physiol **47**(5): 572-80.

Yoine, M., M. A. Ohto, et al. (2006). "The lba1 mutation of UPF1 RNA helicase involved in nonsense-mediated mRNA decay causes pleiotropic phenotypic changes and altered sugar signalling in Arabidopsis." Plant J **47**(1): 49-62.

Zhang, X. C. and W. Gassmann (2007). "Alternative splicing and mRNA levels of the disease resistance gene RPS4 are induced during Defense responses(1[W][OA])." Plant Physiology **145**(4): 1577-1587.

Zhang, Y., S. Goritschnig, et al. (2003). "A gain-of-function mutation in a plant disease resistance gene leads to constitutive activation of downstream signal transduction pathways in suppressor of npr1-1, constitutive 1." Plant Cell **15**(11): 2636-46.

Zhou, J., K. Hidaka, et al. (2000). "The Est1 subunit of yeast telomerase binds the Tlc1 telomerase RNA." Mol Cell Biol **20**(6): 1947-55.

Zhou, N., T. L. Tootle, et al. (1998). "PAD4 functions upstream from salicylic acid to control defense responses in Arabidopsis." Plant Cell **10**(6): 1021-30.

Zipfel, C. (2008). "Pattern-recognition receptors in plant innate immunity." Curr Opin Immunol **20**(1): 10-6.

6 LIST OF ABBREVIATIONS

aa	amino acids
APC	anaphase promoting complex
APS	ammonium persulfate
bp	base pair
CDK	cyclin dependent kinase
cDNA	complementary DNA
Col-0	Columbia ecotype
DAPI	4',6-diamidino-2-phenylindole
dCAPS	derived cleaved amplified polymorphic sequences
DEPC	diethyl pyrocarbonate
DNA	desoxyribonucleic acid
dNTP	deoxyribonucleotide
EDTA	ethylenediaminetetraacetic acid
EJC	exon-junction complex
EMC	embryo-sac mother cell
FISH	fluorescence *in situ* hybridization
FEAR	cdc fourteen early anaphase release
GUS	beta-glucoronidase
h	hour
HH	high humidity
HR	hypersensitive response
kbp	kilo base pair
LH	low humidity
LMM	lesion mimic mutant
MEN	mitotic exit network
min	minute
mRNA	messenger RNA
NMD	nonsense mediated RNA decay
OD	optical density
ORF	open reading frame
PAGE	polyacrylamide gel electrophoresis

PCR	polymerase chain reaction
PEG	polyethylene glycol
PIPES	piperazine-N,N′-bis(2-ethanesulfonic acid)
PMC	pollen mother cell
PTC	premature termination codon
PSI-BLAST	position-specific iterative basic local alignment search tool
RNA	ribonucleic acid
RT-PCR	reverse transcription polymerase chain reaction
SA	salicylic acid
SAC	spindle assembly checkpoint
SAR	systemic acquired resistance
SDS	sodium dodecyl sulfate
sec	second
TCA	trichloroacetic acid
TEMED	N,N,N´,N´Tetramethylethylenediamine
TPR	tetratricopeptide repeat
uORF	upstream open reading frame
U	unit
UTR	untranslated region
Ws	Wassiljewskia ecotype
wt	wild type

ACKNOWLEDGEMENTS

"No (wo)man is an island, entire of itself."
after John Donne, 1624

Thus, I would like to thank all the people who supported, guided and challenged me on my way.

I am very grateful to Karel for his constant support, his motivating spirit and great ideas over all the years.

I want to thank Prof. Schweizer and my PhD committee members Ortrun Mittelsten-Scheid, Claudia Jonak and Michael Jantsch for their good advice and I want to thank Susan Armstrong and Zdravko Lorkovic in advance for reviewing my thesis.

Thanks to all current and former Riha lab members for contributing to the great lab atmosphere, especially Sveta (for constantly being helpful and in good mood), Babsi, Max, Martina, Anita and Honza (for all the scientific / non-scientific chats and good laughs), Matt (who always takes the time and trouble to correct my English), Petra and Marc (for help on the project).

I would like to thank Bettina for performing the salicylic acid analysis. Thanks to all the former and current office mates, especially Gudrun, Stefan and Sascha for all the great discussions. Thanks to Borries, Eva, Jens, Steff, Lucia, Andrea, Ecki and anyway the entire GMI for being more than just a workplace.

Last but not least I want to thank Barry, my mother Renate and my brother Martin for their continuous and full support.

CURRICULUM VITAE

Name: Nina Riehs

Birth: 23.09.1981 in Horn / Austria

Address: GMI – Gregor Mendel Institute of Molecular Plant Biology
Dr. Bohr-Gasse 3
1030 Vienna

E-mail: nina.riehs@gmi.oeaw.ac.at

Education:

2000 – 2005	Studies of Molecular Biology University of Vienna
2003 – 2005	Diploma student at the Gregor Mendel Institute of Molecular Plant Biology (GMI) in Vienna Supervised by Dr. Karel Riha and Prof. Dieter Schweizer. ”Identification of the RNA subunit of telomerase”
2005 – 2009	PhD student at the Gregor Mendel Institute of Molecular Plant Biology (GMI) in Vienna Supervised by Dr. Karel Riha ”Functional analysis of the *Arabidopsis* SMG7 protein”

Publications:

Riehs N, Akimcheva S, Puizina J, Bulankova P, Idol RA, Siroky J, Schleiffer A, Schweizer D, Shippen DE, Riha K. “*Arabidopsis* SMG7 protein is required for exit from meiosis.” J Cell Sci. 2008 Jul 1;121(Pt 13):2208-16.

Presentations at meetings and conferences:

"The *Arabidopsis EVER SHORTER TELOMERE 1* homologue is required for exit from meiosis"
Poster presentation at the 17th Botanical Congress in Vienna, 17-23 July 2005

"*Arabidopsis* EST1/SMG7-like protein is a key regulator of the meiotic cell cycle"
Oral presentation at Vienna Plant Network Meeting, IMP, 19 January 2007

"The *Arabidopsis* EST1/SMG7-like protein is required for exit from meiosis"
Poster presentation at the 32nd FEBS Congress in Vienna, 7-12 July 2007

"The *Arabidopsis* EST1/SMG7-like protein is required for exit from meiosis"
Poster presentation at the 8th European Meiosis EMBO Meeting in Japan, 13-18 September 2007